UNITED NATIONS EDUCATIONAL, SCIENTIFIC AND CULTURAL ORGANIZATION
INTERNATIONAL ATOMIC ENERGY AGENCY
INTERNATIONAL CENTRE FOR THEORETICAL PHYSICS
I.C.T.P., P.O. BOX 586, 34100 TRIESTE, ITALY, CABLE: CENTRATOM TRIESTE

H4.SMR/916 -16

SEVENTH COLLEGE ON BIOPHYSICS:

Structure and Function of Biopolymers: Experimental and Theoretical Techniques.

4 - 29 March 1996

Biological Microcalorimetry - III

Pedro L. MATEO
Department of Physical Chemistry
University of Granada
18071 Granada
SPAIN

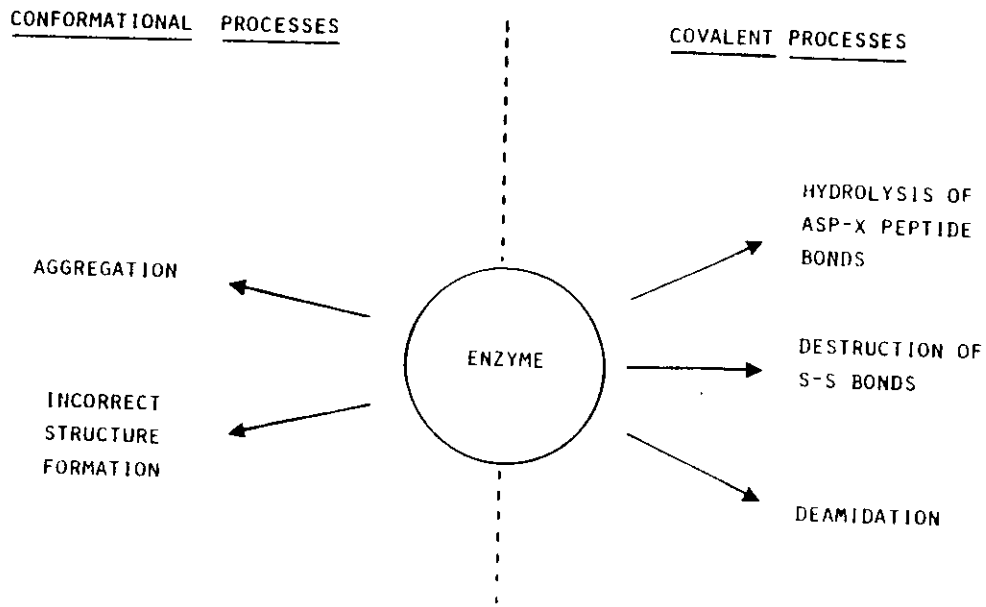

Fig. 2. *The general mechanisms of irreversible thermoinactivation of enzymes.*

LUMRY-EYRING MODEL

$$N \underset{\longleftarrow}{\overset{K}{\longrightarrow}} U \xrightarrow{k} F$$

$$K = \exp\left[-\frac{\Delta H}{R} \cdot \left[\frac{1}{T} - \frac{1}{T_{1/2}} \right] \right]$$

$$k = \exp\left[-\frac{E}{R} \cdot \left[\frac{1}{T} - \frac{1}{T_{*}} \right] \right]$$

$$x_F = 1 - \exp\left\{ -\frac{1}{v} \cdot \int_{T_o}^{T} \frac{k \cdot K}{1 + K} \cdot dT \right\}$$

$$x_U = \frac{K}{1 + K} \cdot \exp\left\{ -\frac{1}{v} \cdot \int_{T_o}^{T} \frac{k \cdot K}{1 + K} \cdot dT \right\}$$

$$x_N = \frac{1}{1 + K} \cdot \exp\left\{ -\frac{1}{v} \cdot \int_{T_o}^{T} \frac{k \cdot K}{1 + K} \cdot dT \right\}$$

$$C_p^{ex} = \frac{K \cdot \Delta H}{(1+K)^2} \cdot \left\{ \frac{k}{v} + \frac{\Delta H}{R \cdot T^2} \right\} \cdot \exp\left\{ -\frac{1}{v} \cdot \int_{T_o}^{T} \frac{k \cdot K}{1 + K} \cdot dT \right\}$$

$$\boxed{C_p^{ex} = C_p^{ex}\ (\Delta H,\ T_{1/2},\ E,\ T_{*},\ v,\ T)}$$

TWO-STATE KINETIC MODEL

$$N \xrightarrow{k} F$$

$$k = \frac{v.C_p^{ex}}{Q_t - Q}$$

$$\ln \frac{v}{T_m^2} = \ln \frac{A.R}{E} - \frac{E}{R.T_m}$$

$$E = \frac{e.R.T_m^2.C_p^m}{Q_t}$$

$$C_p^{ex} = e.C_p^m.\exp\left[\frac{E}{R.T_m^2}.(T-T_m)\right].\exp\left[-\exp\left[\frac{E}{R.T_m^2}.(T-T_m)\right]\right]$$

Biochemistry (1988) 27, 1648-52.

Thermodynamic and Kinetic Analysis of the SH3 Domain of Spectrin Shows a Two-State Folding Transition†

A. R. Viguera,‡ J. C. Martínez,§ V. V. Filimonov,§,∥ P. L. Mateo,*,§ and L. Serrano*,‡

European Molecular Biology Laboratory, Postfach 102209, Meyerhofstrasse, 1, 69012 Heidelberg, Germany, and Departamento de Química-Física, Facultad de Ciencias, Universidad de Granada, 18071 Granada, Spain

Received September 7, 1993; Revised Manuscript Received November 22, 1993•

ABSTRACT: The folding and unfolding reactions of the SH3 domain of spectrin can be described by a two-state model. This domain is a β-sheet barrel containing 62 amino acids. Equilibrium unfolding by urea, guanidine hydrochloride, and heat is completely reversible at pH values below 4.0. At higher pH values the unfolding is reversible as long as the protein concentration is below 1 mg/mL. The Gibbs energy of unfolding in the absence of denaturant, ΔG_{H_2O}, at pH 3.5 and 298 K is calculated to be 12 kJ mol^{-1} for urea, chemical, and temperature denaturation. The stability of the protein does not change noticeably between pH 5.0 and 7.0 and is around 15.5 kJ mol^{-1}. Since heat effects of unfolding are relatively small and, as a result, heat-induced melting occurs in a wide temperature range, the analysis of scanning calorimetry data was performed taking into account the temperature dependence of unfolding ΔC_p. The free energy of unfolding obtained for this domain ($\Delta G_{H_2O} = 14 \pm 2$ kJ mol^{-1}) was, within experimental error, similar to those obtained in this work by other techniques and with those reported in the literature for small globular proteins. Kinetics of unfolding and refolding at pH 3.5, followed both by fluorescence and by circular dichroism, provide evidence of the simplest folding mechanism consistent with the two-state approximation. A value for $\Delta G_{H_2O} = 13 \pm 0.7$ kJ mol^{-1} can be extrapolated from the kinetic data. No intermediate can be seen to accumulate by equilibrium denaturation followed by fluorescence and circular dichroism, refolding kinetics and calorimetry, and a concomitant recovery of secondary and teritary structure is observed during refolding. This suggests that the two-state model can properly describe the folding of this domain from both the equilibrium and kinetic points of view and raises the question of whether the accumulation of kinetic intermediates is merely a result of the size of the protein being studied.

It is clear that a polypeptide chain cannot explore all the conformational space in order to reach the native state, and it thus follows that one or more folding pathways should exist. The analysis of small monomeric proteins has shown that in many cases they follow a single unfolding transition in equilibrium and can consequently be studied as a two-state system. However, there is now increasing evidence for the existence of one or more intermediates in proteins with more than 70 residues. These intermediates have been detected when the folding reactions of these proteins have been studied kinetically or under certain conditions of pH, solvent, etc. (Ikeguchi *et al.*, 1986; Kuwajima *et al.*, 1988; Griko *et al.*, 1988; Udgaonkar & Baldwin, 1990; Briggs & Roder, 1992; Lu & Dahlquist, 1992; Radford *et al.*, 1992; Serrano *et al.*, 1992; Varley *et al.*, 1993; Mann & Matthews, 1993). On the other hand, there are two cases, the chymotrypsin inhibitor CI2 (Jackson & Fersht, 1991) and the G-domain (Alexander *et al.*, 1992b), for which a kinetic or equilibrium intermediate could not be detected, using a wide variety of techniques. The protein inhibitor CI2 has 80 amino acids, but only 60 of them form a globular compact domain (McPhalen & James, 1987). The G-domain forms part of the IgG binding protein and contains around 57 residues (Fahnestock *et al.*, 1986). In both cases there is a central α-helix packing against an antiparallel β-strand (Lyan *et al.*, 1991; Gronenborn *et al.*, 1991; Orban *et al.*, 1992; McPhalen & James, 1987). This raises the following question: are the intermediates accumulating during refolding in other proteins the result of size and consequently of complexity? If this is the case, then we should expect that other proteins or domains with around 60 residues, and no disulfide bridges, should also lack any populated intermediate and behave as true two-state systems.

The SH3 domain is a single small domain of around 60 residues, consisting almost exclusively of β-structure. It is found in a number of proteins and the homology pattern between all of them is well established (Musacchio *et al.*, 1992a). The crystal structures of the SH3 domains of α-spectrin (Musacchio *et al.*, 1992b) and human Fyn (a *src* family tyrosine kinase) (Noble *et al.*, 1993) have recently been determined by X-ray diffraction. Solution structures of SH3 domains from other sources have also been obtained by NMR: human phosphatidylinositol 3′-kinase (PI3K) (Koyama *et al.*, 1993; Booker *et al.*, 1993), *src* (Yu *et al.*, 1992, 1993), and phospholipase Cγ (PLC-γ) (Kohda et al., 1993). All the resolved SH3 domains are highly conserved structures consisting mainly of two antiparallel β-sheets perpendicularly disposed to form a compact β-barrel, with loops of different extensions between the β-strands. This domain is quite interesting, not only because of its small size but also because few all-β-structure proteins (Varley *et al.*, 1993) have been studied from a thermodynamic and kinetic point of view.

† P.L.M. acknowledges financial support from the DGICYT (Spain) (Grant PB90-0876). J.C.M. is a predoctoral fellow of the DGICYT (Spain). A.R.V. is a postdoctoral fellow of the Basque Government (Spain).

‡ EMBL.

§ Universidad de Granada.

∥ Permanent address: Institute of Protein Research, Russian Academy of Sciences, Pushshino, 142292 Russia.

⊥ *Abbreviations*: Gdn-HCl, guanidine hydrochloride; PIPES, piperazine-*N*,*N*′-bis[2-ethanesulfonic acid]; OD, optical density; CD, circular dichroism; SH3, *src* homology region 3; DSC, differential scanning calorimetry.

• Abstract published in *Advance ACS Abstracts*, February 1, 1994.

0006-2960/94/0433-2142$04.50/0

For this paper, we have analyzed the thermodynamic and kinetic behavior of the SH3 domain from α-spectrin to see if it behaves in a similar way as the CI2 protein or the G domain of the IgG binding protein. We have used urea or guanidine hydrochloride to denature the protein, and the changes in fluorescence and/or CD were measured in order to follow the unfolding process. Differential scanning calorimetry experiments were also performed in the pH 2.0–4.0 range. The kinetics of unfolding and refolding, using urea concentration jumps, was used to detect transient intermediates not detected under equilibrium conditions.

EXPERIMENTAL PROCEDURES

Chemicals. Guanidine hydrochloride (Gdn·HCl) and urea were purchased from BRL (Gaithersburg, MD). Buffers for equilibrium denaturation were citric acid, glycine, and sodium phosphate from Merck (Darmstadt, Germany) and PIPES from Sigma (St. Louis, MO). All other reagents were of the highest purity available. Double-distilled deionized water was used throughout.

Expression and Purification of the Recombinant SH3 Domain. pET3c plasmid coding for wild-type SH3 domain was a generous gift from Dr. Saraste. The domain was expressed in *Escherichia coli* BL21 strain. The protein was purified essentially by the method of Musacchio et al. (1992b).

Protein Concentration Determination. The extinction coefficient was calculated by the method of Gill and von Hippel (1989), consisting of the measurement of absorbance at 280 nm of a protein preparation in 6 M Gdn·HCl. Only two tryptophans and the three tyrosines contribute to this signal. The extinction coefficient at 280 nm for the domain in 6 M Gdn·HCl is calculated to be 15 220 and is 16 147 for the native protein.

Chemical Denaturation Experiments. Urea and Gdn·HCl solutions were prepared gravimetrically in volumetric flasks. For each data point 100 or 50 μL of SH3 in the appropriate buffer was mixed with 750 μL of a given denaturant solution. At pH values lower than 3.5, high concentrations of urea changed the pH. Since the stability of this domain is very sensitive to pH values lower than 5.0, we adjusted the pH of the different urea solutions plus buffer, with concentrated hydrochloric acid. The mixtures of the protein plus the buffer in the appropriate urea solutions were left to equilibrate for at least 1 h.

(*a*) *Fluorescence Spectroscopy Analysis.* Fluorescence emission spectra of tryptophan residues in SH3 were used to monitor any changes in the environment of Trp 41 and 42 upon unfolding of the protein. Fluorescence was measured in an Aminco Bowman Series 2 luminescence spectrometer. Excitation was at 290 nm with a 2-nm slit. Fluorescence was detected through an 8-nm slit. In these experiments protein concentration was kept at 3 μM, which renders an OD at 280 nm of 0.05. All experiments were performed at 298 K. The fluorescence spectrum corrected for the instrument response of the SH3 domain is reduced in intensity and red-shifted from 336 to 347 nm upon denaturation with urea or guanidine hydrochloride (data not shown). We found the maximum difference between the native and denatured states to be at 329 nm. However, we have chosen 315 nm to monitor protein denaturation in order to minimize the contribution of Raman scattering from the buffer to the signal. The equilibrium constant for denaturation was calculated, for each denaturant concentration, using

$$K_U = (F_N - F)/(F - F_U) \qquad (1)$$

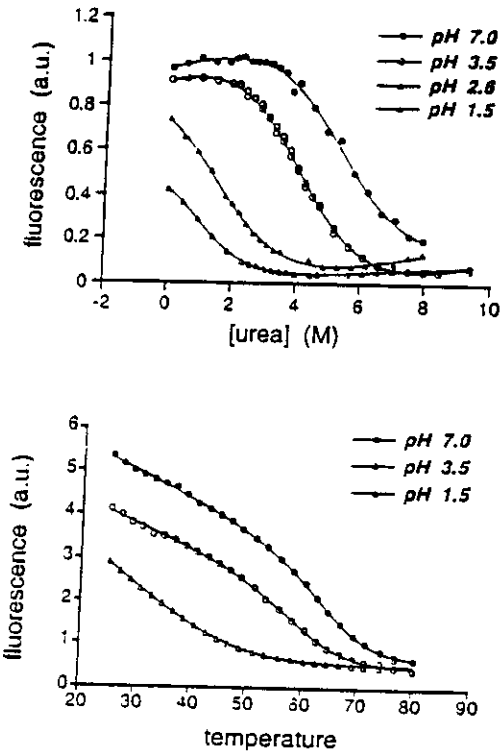

FIGURE 1: Chemical and temperature denaturation profiles of spectrin SH3 domain, followed by fluorescence. Fluorescence emission registered at 315 nm (excitation at 290 nm) after at least 1 h of treatment with denaturant at 298 K. The following buffers were used: 50 mM citric acid, pH 3.5 (○); 50 mM PIPES, pH 7.0 (●); 50 mM glycine, pH 1.5 (△) and 2.5 (▲). Traces were fit to eq 3. (Top) Urea denaturation. (Bottom) Temperature denaturation. In all cases at low pH, a destabilization of the domain can be observed although it cannot be quantified.

where F is the fluorescence value at a certain concentration of denaturant and F_N and F_U are the corresponding fluorescence values for the fully folded and unfolded states in the absence of denaturant. It has been found experimentally that the free energy of unfolding of proteins in the presence of urea is linearly related to the concentration of the denaturant (Pace, 1986):

$$\Delta G_U = \Delta G_{H_2O} - m[\text{denaturant}] \qquad (2)$$

The value of m and ΔG_{H_2O}, the apparent free energy of unfolding in the absence of denaturant, may be calculated from eq 1, because $\Delta G_U = -RT \ln K_U$. The proportionality constant m reflects the cooperativity of the transition and is believed to be related to the difference in hydrophobic surface exposed to the solvent between the native and denatured states.

The quantum yield of the fluorescence of the native and denatured protein increases with urea (Figure 1, top). In the case of Gdn·HCl the fluorescence of the native protein decreases with the denaturant, while that of the unfolded state increases. Consequently the fluorescence yield of the unfolded (F_U) protein in water needs to be linearly extrapolated from higher denaturant concentrations, at which the protein is denatured.

Taking all these dependencies into account, the fluorescence data can be fitted to the following equation

$$F = \{(F_N + a[\text{denat}]) + (F_U + b[\text{denat}])\exp(m[\text{denat}] - \Delta G_{H_2O})/RT\}/\{1 + \exp(m[\text{denat}] - \Delta G_{H_2O})/RT\} \qquad (3)$$

in which the dependence of the intrinsic fluorescence upon

denaturant concentration, in both the native and denatured state, is taken into account by the terms a[urea] and b[urea], respectively (linear approximation). With this kind of analysis we are assuming a two-state model for denaturation, with no species accumulating significantly apart from the native and denatured forms of the domain.

The values obtained for ΔG_{H_2O} and m are only reliable when both a and b can be calculated accurately, in other words, when the total transition can be observed, and we have several values of the fluorescence of the native and denatured states over a large range of denaturant concentrations.

(*b*) *Circular Dichroism.* CD equilibrium measurements were performed in a Jobin-Yvon C-VI machine. Far UV circular dichroism spectra were recorded in a 0.2-cm path length cuvette at 298 K. Secondary structure was followed at 235 nm as a function of urea concentration. We did not find any dependence of the ellipticity of the native or denatured states with the urea concentration and, as a consequence, the data could be fitted to the following simpler equation:

$$F = F_N - \{(F_N - F_U) \exp(m[\text{urea}] - \Delta G_{H_2O})/RT\}/\{1 + \exp(m[\text{urea}] - \Delta G_{H_2O})/RT\} \quad (4)$$

Thermal Denaturation Experiments. Thermally induced unfolding was monitored by fluorescence spectroscopy at different pHs. Fluorescence measurements were made through the temperature range 298–363 K. The temperature was monitored by a thermocouple immersed in the cuvette under observation. Reversibility of the transition can be tested by almost complete recovery of the fluorescence signal after cooling back to 298 K. There is a linear dependence of the fluorescence of the native (F_N) and denatured states (F_U) (Figure 1, bottom) with temperature, and consequently the values of F_N and F_U are estimated at each temperature by linear extrapolation (Pace, 1986).

The enthalpy, $\Delta H_U(T)$, and the enthropy, $\Delta S_U(T)$, of unfolding at a given temperature T can be calculated from the following equations:

$$\Delta H_U(T) = -R[\mathrm{d}(\ln K_U)/\mathrm{d}(1/T)] \quad (5)$$

$$\Delta S_U(T_m) = \Delta H_U(T_m)/(T_m) \quad (6)$$

where T_m is the midpoint of thermal denaturation. van't Hoff plots ($\ln K_U$ vs $1/T$) are approximately linear through the T_m region, thus allowing the estimation of the enthalpy and enthropy of unfolding at T_m. Using the average ΔC_p value obtained from differential scanning calorimetry and applying the following equations

$$\Delta H_U(T) = \Delta H_U(T_m) + \Delta C_p(T - T_m) \quad (7)$$

$$\Delta S_U(T) = \Delta S_U(T_m) + \Delta C_p \ln (T/T_m) \quad (8)$$

$$\Delta G_U(T) = \Delta H_U(T) - T\,\Delta S_U(T) \quad (9)$$

it is possible to calculate the free energy of unfolding, ΔG_U, at a certain temperature T.

Differential Scanning Calorimetry. Calorimetric experiments were performed with the computerized version of the DASM-4 microcalorimeter (Privalov & Potekhin, 1986) at heating rates of 0.5, 1, and 2 K/min. The samples were routinely heated up to 383 K and then cooled slowly inside the calorimeter and reheated once again to check the reversibility of the unfolding. Before filling into the cell, the samples were extensively dialyzed against buffers with the appropriate pH. Since the experiments were conducted between pH 2 and 4, buffers were either 10 mM sodium glycine or 10 mM sodium acetate. The concentration of the protein in calorimetric experiments was between 2 and 5 mg/mL.

The molar partial heat capacity was calculated as previously described (Privalov & Potekhin, 1986) assuming that the partial specific volume of SH3 is 0.73 mL/g (the average value for globular proteins) and its molecular mass equal to 7150 Da. The molar partial heat capacity was further analyzed using SCAL software (Filimonov *et al.*, 1982) and the curve-fitting option of Sigmaplot (Jandel Co.).

The necessity of using a nonlinear $\Delta C_{p,u}$ function to analyze calorimetric experiments was demonstrated by Privalov *et al.* (1989), who showed that $C_{p,u}$ is a nonlinear function of temperature and who suggested a simple procedure for estimating $C_{p,u}$ from the amino acid content of the protein (Makhatadze & Privalov, 1990; Privalov & Makhatadze, 1990). For many years the heat effect of the unfolding was calculated by a direct integration of the C_p^{exc} function in accordance with the following definitions (Filimonov *et al.*, 1982; Privalov & Potekhin, 1986);

$$\langle \Delta C_{p,0}(T) \rangle = C_{p,p}(T) - C_{p,0}(T) = \mathrm{d}\langle \Delta H \rangle/\mathrm{d}T = \delta C_p^{int} + \delta C_p^{exc} \quad (10)$$

$$\delta C_p^{int} = \sum_i \Delta C_{p,i} F_i \qquad \delta C_p^{exc} = \sum_i \Delta H_i \, \mathrm{d}F_i/\mathrm{d}T \quad (11)$$

Here $\langle \Delta C_{p,0} \rangle$ is the excess of C_p over $C_{p,0}$, the heat capacity of the initial state (which from now on will be considered as the reference state), and $\langle \Delta H(T) \rangle$ is the overall excess of the enthalpy, while ΔH_i and $\Delta C_{p,i}$ refer to the increments corresponding to the macroscopic states of protein with relative population F_i. Then $\delta C_p^{int}(T)$ is related to the "internal" heat capacity increase, while $\delta C_p^{exc}(T)$ is the excess heat absorbance of the reaction.

To find δC_p^{exc} from C_p one has to approximate both $C_{p,0}$ and δC_p^{int} by some reasonable functions. Usually the first one is approximated by a linear function of temperature (Privalov, 1979; Privalov & Potekhin, 1986; Privalov *et al.*, 1989) and the second one by a sigmoid proportional to the integral of δC_p^{exc} (Takahashi & Sturtevant, 1981; Filimonov *et al.*, 1982). Such an approximation seems to be very reasonable and will result in a relatively correct estimation of the δC_p^{exc} whenever the following restrictions are fulfilled:

$$\delta C_{p,max}^{int} \ll \delta C_{p,max}^{exc} \quad (12)$$

$$\Delta C_{p,i} \approx k\,\Delta H_i \quad (13)$$

where k is the same constant for all the possible macroscopic states of the protein. Since the first condition is usually valid for proteins with relatively high enthalpy of unfolding (>300 kJ/mol), the error in evaluation of δC_p^{exc} introduced by such approximate estimation of δC_p^{int} is negligible, and δC_p^{exc} is useful for the calculation of T_m and of the overall heat effect. However, the applicability of this simple algorithm to the more detailed thermodynamic analysis, e.g., for simply checking the two-state model validity, is very questionable when conditions 12 and 13 are not valid or ΔC_p of unfolding depends on temperature.

It seems that in general, and in particular in those cases when the heat effects of unfolding are small, the most correct approach to the calorimetric data analysis is to perform the global fitting of the data to some reasonable model, which will impose the restrictions on the variable parameters and reduce

the fitting uncertainty (Filimonov *et al.*, 1982). For example, for SH3 one can assume that

$$C_{p,0}(T) = a_0 + b_0(T - T_0) \quad (14)$$

where a_0 is the partial molar heat capacity of the native protein at some temperature $T = T_0$ and b_0 is the slope. Then, by analyzing the initial parts of all the experimentally accumulated molar heat capacity functions, rather strict constraints on the values of a_0 and b_0 can be deduced. A similar procedure might be used to impose constraints on the $C_{p,u}$ and, as a result, on the δC_p^{int} function. In addition, the heat capacity of the unfolded state can be estimated with the method suggested by Makhatadze and Privalov (1990) and Privalov and Makhatadze (1990).

In our analysis we have performed a direct global fitting of the C_p curves to a two-state model under the assumption of the linearity of $C_{p,0}$ and the variability of $\Delta C_{p,u}$. The latter was presented as $f(T) = a + bT + cT^2$ since, as it will be shown later, a first-order polynomial cannot adequately describe the heat capacity of the unfolded state, $C_{p,u}$.

For a two-state monomolecular process we can write

$$N \overset{K_u}{\rightleftharpoons} U \quad (15)$$

$$K_u = [U]/[N] = f_u/f_n \quad (16)$$

$$f_n + f_u = 1 \quad (17)$$

where N and U stand for the native and unfolded states, f_n and f_u for their fractions, and K_u for the monomolecular equilibrium constant.

Then for excess heat capacity we have

$$\langle \Delta C_{p,0} \rangle = \delta C_p^{int} + \delta C_p^{exc} = \Delta C_{p,u} f_u + \Delta H_u \, df_u/dT \quad (18)$$

Here $\Delta H_u(T)$ and $\Delta C_{p,u}(T)$ are the enthalpy and the heat capacity increments of unfolding. Introducing T_m as the temperature where at given solvent conditions $K_u(T_m) = 1$ and taking into account that

$$d\Delta H_u/dT = \Delta C_{p,u} \quad (19)$$

and that $\Delta C_{p,u}$ is a parabolic function

$$\Delta C_{p,u}(T) = a + bT + cT^2 \quad (20)$$

we get for the enthalpy

$$\langle \Delta H_u(T) \rangle = \Delta H_u(T_m) + a(T - T_m) + [b(T^2 - T_m^2)/2] + [c(T^3 - T_m^3)/3] \quad (21)$$

In a similar way, since

$$d\Delta S_u/dT = \Delta C_{p,u}/T \quad (22)$$

one can find ΔS_u, ΔG_u, and K_u as temperature functions. Finally

$$\delta C_p^{int} = \Delta C_{p,u} K_u/(1 + K_u) \quad (23)$$

$$\delta C_p^{exc} = \frac{\Delta H_u^2}{RT^2} \frac{K_u}{(1 + K_u)^2} \quad (24)$$

Kinetic Analysis. Kinetics were followed in a Biologic stopped-flow machine both by fluorescence and by circular dichroism. For fluorescence experiments the unfolding reaction was performed by dilution of the native SH3 domain in 50 mM citric acid, pH 3.5, with the appropriate ratio of denaturating buffer containing different concentrations of urea in 50 mM citric acid, pH 3.5. For the refolding reaction, the unfolded domain in 50 mM citric acid, pH 3.5, containing 7.5 and 9 M urea, was mixed with an excess of the same buffer without urea to give various final urea concentrations. Fluorescence was measured through a 320-nm cutoff filter (excitation at 290 nm). In the CD refolding experiments the buffer used was 5 mM citric acid, pH 3.5. The CD signal was followed at 235 nm. In all the experiments the pH of the buffer containing the urea solution was adjusted to pH 3.5 with hydrochloric acid. The cell chamber and the syringes were kept at 298 K.

RESULTS

Chemical Denaturation Followed by Circular Dichroism and Fluorescence Spectroscopy. (*a*) *Fluorescence Spectroscopy.* In Figure 1 we show the chemical denaturation by urea (top) of the SH3 domain followed by fluorescence. At pH 3.5 the values for ΔG_{H_2O} and m are 12 ± 0.2 kJ mol^{-1} and 3.1 ± 0.03 kJ mol^{-1} M^{-1}, respectively, depending on the slope of the effect of urea on the denatured state. The stability of the protein decreases at lower pH values and increases at higher pH values. However, it is not possible to quantify the data with reasonable accuracy, due to the lack of points for the native (low pH) or denatured state (high pH) (Figure 1, top). In the case of Gdn·HCl denaturation, there is a sharp dependence of the native fluorescence on the Gdn·HCl concentration (data not shown). This dependency precludes any quantitative analysis at pHs below or equal to 3.5. Only between pH 5.0 and 7.0 is it possible to estimate ΔG_{H_2O} and m with reasonable accuracy. Between these two pHs the values for ΔG_{H_2O} and m are 15.5 ± 1.3 kJ mol^{-1} and 7.85 ± 0.5 kJ mol^{-1} M^{-1}, respectively.

(*b*) *Circular Dichroism.* Tryptophan fluorescence seems to be dependent on very local changes in its environment. In order to test if the transition monitored by fluorescence reflected a total disruption of the overall structure of the domain, or just a local unfolding, we analyzed the chemical denaturation of SH3 by urea at pH 3.5. The SH3 far UV CD spectrum is a complex one (Figure 2, top). It presents two minima at 228 and 203 nm and two maxima at 220 and 235 nm. Upon urea denaturation the overall spectrum flattens, although the spectrum could only be registered down to 220 nm because of the high urea absorbance below this value. For this reason we have chosen 235 nm to follow urea denaturation (Figure 2, bottom). An increase in the negative ellipticity is observed upon urea addition. The fitting of ellipticity data at 235 nm to eq 3 gives ΔG_{H_2O} = 12 ± 0.1 kJ mol^{-1} and m = 3.2 ± 0.06 kJ mol^{-1} M^{-1}.

(*c*) *Thermal Denaturation Followed by Fluorescence.* It is not possible to perform an accurate analysis of the thermal denaturation of the SH3 demain at pH 7.0, due to the high midpoint of the thermal denaturation (Figure 1, bottom). At pH 3.5 the midpoint of the thermal denaturation is good enough to obtain an accurate extrapolation of the fluorescence of the native and denatured states. The T_m of the thermal denaturation was found to be 333 ± 6 K. The $\Delta H_u(T_m)$ of the thermal denaturation at pH 3.5 was calculated from a van't Hoff plot (ln K_u vs $1/T$) (data not shown) and was found to be 196 ± 3 kJ mol^{-1}. Applying eqs 6–9, and using the ΔC_p

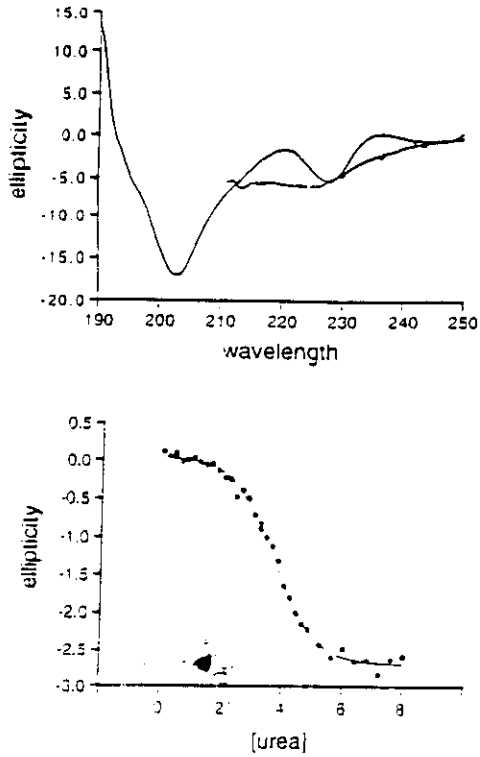

FIGURE 2: Circular dichroism spectra of native and denatured SH3 domain and chemical denaturation profiles of spectrin SH3 domain. (Top) CD spectra at 298 K of different conformations of SH3. Native SH3 in 5 mM citric acid, pH 3.5 (—); unfolded SH3 in 5 mM citric acid, pH 3.5, and 8 M urea (○). (Bottom) Urea denaturation of the SH3 domain in 5 mM citric acid, pH 3.5, at 298 K, followed by changes in the circular dichroism signal at 235 nm.

value at 298 K (3.9 kJ deg^{-1} mol^{-1}) obtained from the calorimetric analysis (see below), we find a value for ΔG_{H_2O} of 13 ± 3 kJ mol^{-1}, which is within experimental error similar to that determined by chemical denaturation.

Differential Scanning Calorimetry. In acidic solutions with pH between 2 and 3.5 and at low ionic strength, the thermal unfolding of SH3 fragment is almost 100% reversible. In other words, the first and the second records of the heat capacity of the protein solutions were indistinguishable within the limits of experimental error. At pH 3.5 and 4.0 the reversibility of unfolding started to decrease, but the recovery was still reasonably high (about 70%) even after heating the samples up to 383 K. Such a decrease in reversibility was expected since the solubility of the native protein also decreases above pH 4 (Musacchio *et al.*, 1992b).

Due to the small size of SH3 its overall molar heat effect of unfolding is not large, i.e., the C_p peaks are small and broad (see Figure 3), which complicates an accurate evaluation of the thermodynamic parameters. To get reliable records of C_p we had to work at relatively high protein concentration (up to 5 mg/mL); nevertheless, neither concentration nor heating rate dependence of the heat capacity was observed. It was concluded, therefore, that under our experimental conditions of low pH and low ionic strength the SH3 unfolding in the calorimeter cell occurs at equilibrium. Careful consideration of the curves presented in Figure 3 reveals two important factors for the data analysis and evaluation of thermodynamic parameters. First, it is seen that the heat capacity of the native SH3 increases with temperature in full agreement with the known behavior of globular proteins (Privalov, 1979; Filimonov *et al.*, 1982; Privalov & Potekhin, 1986). At the same time, the heat capacity of the unfolded state under our

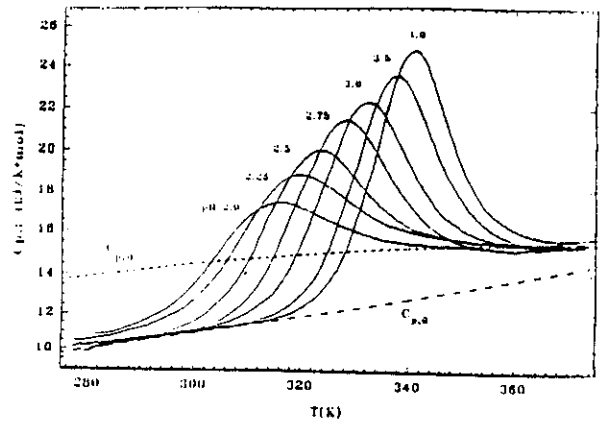

FIGURE 3: Temperature dependence of the molar partial heat capacity of the SH3 at acidic pH (—). The dashed lines show average temperature dependencies of $C_{p,0}$ (– – –) and $C_{p,u}$ (- - -), as found by the global curve-fitting procedure (for the parameters see text). The average value of $C_{p,0}$ at 293 K is equal to 10.5 ± 0.8 kJ K^{-1} mol^{-1}. pH values are shown on top of the curves.

experimental conditions is much less dependent on temperature, at least above 340 K. If the initial state corresponds to the monomer of the native protein and the final state corresponds to the monomer of the unfolded molecule, such a difference in C_p slopes should mean that the ΔC_p of unfolding is not constant and changes with temperature. A similar effect was first pointed out by Takahashi and Sturtevant (1981) and later analyzed and explained by Privalov and co-workers (Privalov *et al.*, 1989; Makhatadze & Privalov, 1990; Privalov & Makhatadze, 1990), who have shown that, in general, the $\Delta C_{p,u}$ (the heat capacity increment of unfolding) of globular proteins depends on temperature. It seems, however, that most of the enthalpy values in the literature are correct within the limits of experimental error, despite the fact that, most frequently, the calorimetric data for globular proteins used to be analyzed under the simplified assumption of a constant ΔC_p (Privalov, 1979) (see Experimental Procedures).

The calculated function $C_{p,u}$ for SH3 fragment is shown in Figure 5. Since the data on partial heat capacities of the elements of protein chemical structure are available only for a few temperatures (Makhatadze & Privalov, 1990), an analytical expression for $C_{p,u}(T)$ was found as a second-order least-square regression through the six calculated data points:

$$C_{p,u}(T) = -9.42 + 0.1366T - 0.0001795T^2 \quad \text{(kJ K}^{-1}\text{ mol}^{-1}\text{)} \tag{25}$$

or after introducing T_0 = 293 K

$$C_{p,u}(T) = 15.2 + 0.137(T - T_0) - 0.0001795(T^2 - T_0^2) \tag{26}$$

For the same T_0, the average values of a_0 and b_0 in function (10) turned out to be equal to 10.5 kJ K^{-1} mol^{-1} and 0.047 kJ K^{-2} mol^{-1} respectively. Thus for the estimated $\Delta C_{p,u}(T)$ function (Figure 4) we have

$$\begin{aligned}\Delta C_{p,u}(T) &= (a - a_0) + (b - b_0)(T - T_0) + c\,(T^2 - T_0^2) \\ &= \Delta a + \Delta b(T - T_0) + c(T^2 - T_0^2) \qquad (27) \\ &= 4.7 + 0.090(T - T_0) - \\ &\qquad (1.795 \times 10^{-4})(T^2 - T_0^2)\end{aligned}$$

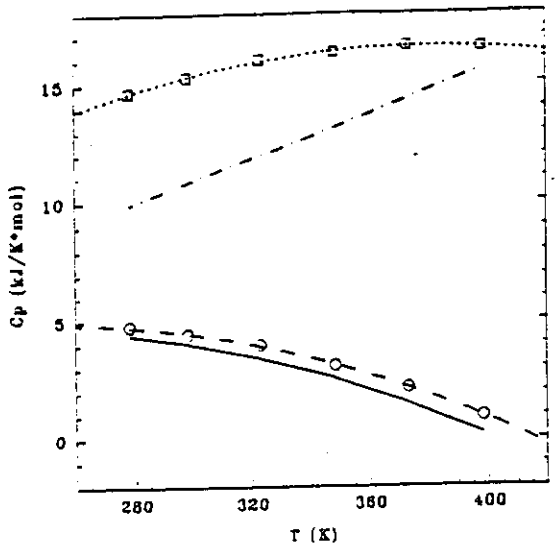

FIGURE 4: Temperature dependencies of the molar heat capacities of SH3. The temperature dependencies of the molar heat capacities of the SH3 in the native state, $C_{p,0}$ (---), were found by global fitting of experimental data, and in the unfolded state, $C_{p,u}$ (□) was calculated according to Privalov et al. (1989), Makhatadze & Privalov (1990). Their difference, $\Delta C_{p,u}^{calc}$, is plotted with (○), while the solid line shows $\Delta C_{p,u}(T)$ found by global fitting of the experimental data.

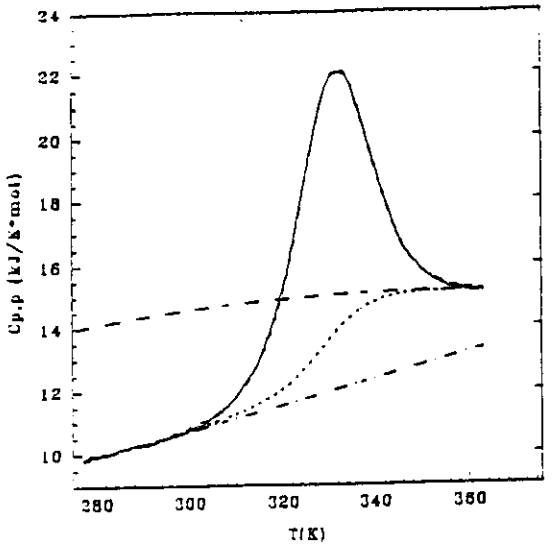

FIGURE 5: Best fit of the experimental temperature dependence of the partial molar heat capacity of SH3 at pH 3.0. The best fit (– – –) of the experimental temperature dependence of the partial molar heat capacity (—) recorded at heating rate 1 K min^{-1} and total protein concentration of 2 mg/mL. The best-fit parameters for this experiment were T_m = 329.7 K; $\Delta H_u(T_m)$ = 176 kJ/mol; $C_{p,0}(T)$ = 10.4 + 0.044(T – 293) (---); $\Delta C_{p,u}(T)$ = –5.95 + 0.087T – (1.795 × 10^{-4})T^2. $C_{p,u} = C_{p,0} + \Delta C_{p,u}$ is shown with (— — —) and δC_p^{int} with (- - -).

In some of our direct global fittings only Δa was allowed to vary. In others b_0 and Δb were also allowed to vary, while c was always kept constant. There are two reasons for unfreezing b_0. First, since only small regions of $C_{p,0}$ could be registered in the case of SH3 (Figure 3), the scatter of b_0 around an average value of 0.047 kJ K^{-2} mol^{-1} was rather high, namely, about 12%. Second, at pH below 2.25 (see Figure 3) even at 280 K about 10% of the protein is already in the unfolded state. Of course, in such a case $C_{p,0}$ is unknown to us and both a_0 and b_0 had to be adjusted.

The typical example of the curve fitting is shown in Figure 5 where the best-fit parameters are listed in the figure legend. In addition to Δa, Δb, and b_0, the fitting gave us the values of T_m and $\Delta H_u(T_m)$, which are shown in Table 1 and plotted in Figure 6 together with the polynomial regression through these points.

It is seen that the dependence of $\Delta H_u(T_m)$ on T_m in the experimentally accessible temperature range fits very well to the linear regression line with the slope of 3.4 ± 0.1 kJ K^{-1} mol^{-1}, despite the fact that in reality $\Delta C_{p,u}$ varies between 3.7 kJ K^{-1} mol^{-1} at pH 2.0 (T_m = 307 K) and 2.8 kJ K^{-1} mol^{-1} at pH 4.0 (T_m = 339 K) (Figure 7). For this reason, $\Delta H_m(T_m)$ points fit better to function 21, although the quality of fitting is not drastically increased. The difference between the two regressions becomes remarkable only below and, in particular, above the experimentally attainable range of T_m. A similar paradox was observed by Privalov and co-workers for some other globular proteins (Privalov *et al.*, 1989).

The global fitting with variable Δa and b_0 introduced some corrections into the $C_{p,u}(T)$ function in comparison with the calculated one (see Figure 4). The experimentally observed heat capacity of the unfolded state is on average about 0.7 kJ K^{-1} mol^{-1} lower than the estimated one. This is a very good agreement, taking into consideration the fact that in the case of SH3 the absolute value of the partial heat capacity of the protein was determined with a precision of about 0.8 kJ K^{-1} mol^{-1}.

The thermodynamic parameters derived from the global calorimetric analysis are shown in Table 1.

Table 1: Thermodynamic[a] Parameters of SH3 Fragment Unfolding at Acidic pH and Low Ionic Strength

pH	T_m (K)	$\Delta H_u(T_m)$ (kJ mol^{-1})	$\Delta G_u(298)$ (kJ mol^{-1})	$\Delta C_{p,u}(T_m)$ (kJ K^{-1} mol^{-1})
2.0	307	93	2.3	3.7
2.25	313	114	4.2	3.6
2.5	320	139	6.9	3.4
2.75	327	162	9.8	3.2
3.0	331	174	11.6	3.0
3.5	336	188	13.9	2.9
4.0	339	197	15.6	2.8

[a] The thermodynamic parameters derived from the calorimeter model are shown. The error is around 8% for $\Delta H_u(T_m)$ and $\Delta C_{p,u}(T_m)$, 20% for ΔG_u, and around 0.7 K for T_m.

Kinetic Analysis of the Folding and Unfolding Reactions of the SH3 Domain. It has been found that in many proteins in which an intermediate in equilibrium conditions is not found, the kinetic analysis of the refolding reaction shows unequivocally the presence of an intermediate (Matouschek *et al.*, 1992). In order to see if we could detect a kinetic intermediate in the refolding of the SH3 domain, we performed a kinetic analysis at pH 3.5. The results of this analysis are shown in Figure 7. As expected for an unfolding reaction in which the strong denaturation conditions preclude the accumulation of an intermediate (Matouschek et al., 1990), there is a linear dependence of the logarithm of the rate constant of unfolding (k_U) with urea. In the refolding reaction two main transitions are observed: a fast transition, completed in less than 5 s, and a slow one with a kinetic constant of 0.0176 ± 0.0023 s^{-1}, which is independent of the urea concentration (data not shown). Contrary to what has been found in many other proteins (Ikeguchi *et al.*, 1986; Kuwajima *et al.*, 1988; Matouschek *et al.*, 1990), the logarithm of the rate constant of refolding (k_F), versus urea, can be fitted to a linear equation. Folding kinetics have also been followed by circular dichroism at 235 nm. Points are totally superimposable with those obtained by fluorescence (Figure 7). This indicates a concomitant recovery of both secondary and tertiary structure

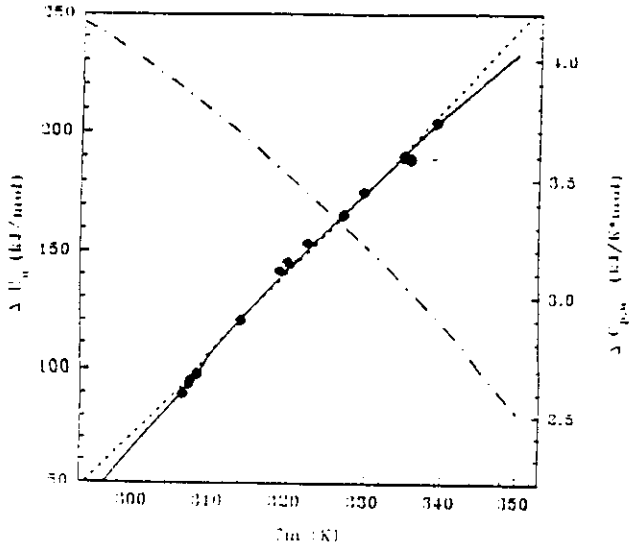

FIGURE 6: Plot of $\Delta H_u(T_m)$ versus T_m. The plot of $\Delta H_u(T_m)$ *versus* T_m as found from the global fitting of the DSC curves for SH3 at acidic pH (●, left axis) is shown. The solid line shows the parabolic function $\Delta H_u(T)$ corresponding to $\Delta C_{p,u} = -5.95 + 0.087T - (1.795 \times 10^{-4})T^2$ (---, right axis), while (- - -) corresponds to the linear regression through the points with the slope of 3.4 kJ K^{-1} mol^{-1}.

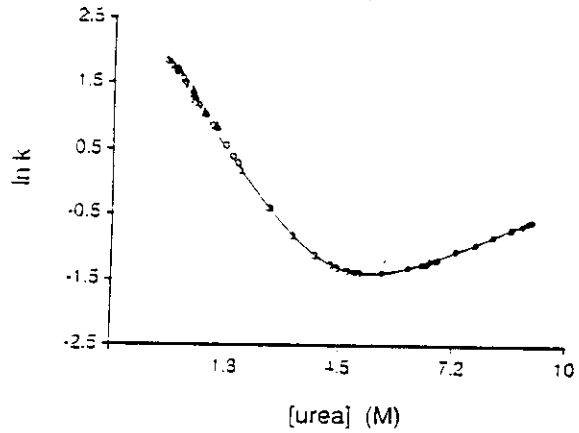

FIGURE 7: Kinetics of unfolding and refolding. Urea concentration dependence of the natural logarithm of the rate constants for refolding and unfolding is shown. The unfolding or refolding reactions were initiated by an urea concentration jump in a stopped-flow machine equilibrated at 298 K. The buffer used for fluorescence measurements was 50 mM citric acid, or 5 mM in the case of CD measurements, at pH 3.5. (○) Refolding experiments followed by fluorescence. (▲) Refolding experiments followed by CD. In this case it was not possible to do the experiments at high urea concentrations due to signal to noise ratio problems. (●) Unfolding experiments followed by fluorescence. The solid curve is the best fit of the whole set of data to eq 28.

upon diluting into refolding buffer. Values within the transition region obtained by either unfolding or refolding experiments were indistinguishable. The whole reaction can be fitted to the following equation (Jackson & Fersht, 1991):

$$\ln k = \ln [k_{f,H_2O} \exp(-m_{kf}[\text{urea}]) + k_{u,H_2O} \exp(-m_{ku}[\text{urea}])] \quad (28)$$

where k is the rate constant at a given concentration of denaturant, k_{f,H_2O} is the rate constant of refolding in water and k_{u,H_2O} is the rate constant of unfolding in water, and m_{kf} and m_{ku} are the slopes of the refolding and unfolding reactions, respectively. The kinetic parameters calculated from this equation are as follows: $k_{f,H_2O} = 8.14 \pm 0.08$ s^{-1}, $k_{u,H_2O} = 0.045 \pm 0.002$ s^{-1}, $m_{kf} = 4 \pm 0.03$ kJ mol^{-1} M^{-1}, and $m_{ku} = -1.14 \pm 0.03$ kJ mol^{-1} M^{-1}.

The spectrin SH3 domain has two proline residues in a *trans* conformation, in the native state. The relative amount of *cis* and *trans* conformation in the unfolded state could, in principle, be calculated by the relative amplitudes of the fast and slow kinetic phases of refolding, as long as the isomerization takes place in the unfolded state. For spectrin SH3 the slow phase of refolding accounts for 4% ± 1% of the total amplitude of fluorescence recovery. This number is small compared with other proteins of similar size with the same number of *trans* prolines (Jackson & Fersht, 1991) and could indicate that the isomerization of at least one of the prolines takes place in a folded conformation.

The values of the free energy of unfolding ΔG_{H_2O} and the constant m, which reflects the cooperativity of the transition, can be estimated from the above parameters, considering the following equilibrium:

$$\text{Uc} \underset{}{\overset{K_{iso}}{\rightleftharpoons}} \text{Ut} \underset{k_{u,H_2O}}{\overset{k_{f,H_2O}}{\rightleftharpoons}} \text{N} \quad (29)$$

K_{iso} is defined as the ratio between the amount of protein in the *cis* and *trans* conformation in the unfolded state. When the native conformation of the proline residues is a *trans* conformation, then the contribution of the *cis–trans* isomerization to the free energy of unfolding is negligible (Jackson & Fersht, 1991) and we can obtain a reasonable estimation of ΔG_{H_2O} from the second equilibrium using

$$\Delta G_{H_2O} = -RT \ln (k_{f,H_2O}/k_{u,H_2O}) \quad (30)$$

$$m = m_{kf} + m_{ku} \quad (31)$$

then $\Delta G_{H_2O} = 12.9$ kJ mol^{-1} and $m = 2.9 \pm 0.06$ kJ mol^{-1} M^{-1}.

DISCUSSION

Criteria for a Two-State Transition. For the equilibrium denaturation of a protein to be described as a two-state process, several criteria must be fulfilled by the protein: (i) the unfolding of the protein by a denaturant agent must fit to a single transition curve and must be independent of the probe used to monitor it, (ii) the DSC unfolding endotherm must fit the $C_p(T)$ function corresponding to the two-state model, and (iii) the fitting of the logarithm of the rate constant of unfolding and refolding, with urea must be linear and the values for ΔG_{H_2O} and m obtained from equilibrium and kinetics must be identical within experimental error. This third criterion is in many cases the most sensitive of the three criteria for the detection of transient intermediates (Jackson & Fersht, 1991).

The equilibrium denaturation of SH3, by urea at pH 3.5, fits a single transition curve and within experimental error seems to be independent of the probe used to monitor it (fluorescence of CD). Differential scanning calorimetry analysis of the protein at different pHs, although somehow complicated because of the dependency of $\Delta C_{p,u}$ on temperature, indicates that the denaturation of this domain follows a two-state transition. The ratio between the van't Hoff's to calorimetric enthalpy is 1.03 ± 0.08, which is within the range of 1.00 ± 0.05 observed for the two-state denaturation of several globular proteins (Privalov, 1979). Kinetic analysis of the folding and unfolding reactions, followed by CD or fluorescence, clearly indicates that there is no intermediate accumulating at low urea concentrations. Also, the values for ΔG_{H_2O} and m obtained from equilibrium chemical denaturation, thermal denaturation, calorimetry, and kinetics

Table 2: Comparison of the Thermodynamic Unfolding Values of SH3 Obtained from Chemical and Temperature Denaturation, Differential Scanning Calorimetry, and Kinetics at pH 3.5 and 298 K

method	ΔG_{H_2O} (kJ mol^{-1})	m (kJ mol^{-1} M^{-1})	T_m (K)	$\Delta H_u(T_m)$ (kJ mol^{-1})
DSC[a]	14 ± 3.0		336 ± 0.8	188 ± 15
temp[b]	13 ± 3.0		333 ± 6	196 ± 3
fluorescence[c]	12 ± 0.2	3.1 ± 0.03		
CD[d]	12 ± 0.1	3.2 ± 0.06		
kinetics[e]	13 ± 0.7	2.9 ± 0.06		

[a] Differential scanning calorimetry. [b] Temperature denaturation followed by fluorescence. [c] Urea chemical denaturation followed by fluorescence. [d] Urea chemical denaturation followed by circular dichroism. [e] Kinetics of urea-induced unfolding and refolding.

are identical within experimental error (Table 2). Therefore, from the equilibrium and kinetic points of view the two-state model applies for the SH3 folding–unfolding reaction. Intermediates of folding in this case should be transient ones, whose energy is indistinguishable from the transition state.

SH3 Stability. The thermodynamic parameters obtained from the equilibrium, kinetic, and calorimetric analysis indicate that the free energy of unfolding of SH3 at pH 3.5 and 298 K must be around 13 kJ mol^{-1} with a value of m around 3.1 kJ mol^{-1}. The stability of the protein at this pH is rather low compared with the majority of the globular proteins. However, we must take into account that this is not the optimal pH for maximum stability of this domain. This optimal pH, which lies between pH 5.0 and 8.0, cannot be used for calorimetry analysis due to the low solubility that this protein has above pH 4.0 at concentrations higher than 1 mg/mL (Musacchio *et al.*, 1992b). Analysis of the stability of this domain between pH 5.0 and 7.0, by Gdn·HCl denaturation, indicates that the stability of the protein is around 15.5 ± 1.3 kJ mol^{-1} with a m value of 7.82 ± 0.5 kJ mol^{-1} M^{-1}. This value for ΔG at pH 7.0, which could be lower than the real value by 10–15% due to the different ways in which urea and Gdn·HCl interact with the protein (Makhatadze & Privalov, 1992), is relatively low for a monomeric globular protein. It has been found for other small monomeric proteins of similar size that the free energy of unfolding at 298 K is around 25–29 kJ mol^{-1} (Jackson & Fersht, 1991; Alexander *et al.*, 1992a). On the other hand this small value is not surprising, taking into account the fact that SH3 is a protein domain and not a monomeric protein. Consequently, it is reasonable to think that interactions with other domains of the protein will stabilize it. The m value is proportional to the average exposure of residues on denaturation. This value is around 10.9–18.8 kJ mol^{-1} M^{-1} for monomeric proteins with 100–150 amino acids, denatured by Gdn·HCl (Pace *et al.*, 1974; Greene & Pace, 1974; Kellis *et al.*, 1989). On the other hand, our m value is quite similar to the value found for the chymotrypsin inhibitor CI2 (7.8 kJ mol^{-1} M^{-1}), which has structured core of 60 amino acids (Jackson & Fersht, 1991).

From the calorimetry point of view, the SH3 domain seems to be an ordinary representative of the small, single-domain globular proteins despite its small molecular weight. Thus the specific heat capacity of the native state at 293 K, 1.47 ± 0.13 J K^{-1} g^{-1}, its temperature dependence, (6.7 ± 1.7) × 10^{-3} J K^{-2} g^{-1}, the specific denaturation enthalpy at the corresponding T_m (e.g., 26.3 ± 2 J g^{-1} at 336 K), and the average specific heat capacity change on denaturation (0.47 ± 0.04 J K^{-1} g^{-1}) all compare very well with what has been described for compact globular proteins (Privalov, 1979; Privalov & Khechinashvili, 1974). In addition, the ΔH_u (mol of amino acid residue)$^{-1}$ reaches a value of 5.2 ± 0.4 kJ (mol of amino acid)$^{-1}$ when $\Delta C_{p,u}$ equals zero, which is close to the values recently found for the ΔH of unfolding of globular proteins at high temperature (Privalov *et al.*, 1989; Privalov & Makhatadze, 1990). For the members of this protein family there is a correlation between $\Delta H_u(298)$ and $\Delta C_{p,u}(298)$, as was pointed out by Murphy *et al.* (1992) (it should be mentioned, however, that these authors used the average values of $\Delta C_{p,u}$ for all proteins). The values found by us for SH3 [$\Delta H_u(298)$ = 917 J (mol of residue)$^{-1}$ and $\Delta C_{p,u}(298)$ = 62 J K^{-1} (mol of amino acid)$^{-1}$] fit rather well to that correlation if the actual value of $\Delta C_{p,u}(298)$ = 3.9 kJ K^{-1} mol^{-1} is taken instead of the average value of 3.4 kJ K^{-1} mol^{-1} (data not shown).

SH3 Folding. As discussed above, the kinetic analysis of protein folding seems to be very sensitive to the presence of kinetic intermediates. In the majority of monomeric domain proteins in which this analysis has been carried out, a significant deviation of linearity has been found which is attributed to the accumulation of a folding intermediate (Ikeguchi *et al.*, 1986; Kuwajima *et al.*, 1988; Matouschek et al., 1990; Schreiber & Fersht, 1993). At least in the last two cases, this intermediate is not due to any *cis–trans* prolyl isomerization. However, in two small monomeric proteins of similar size to the SH3 domain, the CI2 chymotrypsin inhibitor (Jackson & Fersht, 1991) and the G-domain (Alexander *et al.*, 1992b), no intermediate was found to accumulate in the refolding reaction. In the SH3 domain we find the same phenomena for those molecules which in the unfolded state contained the two prolines in the native conformation. It is possible that the slow phase we detected could be due to the isomerization of any of the two prolines in a folded nonnative structure. This will count, in a strict sense, as a folding intermediate. Although the *cis–trans* intermediates are well-known in the literature, the intermediates we are seeking are those accumulating in the folding reactions of unfolded proteins with all the prolines in the native conformation (Matouschek *et al.*, 1989; Schreiber & Fersht, 1993). Our data clearly demonstrate that these intermediates do not accumulate significantly in the refolding reaction of SH3.

Kinetic analysis using quench-flow of a large β-sheet barrel protein, interleukin 1β, has revealed the presence of a kinetic intermediate. It has been suggested, on the basis of this study, that the formation of the β-sheet in β-sheet proteins follows a different folding pathway compared to the formation of the β-sheet in α/β mixed proteins (Varley *et al.*, 1993). In this study it was found that folding to the native structure involves the rapid formation of a β-structure around a hydrophobic core, followed by a slow stabilization of the secondary structure. However, the kinetic analysis by CD and fluorescence of the SH3 domain indicates that this is not the case for all β-sheet proteins.

It is now generally believed that there must be kinetic intermediates in the folding pathway of proteins [for a review see Kim and Baldwin (1990)]. In the case of the CI2 protein, the G-domain, and the SH3 domain, no intermediate can be seen to accumulate. These proteins have in common that they have a very small core within the limits of what has been postulated to be a stable folding domain without disulfide bridges (Privalov & Gill, 1988). On the other hand, their fold is very different. In the case of CI2 (McPhalen & James, 1987) and the G-domain (Lyan *et al.*, 1991; Gornenborn *et al.*, 1991; Orban *et al.*, 1992), there is an α-helix packing against a β-sheet, while in the SH3 domain there is only a β-sheet barrel (Musacchio *et al.*, 1992b). It is puzzling that the only three proteins for which a kinetic intermediate has

not been found to accumulate correspond to proteins which have a globular unit of around 60 residues. Although more proteins of this size should be studied, it is tempting to speculate that only in those proteins for which the size imposes the existence of one or more large hydrophobic cores, or two or more subdomains, will there be kinetic intermediates that will accumulate in the folding pathway, whereas in one-domain proteins with a single small hydrophobic core, the acquisition of secondary structure will be simultaneous with that of the tertiary structure.

CONCLUSIONS

In summary, SH3 represents a very good model for protein folding due to the simplicity of its mechanism, following a pure two-state transition. In addition, the coincidence of Gibbs energy of unfolding from all the methods used, urea and calorimetry, suggest that the final denatured state reached by both methods is energetically the same, and so it is expected to be a fully denatured state. The differential scanning calorimetry of the spectra SH3 domain requires $\Delta C_{p,u}$ to be temperature-dependent in order to carry out an appropriate calorimetric data analysis. This agrees with earlier findings and shows that only under certain conditions would the use of a constant $\Delta C_{p,u}$ lead to the same results within experimental uncertainty.

ACKNOWLEDGMENT

We are very grateful to Dr. M. Saraste and A. Musacchio for the generous gift of the pET3d plasmid used for the expression of the spectrin SH3 domain. We are also grateful to Dr. Cònejero-Lara for helpful discussion.

REFERENCES

Alexander, P., Fahnestock, S., Lee, T., Orban, J., & Bryan, P. (1992a) *Biochemistry 31*, 3597.
Alexander, P., Orban, J., & Bryan, P. (1992b) *Biochemistry 31*, 7243.
Booker, G. W., Gout, I., Downing, A. K., Driscoll, P. C., Boyd, J., Waterfield, M. D., & Campbell, I. D. (1993) *Cell 73*, 813.
Briggs, M., & Roder, H. (1992) *Proc. Natl. Acad. Sci. U.S.A. 89*, 2017.
Fahnestock, S. R., Alexander, P., Nagle, J., & Filpula, D. (1986) *J. Bacteriol. 167*, 870.
Filimonov, V. V., Potekhin, S. A., Matveyev, S. V., & Privalov, P. L. (1982) *Mol. Biol. (USSR) 16*, 435.
Gill, S. C., & von Hippel, P. H. (1989) *Anal. Biochem. 182*, 319.
Griko, Yu. V., Privalov, P. L., Venyaminov, S. Yu., & Kutyshenko, V. P. (1988) *J. Mol. Biol. 202*, 127.
Gronenborn, A. M., Filpula, D. R., Essig, N. Z., Acahri, A., Whitlow, M., Wingfield, P. T., & Clore, G. M. (1991) *Science 253*, 657.
Ikeguchi, M., Kuwajima, K., Mitani, M., & Sugai, S. (1986) *Biochemistry 25*, 6956.
Jackson, S. E., & Fersht, A. R. (1991a) *Biochemistry 30*, 10443.
Kellis, J. T., Nyberg, K., & Fersht, A. R. (1989) *Biochemistry 28*, 4914.
Khechinashvili, N. N. (1989) *J. Mol. Biol. 205*, 737.
Kohda, D., Hatanaka, H., Odaka, M., Madiyan, V., Ullrich, A., Schlessinger, J., & Inagaki, F. (1993) *Cell 72*, 953.
Koyama, S., Yu, H., Dalgarno, D. C., Shin, T. B., Zydowsky, L. D., & Schreiber, S. L. (1993) *FEBS Lett. 324*(1), 93.
Kuwajima, K., Sakuraoka, A., Fueki, S., Yoneyama, M., & Sugai, S. (1988) *Biochemistry 27*, 7419.
Lian, L. Y., Yang, J. C., Derrick, J. P., Sutcliffe, M. J., Roberts, G. C. K., Murphy, J. P., Goward, C. R., & Atkinson, T. (1991) *Biochemistry 30*, 5335.
Lu, J., & Dahlquist, F. W. (1992) *Biochemistry 31*, 4749.
Makhatadze, G. I., & Privalov, P. L. (1990) *J. Mol. Biol. 213*, 375.
Makhatadze, G. I., & Privalov, P. L. (1992) *J. Mol. Biol. 226*, 491.
Mann, C. J., & Matthews, C. R. (1993) *Biochemistry 32*, 5282.
Matouschek, A., Serrano, L., & Fersht, A. R. (1992) *J. Mol. Biol. 224*, 819.
McPhalen, C. A., & James, M. N. G. (1987) *Biochemistry 26*, 261.
Murphy, K. P., Bhakuni, V., Xie, D., & Freire, E. (1992) *J. Mol. Biol. 227*, 293.
Musacchio, A., Gibson, T., Lehto, V.-P., & Saraste, M. (1992a) *FEBS Lett. 307*, 55.
Musacchio, A., Noble, M. E. M., Pautit, R., Wierenga, R., & Saraste, M. (1992b) *Nature 359*, 851.
Noble, M. E. M., Musacchio, A., Saraste, M., Courtneidge, S. A., & Wierenga, R. K. (1993) *EMBO J. 12* (7), 2617.
Orban, J., Alexander, P., & Bryan, P. (1992) *Biochemistry 31*, 3604.
Pace, C. N. (1986) *Methods Enzymol. 131*, 226.
Pace, C. N., Laurents, D. V., & Thomson, J. A. (1990) *Biochemistry 29*, 2564.
Pace, C. N., Laurents, D. V., & Erickson, R. E. (1992) *Biochemistry 31*, 2728.
Privalov, P. L. (1979) *Adv. Protein Chem. 33*, 167.
Privalov, P. L., & Khechinashvili, N. N. (1974) J. Mol. Biol. *86*, 665.
Privalov, P. L., & Potekhin, S. A. (1986) in *Methods in Enzymology*, Vol. 131, p 4, Academic Press, New York.
Privalov, P. L., & Gill, S. J. (1988) *Adv. Protein Chem. 39*, 191.
Privalov, P. L., & Makhatadze, G. I. (1990) *J. Mol. Biol. 213*, 285.
Privalov, P. L., Tiktopulo, E. I., Venyaminov, S. Yu, Griko, Yu. V., Makhatadze, G. I. Radford, S. E., Dobson, C. P., & Evans, A. P. (1992) *Nature 358*, 302.
Schreiber, G., & Fersht, A. R. (1993) *Biochemistry 32*, 11195.
Serrano, L., Matouschek, A., & Fersht, A. R. (1992) *J. Mol. Biol. 224*, 847.
Takahashi, K., & Sturtevant, J. M. (1981) *Biochemistry 20*, 6185.
Udgaonkar, J. B., & Baldwin, R. L. (1988) *Nature 335*, 694.
Varley, P., Gronenborn, A. M., Christense, H., Wingfield, P. T., Pain, R. H., & Clore, G. M. (1993) *Science 260*, 1110.
Yu, H., Rosen, M. K., & Schreiber, S. L. (1993) *FEBS Lett. 324*, 87.
Yu, H., Rosen, M. K., Shin, T. B., Siedel-Dugan, C., Brugge, J. S., & Schreiber, S. L. (1992) *Science 258*, 1665.

Reprinted from Biochemistry, 1994, 33.

A Calorimetric Study of the Thermal Stability of Barnase and Its Interaction with 3′GMP†

Jose C. Martínez,‡ Mohamed El Harrous,‡ Vladimir V. Filimonov,*,‡,§ Pedro L. Mateo,*,‡ and Alan R. Fersht∥

Department of Physical Chemistry, Faculty of Sciences, University of Granada, 18071 Granada, Spain, and University Chemical Laboratory, University of Cambridge, Cambridge CB2 1EW, U.K.

Received September 28, 1993; Revised Manuscript Received January 21, 1994•

ABSTRACT: We have used high-sensitivity differential scanning calorimetry to characterize the thermal stability of barnase from *Bacillus amyloliquefaciens* in the pH range 2.0–5.0. The energetics of the interaction between barnase and its inhibitor 3′GMP have been studied by isothermal titration calorimetry in the temperature range 15–30 °C. Scanning calorimetry experiments were also made with the protein in the presence of various concentrations of 3′GMP at pH 4.5. A novel, simple procedure is proposed to obtain binding parameters from scanning calorimetry data. This method is based on the calculation of the partition functions of the free and the ligand-bound protein. Isothermal calorimetry shows that at 25 °C 3′GMP binds to a single site in barnase with a ΔC_p of -250 ± 50 J/(K·mol). Both free barnase and ligand-bound barnase undergo a highly reversible, two-state thermal unfolding process under our experimental conditions. ΔG and ΔC_p unfolding values are similar to others found for globular proteins, whereas ΔH and ΔS unfolding values are unusually high at the denaturation temperature of barnase. We have also found unexpectedly that the thermodynamic unfolding parameters of barnase fit neither the trend of values described in the literature for the correlation between ΔC_p and ΔH nor the limiting specific enthalpy value in the correlation between ΔH and T_m for globular proteins. These discrepancies might be related to particular features of the folded and/or unfolded states of the protein.

The study of protein folding/unfolding and stability is today of paramount importance both in the academic field and in biotechnology. The equilibrium transition between the folded and unfolded states of small proteins is usually a two-state one (Privalov, 1979); i.e., the protein is either in the native, folded state or in the unfolded, denatured state. The stability of the folded state is only about 20–60 kJ/mol higher than that of the unfolded conformation. This small value is the result of a compromise balance between large enthalpy and entropy values. Protein stability can be affected by many factors, such as the binding to specific effectors, an almost ubiquitous process in *in vivo* protein function. This stability change is obviously related to the energetics of the protein–ligand interaction.

High-sensitivity differential scanning calorimetry (DSC)[1] is a very suitable technique for characterizing the thermal stability of proteins since it provides the calorimetric and van't Hoff enthalpy and other thermodynamic values, and may lead to the analysis of multidomain proteins, as long as the denaturation process occurs under equilibrium conditions (Privalov, 1979, 1982). As for isothermal calorimetry, it allows one the most direct thermodynamic analysis of protein–ligand interactions.

We have applied here both DSC and isothermal titration calorimetry to study barnase and its binding to the inhibitor 3′GMP. Barnase is a single-domain, monomeric, extracellular ribonuclease from *Bacillus amyloliquefaciens*. It consists of a single polypeptide chain with 110 residues, M_r 12 382, without cysteines or methionines and with three *trans*-prolines (Hartley & Barker, 1972). The gene for this enzyme has been cloned and can be expressed in *Escherichia coli* (Paddon & Hartley, 1987). Barnase secondary structure contains two α-helices and a five-stranded antiparallel β-sheet. The X-ray crystal structure has been solved at 2-Å resolution (Mauguen et al., 1982), and the structure in solution has been determined by NMR (Bycroft et al., 1991). The protein undergoes reversible, two-state denaturation induced either by solvent or by heat (Hartley, 1968; Kellis et al., 1989). Barnase is a very appropriate model for studying protein stability and folding in solution, and a large amount of physicochemical data has been published, including detailed information on the thermodynamics and kinetics of the folding of wild-type barnase and many of its mutants (Kellis et al., 1988, 1989; Matouschek et al., 1990, 1992; Serrano et al., 1990, 1992a,b; Fersht et al., 1992).

In this paper, we describe the DSC thermodynamic characterization of the thermal stability of the free protein in the pH range 2.0–5.0, and that of barnase in the presence of increasing concentrations of 3′GMP at pH 4.5. In addition, the interaction of the protein with 3′GMP has been studied by isothermal titration calorimetry at pH 4.5 in the temperature range 15–30 °C. We also propose here a new method of estimating binding parameters by obtaining the partition functions of the free and liganded protein from DSC data. Barnase thermal denaturation follows a reversible, two-state transition; nevertheless, its high unfolding enthalpy does not fit some correlations described in the literature for compact globular proteins.

† This research has been supported by BRIDGE Grant BIOT-CT91-0270 from the European Communities. P.L.M. also acknowledges financial support from DGICYT Grant PB90-0876 (Spain). J.C.M. and M.E.H. are predoctoral fellows from the DGICYT and Ministerio de Asuntos Exteriores (Spain).

* To whom correspondence should be addressed. Telephone: +34-58-243333/1. Fax: +34-58-274258.

‡ University of Granada.

§ Permanent address: Institute of Protein Research, Russian Academy of Sciences, Pushchino, Moscow Region, 142292 Russia.

∥ University of Cambridge.

• Abstract published in *Advance ACS Abstracts*, March 1, 1994.

[1] Abbreviation: DSC, differential scanning calorimetry.

0006-2960/94/0433-3919$04.50/0

EXPERIMENTAL PROCEDURES

Biochemicals and Calorimetric Experiments. Wild-type barnase was expressed and purified as described elsewhere (Serrano et al., 1990). Before calorimetric experiments, the protein was extensively dialyzed against the appropriate buffer. The concentration of barnase was calculated from the UV absorbance of the solution at 280 nm, using an extinction coefficient of 2.21 mg^{-1}·mL·cm^{-1} (2.74 × 10^4 M^{-1}·cm^{-1}; Loewenthal et al., 1991).

In the DSC experiments with 3′GMP (Sigma), the ligand dissolved in buffer at a concentration of 50 mM was added to the dialyzed protein sample to give the desired concentrations of protein and of 3′GMP. If not specified otherwise, the solutions contained either 50 mM sodium or potassium acetate or 50 mM glycine (Sigma).

Scanning calorimetry was performed in a computerized version of the DASM-4 microcalorimeter (cell volume 0.47 mL; Privalov & Potekhin, 1986) at heating rates of 2 and 1 K/min with protein concentrations of about 1.5 mg/mL (a wider range of concentrations from 0.8 up to 4 mg/mL was checked at pH 4.5, used for 3′GMP studies, and also at pH 2.5). In addition, some DSC experiments were made in the DASM-1M microcalorimeter (Privalov et al., 1975) with a different cell configuration and volume (1 mL). An extra pressure of 1.5 atm was maintained during all DSC runs to prevent possible degassing of the solutions on heating. The molar partial heat capacity of the protein, C_p, was evaluated according to standard procedures (Privalov & Potekhin, 1986), taking 0.73 mL/g for the partial specific volume (an average value for globular proteins, confirmed by calculations according to Makhatadze et al., 1990) and 12.4 kDa for the molecular mass of barnase (Hartley & Barker, 1972). The reversibility of the unfolding was checked routinely by sample reheating after cooling inside the calorimetric cell.

Isothermal calorimetric titration experiments were conducted using a mixing calorimeter designed and built at the University of Granada according to McKinnon et al. (1984). The heat of mixing barnase with 3′GMP was measured by adding 10-μL portions of the 0.6 mM ligand stock solution to the calorimetric cell (volume 0.2 mL) containing the protein solution at about 0.2 mM concentration. To compensate for dilution of the enzyme, the 10-μL injection solution had the same protein concentration as that in the cell. Experimental heat binding values were corrected for thermal contributions of the stirring effect and that of the ligand dilution, which were always very small (≃8 μJ). The experiments were performed in 50 mM potassium acetate, pH 4.5, between 15 and 30 °C.

Analysis of Calorimetric Titration Data. Prior to any data analysis, the number of protons exchanged upon binding was obtained by potentiometric titration of the protein with 3′GMP. We found that about 0.12 proton was released by the system within the temperature range 15–30 °C. Given the small heat of ionization of acetate, this thermal correction was almost negligible. The dependence of the heat effect on the total amount of ligand added was recorded and analyzed to evaluate the number of binding sites n_b, binding enthalpy ΔH_b, and binding constant K_b, assuming a noncooperative binding of the ligand. An iterative, nonlinear, least-squares fitting of the molar enthalpy change, ΔH, for a given free-ligand concentration, [L], was used according to the equation:

$$\Delta H = n_b \Delta H_b K_b [L]/(1 + K_b[L]) \quad (1)$$

The free-ligand concentration was obtained from the total ligand, $[L_0]$, and protein, $[P_0]$, concentrations according to

$$[L] = \{\sqrt{(1 - K_b[L_0] + n_b K_b[P_0])^2 + 4K_b[L_0]} + K_b[L_0] - n_b K_b[P_0] - 1\}/2K_b \quad (1a)$$

The results calculated at each temperature (15, 20, 25, and 30 °C) were further analyzed to determine the temperature dependence of thermodynamic functions. For that purpose, the data on binding enthalpy have been fitted using a linear least-squares regression to estimate the ΔC_p of binding, taking into account that only one binding site for 3′GMP was found. After estimating $\Delta C_{p,b}$, the final fitting of the observed temperature dependence of binding parameters was made according to the equations:

$$\Delta H_b = \Delta H_{b,0} + \Delta C_{p,b}(T - T_0) \quad (2)$$

$$\Delta S_b = \Delta S_{b,0} + \Delta C_{p,b} \ln(T/T_0) \quad (3)$$

$$\Delta G_b = -RT \ln K_b \quad (4)$$

The adjustable parameters were $\Delta H_{b,0}$ and $\Delta S_{b,0}$, the enthalpy and entropy of binding at a given temperature, T_0 (normally 288.2 K).

Analysis of Scanning Calorimetry Data. We have also tried to use scanning calorimetry not only to characterize protein unfolding but also to evaluate the parameters of barnase interaction with 3′GMP. The applicability of DSC to protein–ligand binding studies has been analyzed recently by a number of authors (Robert et al., 1988; Shrake & Ross, 1990, 1992; Brandts & Lin, 1990; Straume & Freire, 1992). Thus, it has been shown that scanning calorimetry is an appropriate technique for measuring very strong affinity constants. As concerns weak binding, such as the one taking place on the interaction of 3′GMP with barnase, the traditional isothermal techniques give more precise results below 50 °C. Nevertheless, even in such cases, scanning calorimetry should be more useful to evaluate binding parameters at higher temperatures since with DSC long extrapolations of thermodynamic functions from low to high temperature are unnecessary. Here we show that by using a combination of the two techniques the ligand binding parameters can be determined with sufficient accuracy over a wide temperature range.

We have extensively checked several analytical procedures used for calculating thermodynamic parameters from scanning calorimetry data. First, we applied nonlinear fitting algorithms to calculate the binding and unfolding parameters from the temperature dependence of C_p. Manipulating such parameters as the van't Hoff enthalpy and its ratio to the calorimetry heat effect can be avoided by using modern analytical software. These parameters are only rough estimates but are widely used in the literature due to the simplicity of their determination from calorimetric data. It can be shown, however, that the van't Hoff enthalpy, which is usually estimated from peak sharpness, might be misleading if the melting profile is distorted by factors that do not alter the height-to-area ratio. Therefore, the computer global fitting of calorimetric curves *over the whole temperature range of the transition*, according to a suitable model, seems to be a more precise and informative procedure for data evaluation and analysis. To check the validity of a two-state model for barnase heat denaturation, as well as to calculate the thermodynamic parameters of unfolding, we used the computer programs developed by Filimonov et al. (1982) at the Institute of Protein Research (Pushchino, Russia). An example of the excellent fitting of

Table 1: Thermodynamic Parameters of 3'GMP Binding to Barnase at pH 4.5 Calculated from Isothermal Titration Calorimetry Data

T (K)	n_b[a] (sites)	ΔH_b[a] (kJ/mol)	ΔH_b[b] (kJ/mol)	K_b[a] × 10^{-5} (M^{-1})	K_b[b] × 10^{-5} (M^{-1})	ΔG_b[a] (kJ/mol)	ΔG_b[b] (kJ/mol)	ΔS_b[a] [J/(K·mol)]	ΔS_b[b] [J/(K·mol)]
288.2	0.98	−46.9 ± 0.4	−46.7	7.4 ± 0.8	6.98	−32.4 ± 0.3	−32.7	−49.8	−48.6
293.2	1.00	−47.3 ± 0.6	−47.9	4.7 ± 0.6	5.01	−31.8 ± 0.3	−32.4	−52.3	−52.8
298.2	0.92	−49.8 ± 0.6	−49.2	3.4 ± 0.3	3.60	−31.6 ± 0.2	−32.!	−60.7	−57.3
303.2	0.99	−50.2 ± 0.8	−50.4	2.2 ± 0.3	2.68	−31.0 ± 0.3	−31.9	−64.0	−60.9

[a] Parameters calculated by fitting the experimental titration curves to eq 1 and 1a. [b] Values obtained by further fitting of the parameters[a] to eqs 2–4 as described in the text; a linear regression through enthalpy (eq 2) corresponded to $\Delta H_b^b(T) = -46.7 - 0.25(T - 288.2)$; therefore, the value −0.25 kJ/(K·mol) was taken as the $\Delta C_{p,b}$ for subsequent calculations.

the calorimetric records at pH 2.0 and pH 4.5 with two-state heat absorbance peaks is shown in the upper half of Figure 1.

To calculate binding parameters from calorimetric data, we adopted two main approaches. First, we have developed and applied a novel and rather simple procedure to evaluate the binding constant from the melting curves of free and ligand-bound protein, as will be described under Results. The advantage of this approach is that no parameter has to be assumed *a priori* except for the scheme of the reaction. In addition, this simple procedure permits the direct estimation of the temperature dependence of the binding constant as soon as the calorimetric melting profiles are accurately recorded.

Second, we performed a more complex global fitting analysis of the DSC data, as suggested by Brandts and Lin (1990). For this purpose, we mainly used the curve-fitting option of the SigmaPlot software (Jandel Co.) and a program for a nonlinear multidimensional fitting developed by Freire at Johns Hopkins University (Straume & Freire, 1992). The fitting has the advantage of not being constrained by the conditions when the free ligand, [L], is in great excess, since free ligand concentration is explicitly expressed with a formula similar to eq 1a. On the other hand, the cases where [L] changes during melting are much more informative and interesting (Brandts & Lin, 1990; Straume & Freire, 1992; Shrake & Ross, 1992). The general treatment of the expressions (eq 6–8) leads to simple quadratic equations describing populations of each state of the protein. After these equations are solved in analytical form, the functions of $\langle \Delta H(T) \rangle$ can be simulated and fitted to the experimental data. A multidimensional fitting was performed simultaneously over the set of $C_p(T)$ curves recorded at different total ligand concentrations to adjust $\Delta H_d(T_m)$ and $K_d(T_m)$ while $\Delta C_{p,d}$ was fixed at 300 J/(K·mol) as explained under Results. The reaction scheme can also be extended to the case of multiple binding, which will, however, simultaneously increase the number of adjustable parameters and make the fitting of the results more ambiguous. Finally, we applied the first approach to estimate roughly the binding parameters and then used them as the initial values to make the global fitting of the DSC traces.

RESULTS

Determination of Binding Parameters by Mixing Calorimetry. The parameters calculated from the isothermal calorimetry data at pH 4.5, as described under Experimental Procedures, appear in Table 1. This set of thermodynamic parameters corresponds closely with those calculated from the scanning calorimetry results (see below). The greatest uncertainty was in the determination of the ΔC_p of binding since the titration data were measured over a rather small temperature range with an accuracy comparable to the heat capacity change itself.

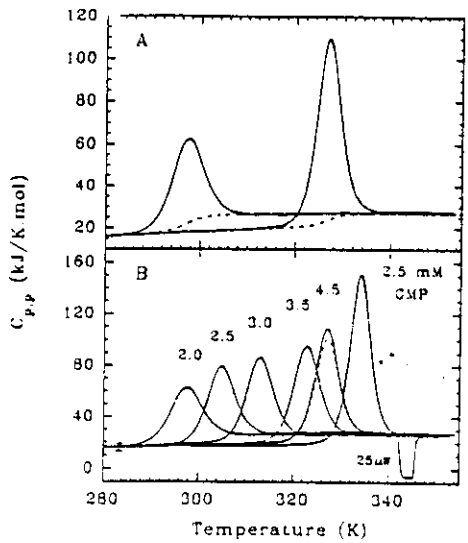

FIGURE 1: (A) DSC records of the molar partial heat capacity of barnase at pH 2.0 and 4.5 (solid lines) and their best fits to a two-state transition (dashed lines). The dashed sigmoid lines correspond to the internal or chemical heat capacity calculated during fitting. (B) Temperature dependencies of the molar partial heat capacity of barnase at various pH values (marked at the tops of the peaks). Curves corresponding to pH 2.5, 3.5, and 4.5 were registered at a heating rate of 1 K/min, while the others were at 2 K/min. Concentrations of protein were between 1 and 2 mg/mL, while for the pH 4.5 curve the concentration was 3.6 mg/mL. The dashed line represents the curve recorded for sample reheating at pH 4.5. The calibration mark of 25 μW [31.9 kJ/(K·mol)] was recorded at a heating rate of 1 K/min. The error bar at 283 K shows the scatter in the position of the curves on the C_p scale. The melting curve of barnase in the presence of 2.5 mM 3'GMP, pH 4.5, is also shown for comparison.

Thermal Unfolding of Barnase. The thermal unfolding of barnase is a highly reversible process below pH 5.0 and above pH 10.0, while at neutral pH the reversibility of melting is much lower, presumably because of aggregation of the unfolded molecules with a net charge close to zero. The alkaline region is much less suitable for temperature unfolding studies because of the high ionization heat effects of the amino groups and the high temperature dependence of the pH of the buffers. For this reason, we have varied protein stability by changing the pH within the acid range. Between pH 2.0 and 5.0 and at 50 mM buffer concentration, the melting curves of barnase do not depend upon the heating rate or protein concentration and follow the two-state model very closely (Figure 1A). Thus, the values of ΔH_m obtained by the fitting procedure (see Figure 2 and Table 2) coincide within the limits of experimental error both with the "calorimetric" and with the "van't Hoff" enthalpies evaluated in a traditional way, *i.e.*, from the area and sharpness of the individual peaks [cf. Privalov and Potekhin (1986)]. The melting curves obtained with fresh barnase preparations (Figure 1) are not distorted in any way, while C_p functions recorded at sample

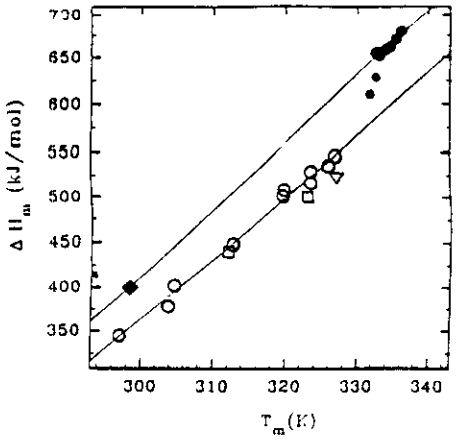

FIGURE 2: Dependence of ΔH_m on T_m for free barnase (open symbols) and ligand-bound protein (filled symbols) according to this study (circles and diamond) and the literature. The data for ligand-bound protein were obtained at a total 3'GMP concentration of between 0.2 and 10 mM, pH 4.5, and at a protein concentration of about 0.15 mM. For comparison, the van't Hoff enthalpies reported by Kellis et al. (1989) (squares) and Hartley (1968) (triangle) are also shown. The straight lines correspond to the least-squares fitting of our own values. The $\Delta H_L(298)$, calculated as described in the text, is shown by the filled diamond.

Table 2: Thermodynamic Parameters for the Thermal Unfolding of Barnase as a Function of pH

pH	T_m (K)	$\Delta H_m(T_m)$ (kJ/mol)	$\Delta S_m(298)^a$ [kJ/(K·mol)]	$\Delta G_m(298)^a$ (kJ/mol)	$\Delta G_m(298)^b$ (kJ/mol)
2.0	297.0	345.0	1.189	−3.4	−1.9
2.5	304.6	394.0	1.151	7.8	7.6
3.0	312.6	449.0	1.115	18.4	21.7
3.5	319.7	497.0	1.082	28.4	31.7
4.0	323.5	523.0	1.063	34.0	35.6
4.5	326.0	540.0	1.051	37.7	37.9
5.0	326.9	546.0	1.046	39.1	38.7

[a] These parameters were calculated from linear regression of experimental data according to eq 5 and the experimental values of T_m as a function of pH. [b] The Gibbs energy changes calculated with temperature-dependent $\Delta C_{p,m}$ specified by eq 17 at $\Delta H_m(298.2) = 344$ kJ/mol (best fit value for polynomial regression).

reheating or after long storage exhibited a small pretransition shoulder.

We determined ΔH_m to an accuracy of 5%, although the $\Delta C_{p,m}$ values calculated directly from the calorimetric records were more scattered. When melting is completely reversible, such a scatter usually arises from an uncertainty in the extrapolation of the initial C_p over the whole transition range and becomes larger when T_m decreases. Since below pH 3.5 barnase starts to unfold at room temperature, there are difficulties in the estimation of the initial heat capacity slope. For this reason and, probably, due to the temperature dependence of $\Delta C_{p,m}$ (see Discussion), the uncertainty of its direct determination from calorimetric records was about 13%, with the average value of $\Delta C_{p,m}$ being about 6.2 kJ/(K·mol). This is only 10% lower than the slope of the least-squares regression line (Figure 2), which corresponds to the following empirical dependence of ΔH_m on temperature:

$$\Delta H_m(T) = \Delta H_{m,0} + \Delta C_{p,m}(T - T_0) = 351 + 6.8(T - 298.2)\ \text{(kJ/mol)} \quad (5)$$

Using this function, we have calculated the changes of the thermodynamic parameters at different pH values (Table 2).

Thermal Unfolding of Barnase in the Presence of 3'GMP. As was mentioned under Experimental Procedures, we have developed and used a simple approach for estimating binding parameters from DSC data. To describe this approach, we shall use the formulations originally suggested by Freire and Biltonen (1978). We shall consider here a rather simple case, but similar equations can be deduced for more complex multistate schemes.

Let us assume that protein unfolding in the presence of a ligand obeys a simple two-step model and that there is only one binding site for the ligand on the native protein:

$$NL \overset{K_d}{=} N + L \overset{K_m}{=} U + L \quad (6)$$

If [NL] stands for the concentration of the protein–ligand complex, [N] and [U] for the concentrations of native and unfolded proteins, respectively, and [L] for the concentration of the free ligand, the dissociation, K_d, and unfolding, K_m, constants, can be expressed as

$$K_d = [N][L]/[NL];\ K_m = [U]/[N] \quad (7)$$

For the total protein $[P_0]$ and ligand $[L_0]$ concentrations, we have

$$[P_0] = [NL] + [N] + [U];\ [L_0] = [NL] + [L] \quad (8)$$

If $[L_0] \gg [P_0]$, then $[L] \approx [L_0] =$ constant, and K_d can be replaced by an effective monomolecular constant, $K_e = K_d/[L_0] = [N]/[NL]$. Hence, the partition function, Q_L, for eq 6 with the liganded native protein taken as the reference state, may be written as

$$Q_L = 1 + K_e + K_eK_m = 1 + K_e(1 + K_m) = 1 + K_eQ \quad (9)$$

Thus

$$K_e = (Q_L - 1)/Q \quad (10)$$

where Q is a partition function for the free protein under the same solvent conditions. Both Q_L and Q are easily calculated from scanning calorimetry data since (Freire & Biltonen, 1978):

$$(\partial \ln Q_L/\partial T)_L = \langle \Delta H_L \rangle / RT^2;\ \partial \ln Q/\partial T = \langle \Delta H_m \rangle / RT^2 \quad (11)$$

and $\langle \Delta H(T) \rangle = H(T) - H_0(T)$ can be found correspondingly from $\langle \Delta C_p(T) \rangle = C_p(T) - C_{p,0}(T)$, since

$$d\langle \Delta H(T) \rangle / dT = \langle \Delta C_p \rangle \quad (12)$$

where subscript "0" refers to the initial state of the protein and ΔH_L is the total heat of unfolding in the presence of the ligand. In practice, to obtain the partition function, a double integration of the $C_p(T)$ function has to be made after subtracting the heat capacity of the initial state. This approach is straightforward, although some complications are again caused by having to approximate the heat capacity of the initial state over the whole transition range. Its extrapolation and subtraction from the total C_p according to standard procedures introduce some errors which are amplified during the evaluation of Q by the double integration procedure. As a result, the factor $Q_L - 1$ is knowable with satisfactory precision almost at the midpoint of protein unfolding. Therefore, $K_d(T)$ calculated in this way is reliably known only at $T > T_m$ of the ligand-bound protein (Figure 3). To overcome this difficulty, we have carried out a global fitting of all individual K_d functions, calculated at each concentration

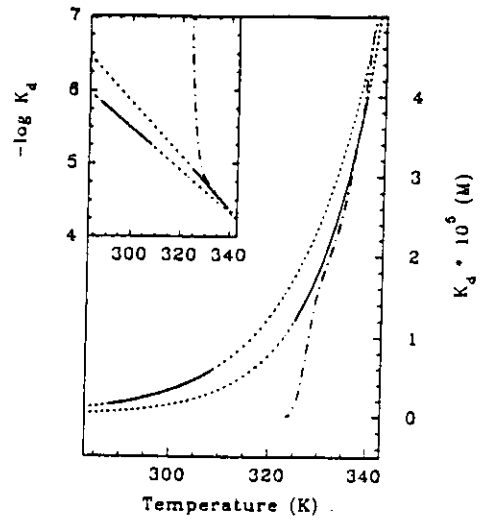

FIGURE 3: Temperature dependencies of the dissociation constant, K_d, of 3'GMP from barnase at pH 4.5, calculated from isothermal titration data (solid line at low temperature extrapolated by dotted line), by applying the partition function method at 5 mM 3'GMP concentration (eq 10, dash-and-dot line) and by global fitting of DSC data in the presence of ligand (solid line at high temperature extrapolated by dotted line). The insert shows the same data in logarithmic scale. Solid lines correspond to the working temperature range for each method.

of the ligand, to the overall analytical expression for the dissociation constant assuming a constant $\Delta C_{p,d}$. This $K_d(T)$ is also shown in Figure 3 together with the temperature dependence of the dissociation constant determined from the mixing calorimetry experiments.

The ΔH_L values measured at pH 4.5 and increasing concentrations of 3'GMP are shown in Figure 2, together with the data for free protein. From a comparison between the two correlations, it is clear that any difference between the two sets of data can be put down exclusively to the effect of ligand binding. With a high excess of ligand, the heat capacity peak is adequately fitted by a two-state unfolding transition, since under these conditions the intermediate state, N in eq 6, is only slightly populated; when the total ligand concentrations were comparable or even smaller than $[P_0]$, the melting curves were somewhat distorted, in full accordance with theory (Brandts & Lin, 1990; Straume & Freire, 1992; Shrake & Ross, 1992). The linear regression line for the ligand-bound protein in Figure 2 is plotted only through the points corresponding to saturating conditions (more than 10-fold molar excess of the ligand over the protein). As can be seen from Figure 2, the points obtained in the presence of ligand are too close to each other to provide a reliable linear regression through them. To decrease the uncertainty in the slope of the regression line, we have plotted on the same graph the value $\Delta H_L(298) = \Delta H_m(298) + \Delta H_d(298)$ (filled diamond in Figure 2). The first term in the sum is the unfolding enthalpy calculated for free protein from eq 5, and the second one is the dissociation heat measured directly with mixing calorimetry (Table 1). The regression line, drawn as shown in Figure 2, has a slope of 7.3 kJ/(K·mol) and corresponds to the equation:

$$\Delta H_L(T) = \Delta H_m + \Delta H_d = 400 + 7.3(T - 298.2) \text{ (kJ/mol)} \quad (13)$$

The difference between eq 13 and 5 should obviously correspond to the temperature dependence of ΔH_d, which is

$$\Delta H_d(T) = 49 + 0.5(T - 298.2) \text{ (kJ/mol)} \quad (14)$$

The value 0.5 in the above equation is twice as high as the $\Delta C_{p,d}$ found from isothermal calorimetry (Table 1). From the global fitting of the $K_d(T)$ functions calculated with the partition function approach (Figure 3), we also got a $\Delta C_{p,d}$ equal to 0.45 kJ/(K·mol). These two $\Delta C_{p,d}$ values estimated from the preliminary analysis of the DSC data compare well. Nevertheless, taking into account the rather large error in their determination [about ±0.35 kJ/(K·mol) in both cases] during the final multidimensional global fitting of the DSC curves, $\Delta C_{p,d}$ was fixed at a weighted-average value of 0.3 kJ/(K·mol), which is clearly closer to the more precise parameter found by isothermal calorimetry. For this multidimensional fitting, the T_m, ΔH_m, and $\Delta C_{p,m}$ values (Table 2) were also fixed, whereas $K_d(T_m)$ and $\Delta H_d(T_m)$ obtained with the partition function approach were used as initial, adjustable parameters. The results of this final fitting are shown in Table 3 and Figure 4.

DISCUSSION

The energetics of the interaction of 3'GMP with barnase have been studied by both isothermal titration and differential scanning microcalorimetry. The direct isothermal experiments have shown that the affinity of the ligand to its single site on the protein is not very high and comparable to that found for other nucleotide binding proteins, in particular that for ribonucleases (Flogel et al., 1975). Taking into account the pH dependence of the binding constant, our value of 3.6×10^5 M^{-1} found for K_b at 298 K and pH 4.5 is in close accord with the value of 4.35×10^5 M^{-1}, determined by Sancho et al. (1991) from kinetic studies at pH 6.3 and the same temperature.

The value of $\Delta C_{p,b}$ found by both techniques has a negative sign, as might be expected from the data reported for ligand-to-protein binding (Sturtevant, 1977; Wiesinger & Hinz, 1986). The magnitude of $\Delta C_{p,b}$ is, however, slightly lower than the values found for the binding of various nucleotides and nucleoside monophosphates to other proteins (Wiesinger & Hinz, 1986; Mateo et al., 1986; Baron et al., 1989).

The effect of 3'GMP binding on the stability of barnase against heat denaturation is similar to the stabilizing effect of other ligands described in the literature (Fukada et al., 1983; Brandts & Lin, 1990; Straume & Freire, 1992). It can easily be explained by the mass action principle without any recourse to "ligand-induced stabilizing conformational changes".

We have found that the most precise and reliable determination of the binding parameters from scanning calorimetry data is provided by the global fitting of the C_p records obtained at various ligand concentrations. Nevertheless, a new approach based on the evaluation of K_d and ΔH_d from the partition functions of the ligand-bound and free proteins provides a very good approximation to the temperature dependence of the binding parameters. This approach, followed by the fitting of the $C_p(T)$ curves (see Results), is recommended for determining the binding parameters when not enough material is available to make a complete calorimetric study with changing ligand concentrations, or when there are problems with ligand solubility.

It must be pointed out, however, that only K_d was determined from our DSC data analysis with any reasonable precision. ΔH_d and, in particular, $\Delta C_{p,d}$ are known much less accurately for several reasons, the most important of which is that ΔH_d, being much smaller than the overall heat of unfolding, is

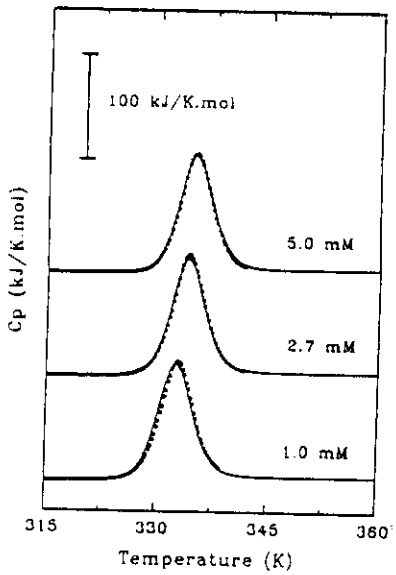

FIGURE 4: Results of nonlinear least-squares global fitting (solid line) of heat capacity excess functions (dots) for barnase in the presence of different concentrations (mM) of 3'GMP.

calculated as the difference between two large values. Therefore, the standard error in determining ΔH_m and ΔH_L, which is about 15 kJ/mol, must serve as the lower limit of the standard error for ΔH_b calculated from DSC data. An even more uncertain situation occurs with $\Delta C_{p,d}$ since (as we know from isothermal calorimetric titrations) it is of the same magnitude and even smaller than the error of direct determination of ΔC_p from DSC records. On the other hand, the overall shape and $T_{m,L}$ of each individual melting curve in the presence of the ligand excess seem to depend mainly on $K_d(T)$ and $\Delta H_d(T_{m,L})$ and much less so on $\Delta C_{p,d}$. For this reason, for example, on making a global fitting of DSC data for liganded protein, we got practically the same results by fixing $\Delta C_{p,d}$ either at 0.3 or at 0.25 kJ/(K·mol). To overcome these problems, one has to determine $\Delta C_{p,d}$ from the temperature dependence of ΔH_d. Nevertheless, because of solubility problems we could not vary the ligand concentration over sufficiently wide limits. So the melting temperature for the liganded protein in our experiments changed within a narrow temperature range, thus introducing a large error into our $\Delta C_{p,d}$ determination from the $\Delta H_d(T)$ slope, unless the independent mixing calorimetry data were used to extend the working temperature range. Finally, with the current levels of DSC experimental error, it is practically impossible to detect any temperature dependence of $\Delta C_{p,d}$, although it can be expected that its relative variation may be as high as the temperature-induced relative changes in $\Delta C_{p,m}$.

The thermodynamic parameters of barnase unfolding, either with or without a ligand, unambiguously show that under our experimental conditions barnase behaves as a single-domain protein, the structure of which melts in an essentially two-state way; *i.e.*, under equilibrium conditions, all intermediate states are much less populated than the native and unfolded ones. This conclusion agrees with previous noncalorimetric results (Hartley, 1968). Recently, however, Makarov et al. (1992) have shown that the C_p endotherm becomes asymmetric when barnase is heated at pH 2.4 in a buffer of low ionic strength (10 mM). We have also found an asymmetry in the calorimetric traces at pH 2.5 and 10 mM buffer. It seems that under these conditions the distortion of the melting peak is caused by a slow, nonspecific oligomerization of the native protein, as was found by analytical methods at the Cambridge laboratory. The oligomerization is reversible and is suppressed by an increase of the ionic strength to above 50 mM and/or of pH to above 3.5. The slow kinetics of nonmonomolecular processes responsible for curve distortion were confirmed by our observation that at low ionic strength the peak shape and position were heating rate dependent and much more evident at sample heating in the cylindrical cells of the DASM-1M calorimeter (this model was the one actually used by Makarov et al.) than in the capillary cells of the DASM-4 (results not shown).

Barnase does not belong to the protein group that have a particularly stable native conformation, as can be seen from the analysis of Gibbs energy changes accompanying unfolding (see Table 2). The ΔG_m values obtained here by DSC agree very well with measurements made using other techniques (Kellis et al., 1988, 1989; Clarke & Fersht, 1993).

Since barnase appears to be a typical representative of the family of small, single-domain globular proteins, it was interesting to compare its specific thermodynamic parameters of unfolding with those of other members of the family. Thus, its specific heat capacity of unfolding, 0.55 J/(K·g) [0.13 cal/(K·g)], compares very well with that of other compact globular proteins (Privalov, 1979). Some time ago Privalov (1979) also found that the extrapolated values of specific heats of unfolding (Δh_m) for globular proteins intersect close to 385 K, where the Δh_m for all of them is about 54 J/g. The exceptions are either very small proteins, extensively cross-linked by S–S bridges, or those with an elongated rather than globular structure.

Initially those extrapolations were made under the assumption of a constant $\Delta C_{p,m}$, but later on Privalov et al. (1989) suggested that $\Delta C_{p,m}$ would be a sort of bell-shaped function of temperature with a maximum close to 310 K and reaching zero at about 413 K. With such a ΔC_p function, the specific heats of unfolding would approach the same value of 54 J/q asymptotically instead of intersecting with it at 373 K. Nevertheless, since the top of the "bell" is rather wide, the absolute variations of $\Delta C_{p,m}$ in the temperature range of protein melting are relatively small, and, consequently, the plots of ΔH_m versus T_m might fit the linear functions very well, with a slope corresponding to an average value of the actual $\Delta C_{p,m}$ (Figure 5). When calculated directly from the calorimetric records, however, the latter must depend on T_m, and these variations might account, at least partly, for the observed scatter of the $\Delta C_{p,m}$ values.

Bearing in mind that the long extrapolations made by Privalov et al. (1989) might be ambiguous, it is also interesting to look for other correlations, which eventually might be more reliable. Murphy et al. (1990) have pointed out that such behavior of the Δh_m dependence on temperature should also provide a strong correlation between $\Delta C_{p,m}$ and Δh_m calculated per mole of amino acid residue at a standard temperature of 298 K, as they have indeed found for more than 10 proteins (Figure 6). Later on, the list of proteins obeying this correlation was extended by Murphy et al. (1992) and Spolar et al. (1992). The latter authors have only found the single exception of ribonuclease T1, the Δh_m vs $\Delta C_{p,m}$ point of which [calculated from the DSC data of Hu et al. (1992)] did not fit into the above-mentioned correlation, primarily due to the high ΔC_p value. Nevertheless, further analysis of the DSC curves for T1 made by Plaza del Pino et al. (1992) gave much a lower $\Delta C_{p,m}$ value [1.16 kcal/(K·mol) or 11.15 cal/(K·mol-residue) instead of 1.59 kcal/(K·mol)], which, in combination with 573 cal/(K·mol-residue) for the $\Delta h_m(298)$, fits perfectly well into Murphy's plot.

Table 3: Thermodynamic Parameters of 3'GMP Binding to Barnase at pH 4.5 and $T = T_m = 326$ K Obtained by Global Fitting of the Temperature Dependencies of the Molar Heat Absorbance with and without Ligand Added to the Protein Solution

T_m (K)	ΔH_m (kJ/mol)	$\Delta C_{p,m}$ [kJ/(K·mol)]	ΔH_d (kJ/mol)	$\Delta C_{p,d}$ [J/(K·mol)]	$K_d \times 10^5$ (M)	$K_b \times 10^{-4}$ (M^{-1})
326.0[a]	540 ± 15[a]	6.8 ± 0.4[a]	59 ± 15[b]	300 ± 100[b]	1.1[b]	9.1[b]
			56 ± 1.5[c]	250 ± 50[c]	1.7[c]	5.9[c]

[a] Parameters defined from linear fitting of DSC data for free protein according to eq 5. [b] Parameters of 3'GMP binding found by fitting the DSC data for ligand-bound protein according to eqs 6–8 as described in the text. The $\Delta C_{p,d}$ value was fixed during fitting. [c] Parameters calculated by extrapolation of mixing calorimetry values to 326 K.

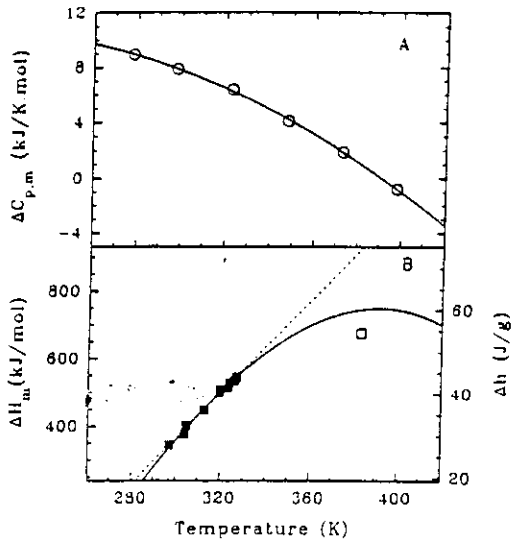

FIGURE 5: (A) Temperature dependence of $\Delta C_{p,m}$, calculated as described in the text. (B) Experimental dependence of ΔH_m on T_m for barnase (solid squares) plotted together with $\Delta H_m(T)$ functions simulated assuming a constant $\Delta C_{p,m}$ of 6.8 kJ/(K·mol) (dotted line) and a variable $\Delta C_{p,m}$ (eq 17, part A of this figure; solid line). The open square corresponds to the Privalov's "limiting value" of 54 J/g at 383 K.

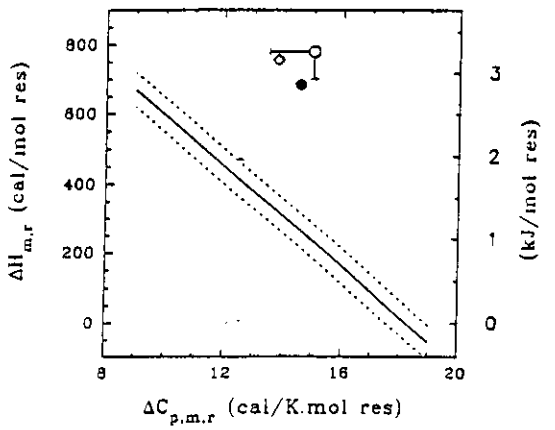

FIGURE 6: Linear correlation between $\Delta H_{m,r}(298)$ and $\Delta C_{p,m,r}$ (both calculated per mole of amino acid residue) as found by Murphy et al. (1990) for more than 10 globular proteins (solid line). The dotted lines show the limits into which all the data for those proteins fit. The open circle with error bars shows our data for barnase. The filled circle corresponds to the value for wild-type barnase, and the opened diamond shows an average of the values for eight single barnase mutants, both calculated from the unpublished data of Matouschek and Fersht.

We have added our data to the plots of both Privalov et al. (1989) and Murphy et al. (1990) and found very unexpected results. First, *at any temperature* barnase has the highest Δh_m of *all globular proteins* studied so far. As a result, the linear extrapolation of Δh_m to 373 K gives a value close to 75 J/g, which is about 40% higher than the universal value of 54 J/g (Figure 5).

We tried to find out then how such an extrapolation would work when a temperature-dependent function of ΔC_p is assumed instead of a constant one. To do this, we estimated the ΔC_p by the procedure suggested by Privalov and Makhatadze (1990). We calculated the C_p of the denatured state from the amino acid content of barnase, which turned out to be a nonlinear function of temperature:

$$C_{p,u}(T) = -14.4 + 0.218T - 0.00028T^2 \text{ [kJ/(K·mol)]} \quad (15)$$

Then, analyzing our calorimetric data we found that an average temperature dependence of C_p for the native state of barnase can be adequately approximated by the *linear* function

$$C_{p,n}(T) = 17.8 + 0.11(T - 298.2) \quad (16)$$

(where each of the numerical parameters is known to 10% accuracy). The difference between the last two functions gives the following empiric formula for $\Delta C_{p,m}$:

$$\Delta C_{p,m}(T) = 0.6 + 0.108T - 0.00028T^2 \quad (17)$$

It can be seen from Figure 5 that the function $\Delta H_m(T)$ simulated with a nonconstant $\Delta C_{p,m}$, using

$$d\Delta H_m/dT = \Delta C_{p,m} \quad (18)$$

fits our experimental data even more precisely than the linear regression. Nevertheless, despite the fact that the extrapolated value of Δh_m at 383 K decreased somewhat it did not reach the universal intersection point. Hence, the temperature dependence of $\Delta C_{p,m}$ cannot account for our observation.

An even higher discrepancy was observed after adding our data point to the plot of Murphy et al. (1990). Again, the barnase data lie far from the correlation found by these authors for other proteins (Figure 6). To obey that correlation, barnase must have either about a 3-fold lower Δh_m per residue or about a 2-fold lower $\Delta C_{p,m}$ value, or lower values for both parameters simultaneously.

Could such a big discrepancy be caused by errors in the determination of the thermodynamic parameters for barnase unfolding? It is very unlikely for the following reasons. First, as was pointed out above, under our experimental conditions the melting of barnase is a highly reversible process and is two-state in character. This observation rules out the possibility of high errors in concentration measurements, which frequently arise from using wrong extinction coefficients [besides, the extinction coefficient used here is in very close agreement with the value of 2.6×10^4 M^{-1}·cm^{-1} reported recently by Hartley (1993)]. Second, under our solvent conditions, the melting curves of barnase are highly symmetrical and did not depend either on heating rate or on protein concentration, which excludes any nonmonomolecular unfolding mechanism. Third, some estimations of the van't Hoff unfolding enthalpy from noncalorimetric measurements are available in the literature, and, as can be seen in Figure 2, they are adequately close to our data. In addition, there are also unpublished DSC data of Matouschek and Fersht which fit the linear dependence of ΔH_m on T_m with a slope

corresponding to a $\Delta C_{p,m}$ value of 6.7 kJ/(K·mol) and a $\Delta H_m(298)$ of 325 kJ/mol (for a comparison, see eq 5 and Figure 6). Finally, the Gibbs energy changes calculated from ΔH_m, T_m, and $\Delta C_{p,m}$ at different pH values (see Table 2) correspond very well with those obtained from urea denaturation studies, usually carried out at much lower protein concentrations because protein unfolding was monitored by fluorescence (Kellis et al., 1988, 1989; Pace et al., 1991; Clarke & Fersht, 1993).

Thus, it is impossible to fit the melting parameters of barnase into the correlations of Privalov et al. (1989) and Murphy et al. (1990). In addition to these simple correlations, different groups working in the field, including those mentioned above, have recently developed methods and algorithms for evaluating the thermodynamic parameters of unfolding from protein structure based on calculations of the buried hydrophobic and hydrophilic areas, the number of internal hydrogen bonds, and so on. So far we have not developed our own methods of structural analysis to form a coherent explanation for our observations. We believe, though, that such an explanation might lie in the properties of the native and unfolded states of barnase. It is highly probable, for example, that the temperature-induced unfolded state of barnase has much less residual structure than that of other proteins *even at low temperature*. This means that its unfolded state should be very specific and very close to random coil. If this were to be the case, a cooperative melting of all structural elements, including the secondary structure, would be accompanied by higher than average enthalpy and entropy changes.

Recently, the X-ray structures of barnase in complex with 3′GMP (Guillet et al., 1993b) and barstar (Guillet et al., 1993a) have been published. The authors of the latter publication have made a very interesting observation about water molecules trapped inside the barnase–barstar complex. It turns out that barstar does not enter the hydrophobic guanine binding pocket of barnase, which appears to be filled with structured water molecules. Since water might be structured in a similar way by unliganded barnase, the melting of this protein–water cluster on protein unfolding may well increase both the enthalpy and entropy of unfolding.

ACKNOWLEDGMENT

We thank Dr. F. Conejero-Lara for his suggestions on the manuscript, and Dr. J. Trout for revising the English text.

REFERENCES

Baron, C., Gonzalez, J. F., Mateo, P. L., & Cortijo, M. (1989) *J. Biol. Chem. 264*, 12872–12878.

Brandts, J. F., & Lin, L.-N. (1990) *Biochemistry 29*, 6927–6940.

Bycroft, M., Ludvigsen, S., Fersht, A., & Poulsen, F. M. (1991) *Biochemistry 30*, 8697–8701.

Clarke, J., & Fersht, A. R. (1993) *Biochemistry 32*, 4322–4329.

Fersht, A. R., Matouschek, A., & Serrano, L. (1992) *J. Mol. Biol. 224*, 771–782.

Filimonov, V. V., Potekhin, S. A., Matveyev, S. V., & Privalov, P. L. (1982) *Mol. Biol. (USSR) 16*, 435–444.

Flogel, M., Albert, A., & Biltonen, R. L. (1975) *Biochemistry 14*, 2616–2621.

Freire, E., & Biltonen, R. L. (1978) *Biopolymers 17*, 463–479.

Fukada, H., Sturtevant, J. M., & Quiocho, F. A. (1983) *J. Biol. Chem. 258*, 13193–13198.

Guillet, V., Lapthorn, A., Hartley, R. W., & Mauguen, Y. (1993a) *Curr. Opin. Struct. Biol. 1*, 165–177.

Guillet, V., Lapthorn, A., & Mauguen, Y. (1993b) *FEBS Lett. 330*, 137–140.

Hartley, R. W. (1968) *Biochemistry 7*, 2401–2408.

Hartley, R. W. (1993) *Biochemistry 32*, 5978–5984.

Hartley, R. W., & Barker, E. A. (1972) *Nature (London), New Biol. 235*, 15–16.

Hu, C. Q., Sturtevant, J. M., Thomson, J. A., Erickson, R. E., & Pace, C. N. (1992) *Biochemistry 31*, 4876–4882.

Kauzmann, W. (1959) *Adv. Protein Chem. 14*, 1–63.

Kellis, J. T., Jr., Nyberg, K., Šali, D., & Fersht, A. R. (1988) *Nature 333*, 784–786.

Kellis, J. T., Jr., Nyberg, K., & Fersht, A. R. (1989) *Biochemistry 28*, 4914–4922.

Loewenthal, R., Sancho, J., & Fersht, A. R. (1991) *Biochemistry 30*, 6775–6779.

Makarov, A., Protasevich, I., Kuznetsova, N., Fedorov, B., Korolev, S., Struminskaya, N., Leshchinskaya, I., Yakovlev, G., & Esipova, N. (1992) in *Stability and Stabilization of Enzymes* (van den Tweel, W. J. J., Harder, A., & Buitelaar, R. M., Eds.) pp 377–382, Elsevier, The Netherlands.

Makhatadze, G. I., Medvedkin, V. N., & Privalov, P. L. (1990) *Biopolymers 30*, 1001–1010.

Mateo, P. L., Gonzalez, J. F., Baron, C., Mayorga, O. L., & Cortijo, M. (1986) *J. Biol. Chem. 261*, 17067–17072.

Matouschek, A., Kellis, J. T., Jr., Serrano, L., Bycroft, M., & Fersht, A. R. (1990) *Nature 346*, 440–445.

Matouschek, A., Serrano, L., & Fersht, A. R. (1992) *J. Mol. Biol. 224*, 819–835.

Mauguen, Y., Hartley, R. W., Dodson, E. J., Dodson, G. G., Bricogne, G., Clothia, C., & Jack, A. (1982) *Nature 297*, 162–164.

McKinnon, I. R., Fall, L., Parody-Morreale, A., & Gill, S. J. (1984) *Anal. Biochem. 139*, 134–139.

Murphy, K. P., Privalov, P. L., & Gill, S. J. (1990) *Science 247*, 559–561.

Murphy, K. P., Bhakuni, V., Xie, D., & Freire, E. (1992) *J. Mol. Biol. 227*, 293–306.

Pace, N. C., Laurents, D. V., & Erickson, R. E. (1992) *Biochemistry 31*, 2728–2734.

Paddon, C. J., & Hartley, R. W. (1987) *Gene 53*, 11–19.

Plaza del Pino, I. M., Pace, C. N., & Freire, E. (1992) *Biochemistry 31*, 11196–11202.

Privalov, P. L. (1979) *Adv. Protein Chem. 33*, 167–241.

Privalov, P. L. (1982) *Adv. Protein Chem. 35*, 1–104.

Privalov, P. L., & Potekhin, S. V. (1986) *Methods Enzymol. 114*, 4–51.

Privalov, P. L., & Makhatadze, G. I. (1990) *J. Mol. Biol. 213*, 385–391.

Privalov, P. L., Plotnikov, V. V., & Filimonov, V. V. (1975) *J. Chem. Thermodyn. 7*, 41–47.

Privalov, P. L., Tiktopulo, E. I., Venyaminov, S. Yu, Griko, Yu. V., Makhatadze, G. I., & Khechinashvili, N. N. (1989) *J. Mol. Biol. 205*, 737–750.

Robert, C. H., Gill, S. J., & Wyman, J. (1988) *Biochemistry 27*, 6829–6835.

Sancho, J., Meiering, E. M., & Fersht, A. R. (1991) *J. Mol. Biol. 221*, 1007–1014.

Serrano, L., Horovitz, A., Avron, B., Bycroft, M., & Fersht, A. R. (1990) *Biochemistry 29*, 9343–9352.

Serrano, L., Kellis, J. T., Jr., Cann, P., Matouschek, A., & Fersht, A. R. (1992a) *J. Mol. Biol. 224*, 783–804.

Serrano, L., Matouschek, A., & Fersht, A. R. (1992b) *J. Mol. Biol.* 224, 805–818.

Shrake, A., & Ross, P. D. (1990) *J. Biol. Chem. 265*, 5055–5059.

Shrake, A., & Ross, P. D. (1992) *Biopolymers 32*, 925–940.

Spolar, R. S., Livingstone, J. R., & Record, M. T., Jr. (1992) *Biochemistry 31*, 3947–3955.

Straume, M., & Freire, E. (1992) *Anal. Biochem. 203*, 259–268.

Sturtevant, J. M. (1977) *Proc. Natl. Acad. Sci. U.S.A. 74*, 2236–2240.

Wiesinger, H., & Hinz, H.-J. (1986) in *Thermodynamic data for Biochemistry and Biotechnology* (Hinz, H.-J., Ed.) pp 221–226, Springer-Verlag, Heidelberg.

Reprinted from Biochemistry, 1995, 34.

A Calorimetric Study of the Thermal Stability of Barstar and Its Interaction with Barnase†

José C. Martínez,‡ Vladimir V. Filimonov,*,‡,§ Pedro L. Mateo,*,‡ Gideon Schreiber,|| and Alan R. Fersht||

Department of Physical Chemistry, Faculty of Sciences, and Institute of Biotechnology, University of Granada, 18071 Granada, Spain, University Chemical Laboratory, University of Cambridge, Cambridge CB2 1EW, U.K., and Institute of Protein Research, Russian Academy of Sciences, Pushchino, Moscow Region 142292, Russia

Received October 27, 1994; Revised Manuscript Received December 28, 1994®

ABSTRACT: The temperature-induced unfolding of single, double, and triple mutants of barstar, the specific intracellular protein inhibitor of barnase from *Bacillus amyloliquefaciens*, has been studied by high-sensitivity differential scanning calorimetry. The thermal unfolding of barstar mutants, where at least one of the two cysteine residues in the molecule had been replaced by alanine, follows a two-state mechanism at neutral and alkaline pH. The unfolding enthalpy and heat capacity changes are slightly lower than those accepted for highly compact, small, globular proteins. We have found that at pH 2.5, where barstar seems to be in a molten globule state, the protein has a heat capacity between that of the native and the unfolded states and shows some tendency for association. Scanning calorimetry experiments were also extended to the barstar–barnase complex in the neutral and alkaline pH range. The binding constants obtained from DSC studies are similar to those already obtained from other (kinetic) studies. The interaction of barstar and barnase was also investigated by isothermal calorimetry in various buffers within the pH range 6.0–10.0 and a temperature range of 15–35 °C. The favorable enthalpy contribution to the binding is about 4 times higher than the entropic one at 25 °C. The overall data analysis of the combined calorimetric results has led to the thermodynamic characterization of barstar unfolding and the interaction of barstar and barnase over a wide range of temperatures.

The study of biopolymer interaction and recognition is of importance because of the role these interactions play in many crucial biological processes. Thus, the way proteins recognize each other and bind is critical to the understanding of such processes as antigen–antibody interactions, the inhibition of some enzymes, membrane–receptor interactions, and monomer–monomer interactions to give the functional oligomeric protein and can be of invaluable help in protein folding studies (Janin & Chothia, 1990). In addition to structural aspects, the energetic and dynamic characterization of protein recognition is also essential for a rationalization of these macromolecular binding processes. The thermodynamic description of the interaction is best achieved by differential scanning (DSC)[1] and isothermal titration (ITC) calorimetry as direct methods to measure the energetics of these processes and particularly by the complementary combination of both techniques (Martínez et al., 1994).

Here, we show the application of DSC and ITC to study barstar and its interaction with barnase. Both proteins, barnase, an extracellular ribonuclease of 110 residues, and barstar, a specific intracellular barnase inhibitor of 89 residues, are produced by *Bacillus amyloliquefaciens*. Barnase is a very well characterized protein, the structure of which is known both in the crystal state (Maugen et al., 1982) and in solution (Bycroft et al., 1991), which undergoes a reversible, two-state unfolding (Hartley, 1968; Kellis et al., 1989; Martínez et al., 1994). The structure of free barstar has been studied in solution by NMR (Lubienski et al., 1993, 1994), and some of its unfolding properties have also been described (Hartley, 1989; Schreiber & Fersht, 1993b; Khurana & Udgaonkar, 1994). The two proteins form a tight 1:1 complex in solution (Hartley, 1993; Schreiber & Fersht, 1993a), the structure of which has been elucidated (Jones et al., 1993; Guillet et al., 1993; Buckle et al., 1994).

In this paper, we describe a DSC thermodynamic study of the thermal stability of free barstar and that of the barstar–barnase complex in the pH range 6.0–11.0. Wild-type barstar gives rise to complex, sometimes irreproducible, endotherms because of complications caused by the oxidation of the two cysteines, 40 and 82, present in the molecule (Hartley, 1989; Schreiber & Fersht, 1993b). Therefore, single, double, and triple barstar mutants, where at least one of the cysteines was replaced by alanine, were used throughout this work. In addition, the binding of the two proteins has been investigated by ITC in the pH range 6.0–10.0, with different buffer systems of different heats of protonation, and at four temperatures within the range 15–35 °C. The overall data analysis of the two sets of experimental calorimetric results has led to a complete thermodynamic characterization of barstar thermal denaturation and of the barstar–barnase interaction. The results are discussed in the light of the structural information available for the two proteins.

† This research has been supported by BRIDGE Grant BIOT-CT91-0270 from the European Union. P.L.M. also acknowledges financial support from DGICYT Grant PB90-0876 (Spain). J.C.M. is a predoctoral fellow of the DGICYT.

* To whom correspondence should be addressed [telephone, +34-(9)58-243333/1; Fax, +34-(9)58-274258].

‡ University of Granada.

§ Russian Academy of Sciences.

|| University of Cambridge.

® Abstract published in *Advance ACS Abstracts*, April 1, 1995.

[1] Abbreviations: DSC, differential scanning calorimetry; ITC, isothermal titration calorimetry.

0006-2960/95/0434-5224$09.00/0

MATERIALS AND METHODS

Wild-type barnase was purified as described (Serrano et al., 1990). Barstar, its single mutants C40A and C82A (with cysteines 40 or 82 replaced by alanine), double mutant C40A-C82A (DM), and triple mutants C40A-C82A-P48A (TMPA) and C40A-C82A-P48L (TMPL) (with proline 48 of the DM replaced by alanine or leucine, correspondingly) were obtained according to Schreiber and Fersht (1993a). Before the calorimetric experiments, the protein samples were extensively dialyzed against the appropriate buffer. The 1:1 complex of barnase with barstar mutants was usually made before dialysis and passed through a gel-filtration column to remove any traces of monomers. Gel chromatography was performed using a Sephadex G-50 column (1 × 30 cm) at a flow rate of 0.8 mL/min under the appropriate solvent conditions. All chemicals were of analytical grade (Sigma), and distilled, deionized water was used throughout.

The purified protein samples were prepared in Cambridge and sent to Granada where they were stored frozen in 50 mM Tris-HCl buffer, pH 8.0. Before calorimetric experiments, their purity was checked by electrophoresis, both in $NaDodSO_4$ at pH 8.8 and under native conditions with Tris–glycine buffer systems, pH 8.3. According to $NaDodSO_4$ gel electrophoresis, more than 95% of each barstar sample appeared in a major band corresponding to a polypeptide with a molecular mass of about 10 kDa.

The concentrations of the individual proteins were measured spectrophotometrically using the following extinction coefficients at 280 nm (in mg^{-1} mL cm^{-1})—2.21, barnase; 2.22, barstar; 2.26, C40A; 2.16, C82A; 2.21, DM; 2.45, TMPA; and 2.30, TMPL—as determined by the method of Gill and von Hippel (1989). An extinction coefficient of 2.2 mg^{-1} mL cm^{-1} for the barnase–DM complex was also found (other complexes between barnase and barstar mutants were not studied in this work). In all calculations, the molecular masses of barnase and barstar mutants were rounded to 12.4 and 10.2 kDa, respectively.

The calorimetric experiments on barstar and barstar–barnase complexes were routinely performed at a 0.05 M concentration of various buffers: CAPS and glycine were used in the alkaline range; PIPES, HEPES, and sodium citrate at neutral pH; and acetate and glycine at acidic pH. Scanning calorimetry was done in a computerized version of the DASM-4 calorimeter (Privalov & Potekhin, 1986) at heating rates of 0.5, 1, and 2 K/min with sample concentrations of 1.5–4 mg/mL for barstar or barnase alone and 0.6–1.2 mg/mL for the barstar–barnase complex. The reversibility of protein unfolding inside the calorimeter cell and the baseline of the instrument were routinely checked after each protein heating, as described (Privalov & Potekhin, 1986). To calculate the molar partial heat capacity of the protein, from calorimetric records, a partial specific volume of 0.73 mL/g (an average value for small globular proteins) was adopted for barnase, barstar, and their complex. The maximum possible deflection of the real partial specific volumes from the average one (4%) is much lower than the errors in C_p calculations caused by calorimetric baseline shifts from the mean position. The isothermal calorimetry experiments of barnase–barstar complexing were conducted using an isothermal titration calorimeter built at the University of Granada as described by Martínez et al. (1994).

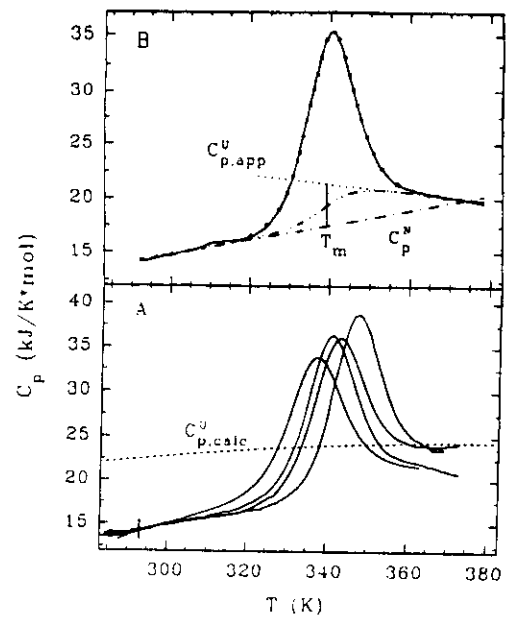

FIGURE 1: (A) Selected temperature dependencies of the partial molar heat capacities of some barstar mutants at various conditions. In order of decreasing stability: DM, 50 mM sodium citrate, pH 6.0, 1.75 mg/mL, 1 K/min; TMPL, 50 mM CAPS, pH 10.0, 1.0 mg/mL, 2 K/min; DM, 50 mM glycine, pH 10.3, 3.2 mg/mL, 1 K/min; DM, 50 mM CAPS, pH 10.8, 2.0 mg/mL, 2 K/min. The DSC traces were aligned to make their C_p coincide at 293 K with an average value of 14.3 kJ/(K·mol) [the vertical bar shows the limits of C_p(293 K) scatter]. The short-dashed line corresponds to the calculated $C^U_{p,calc}(T)$ function (see text). (B) The best fitting of one of the DSC curves for the barstar DM at pH 10.3, 50 mM CAPS, 1 K/min, 2.0 mg/mL. The solid line corresponds to the experimental $C_p(T)$ curve, and dots refer to its best fitting to the two-state model. Curves: best fit of the $C^U_{p,app}(T)$ (···), $C^N_p(T)$ (– · –), and $C^{nt}_p(T)$ (– · · –) functions. The bar at T_m shows the best-fit value of $\Delta C^U_{p,m}$ (eq 4), which in this particular case was 3.9 kJ/(K·mol).

RESULTS

Thermal Stability of Barstar Mutants. Wild-type barstar exhibits a complex unfolding transition upon heating. This problem was attributed (Hartley, 1989) to two cysteine residues (40 and 82) which, as was found later (Guillet et al., 1993; Lubienski et al., 1994), are situated in rather close proximity in the native protein structure. The melting curves of wild-type barstar, determined by DSC in this study, are also rather complex and irreproducible. To avoid all these problems in our DSC studies, we used barstar mutants in which at least one of the cysteines was replaced by alanine. All the barstar mutants exhibit quite simple and reproducible melting curves at neutral and alkaline pH values (Figure 1A). Thus, it seems that the complex unfolding pattern of the wild-type protein does result from the intramolecular cross-bridge formation upon protein heating.

Barstar loses its native conformation in the acid pH range at room temperature (Schreiber & Fersht, 1993b; Khurana & Udgaonkar, 1994) (cf. below) so that its heat-induced unfolding can be studied at only neutral or alkaline pH. These solvent conditions have been used throughout this work to change the stability of the native conformation.

At pH ≥ 6, the reversibility of unfolding for all the barstar mutants studied is rather high (up to 80%), unless the sample had been heated for too long after completion of unfolding. Although there is no dependence of the peak shape and

position on the heating rate, continued heating at high temperatures usually results in a gradual decrease of the area of the main peak. This decrease in the reversibility of the thermal unfolding must result from some irreversible processes that follow the unfolding. Such processes might be, for example, related to irreversible oligomerization of the unfolded polypeptide and/or its chemical modification (Klibanov & Ahern, 1987). No visible precipitates were formed, however, upon heating barstar solutions to 100 °C. In addition, NaDodSO$_4$ gel electrophoresis of all these samples heated inside the calorimeter revealed no additional bands with any molecular mass other than that of intact barstar, which excludes the possibility of chemical degradation of the protein. Conversely, electrophoresis under nondenaturing conditions (pH 8.3) of protein samples heated at pH $\geq$ 6 reveals minor bands with a mobility exceeding that of the native protein (results not shown). This observation suggests chemical modifications and/or incorrect refolding of the barstar mutants after their exposure to high temperatures. The slow kinetics of the irreversible processes following protein unfolding is consistent with chemical modifications. This conclusion has some support from our being unable to refold the protein that had been heated in the calorimeter, even by the addition and slow removal of 6 M urea (the degree of refolding after such treatment was always found by DSC to be incomplete).

The heat capacity of the initial, native state of fresh preparations of barstar mutants, $C_p^N(T)$, linearly increases with temperature in a typical manner for small globular proteins. The following empirical formula was deduced after averaging the initial parts of all the melting curves of barstar mutants:

$$C_p^N(T) = (14.3 \pm 1.5) + (0.08 \pm 0.008)(T - 293.2) \quad [\text{kJ/(K·mol)}] \quad (1)$$

In general, the baseline of the DASM-4 calorimeter has a very reproducible shape, but it can be shifted from its average position, which adds the greatest contribution (about 5−10%, depending on protein concentration) to the overall error in the C_p determination. The dispersion of the initial C_p slopes is usually much smaller as long as the protein solution is well equilibrated against the solvent by dialysis. In our experiments, because of using relatively low concentrations for a small protein, the dispersion of the initial slope also reached 10%. Such changes in the initial slope lead to quite large displacements of the melting curve at high temperature, which complicates the determination of the heat capacity for the unfolded state, $C_p^U(T)$. In fact, the absolute $C_p^U(T)$ values of barstar are much more widely scattered than the $C_p^N(T)$ values, and we also observed a systematic tendency for the apparent heat capacity of the denatured state to decrease with temperature (Figure 1A), instead of remaining almost constant as has been reported for many other small globular proteins (Privalov, 1979, 1989; Privalov et al., 1989; Martinez et al., 1994). Our experience in heat-induced protein denaturation has shown us that many irreversible modifications of the polypeptide chain, similar to those mentioned above, can be accompanied by an exothermic heat effect, which, depending on the kinetics of those processes, might result in an apparent stepwise decrease in the heat capacity, as will be commented upon in the Discussion. Similar decreases in the posttransitional C_p function have also been reported for some other globular proteins (Takahashi & Sturtevant, 1981; Azuaga et al., 1992). Takahashi and Sturtevant (1981) suggested a general procedure of data analysis for such cases, based on a linear approximation of the initial and final heat capacity over the transition temperature range. We have used a similar approach here with minor modifications.

Let us assume that the heat capacities of the initial and final conformational states can be represented as

$$C_p^N(T) = a_n + b_n(T - T_m) \quad (2)$$

$$C_{p,app}^U(T) = a_u + b_u(T - T_m) \quad (3)$$

Here a_n, a_u, b_n, and b_u are independent variable parameters, specific for each individual melting curve. The transition midpoint, T_m, was chosen as a reference temperature for convenience, since this parameter enters into all formulas determining the peak shape and position. If the heat capacities of the initial and final conformations are defined, and we assume that only these two conformations are populated at equilibrium and choose the initial (native) state as the reference one, then any individual function $C_p(T)$ might be described by the equations:

$$\Delta C_{p,app}^U(T) = (a_u - a_n) + (b_u - b_n)(T - T_m) = \Delta C_{p,m}^U + \Delta b_u(T - T_m) \quad (4)$$

$$\delta C_p^{exc}(T) = (\langle \Delta H^U(T) \rangle^2 / RT^2)(K/(1 + K)^2) \quad (5)$$

$$C_p^{int}(T) = C_p^N(T) + \Delta C_{p,app}^U(T)K/(1 + K) \quad (6)$$

$$C_p(T) = C_p^{int}(T) + \delta C_p^{exc}(T) \quad (7)$$

$$\Delta H^U(T) = \Delta H_m^U + \Delta C_{p,m}^U(T - T_m) + \Delta b_u(T - T_m)^2/2 \quad (8)$$

$$\Delta S^U(T) = \Delta H_m^U/T_m + (\Delta C_{p,m}^U - \Delta b_u T_m) \ln(T/T_m) + \Delta b_u(T - T_m) \quad (9)$$

$$K(T) = \exp[(\Delta S^U(T) - \Delta H^U(T)/T)/R] \quad (10)$$

where K is the equilibrium constant of unfolding, $\Delta H^U(T)$ and $\Delta S^U(T)$ are the enthalpy and entropy changes, and $\Delta C_{p,m}^U$ and ΔH_m^U are the variations in the heat capacity and the enthalpy at the transition midpoint, T_m [$K(T_m) = 1$]. These equations contain six independent parameters (a_n, b_n, a_u, b_u, ΔH_m^U, and T_m) to be adjusted by a fitting procedure. Nevertheless, because of the relatively high stability of barstar the unperturbed initial heat capacity, $C_p^N(T)$, was usually measured over a wide temperature range and could be approximated separately with high accuracy, which reduces the number of truly independent adjustable parameters to four.

The application of this fitting procedure to a typical individual melting curve is shown in Figure 1B. Both the linear approximations of the initial and final heat capacities are illustrated, as found by the curve fitting, as well as the $C_p^{int}(T)$, the T_m and the $\Delta C_{p,m}^U$, which in this case comprises as much as 20% of the total peak height. The experimental

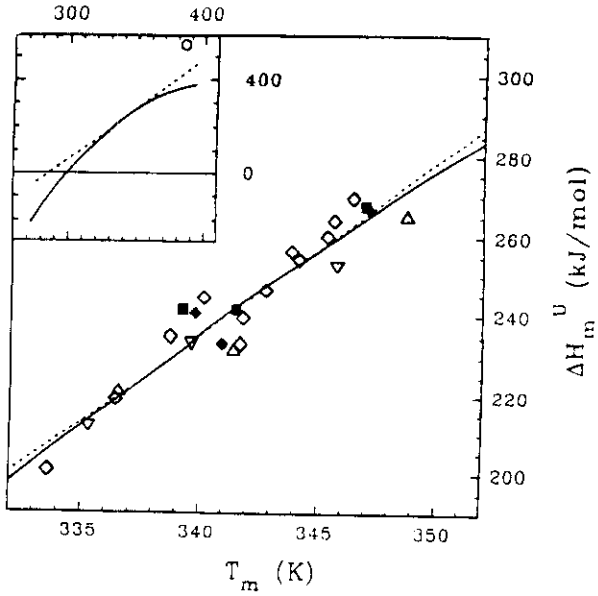

FIGURE 2: Correlation between the unfolding enthalpy and the melting temperature for barstar mutants as found by DSC data analysis: C40A (△), C82A (▽), DM (◇), TMPA (◆), and TMPL (■). Data were obtained in the pH range 6.0−10.8 for DM and 7.0−10.3 for the other mutants. The linear regression through the experimental points (- - -) and the parabolic regression made are as described in the text (—). The insert in the upper left corner shows the same two regressions at wider scales, where the open circle refers to Privalov's "limiting enthalpy" (see text).

melting curve fits the two-state curve very well, as shown by the dotted line in Figure 1B.

The ΔH_m^U values found by applying this fitting procedure to the individual melting curves of various barstar mutants are plotted in Figure 2 *versus* the corresponding melting temperatures. The linear least-squares regression line through these experimental points is represented by the equation:

$$\Delta H_m^U(T_m) = -56 + 4.35(T_m - 273.2) \quad \text{(kJ/mol)} \quad (11)$$

with standard errors in ΔH_m^U and T_m of about ±15 kJ/mol and ±0.5 K, respectively. The average of the $\Delta C_{p,m}^U$ values found by the fitting procedure over the barstar melting range, 334−349 K, was found to be 4.1 kJ/(K·mol) with a standard error as high as ±2.5 kJ/(K·mol).

Barstar Melting at Acid pH. The mutant DM at pH 2.5 does not show a DSC transition similar to that at pH ≥ 6, and neither is its $C_p(T)$ function typical for a completely unfolded protein (Figure 3). At low temperature, the protein has a much higher apparent molar heat capacity than the average value of 14.3 kJ/(K·mol) found for the native protein at 293 K and, at the same time, somewhat lower than the $C_p^U(T)$ value calculated as described in the Discussion (Figure 3). The first heating of the sample in the calorimeter cell resulted in a typical almost linear increase of C_p at temperatures below 325 K. The position and slope of the heat capacity for this initial state do not depend on the heating rate within the limits of experimental error. Increasing the temperature to above 325 K, however, caused a wide endothermic process, followed at about 365 K by a very sharp exotherm. Such sharp exotherms are typical of protein aggregation, and in fact, the position and shape of this exothermic peak depend on the heating rate in a manner expected for a kinetically controlled process. Reheating the sample showed that at low temperatures its apparent heat

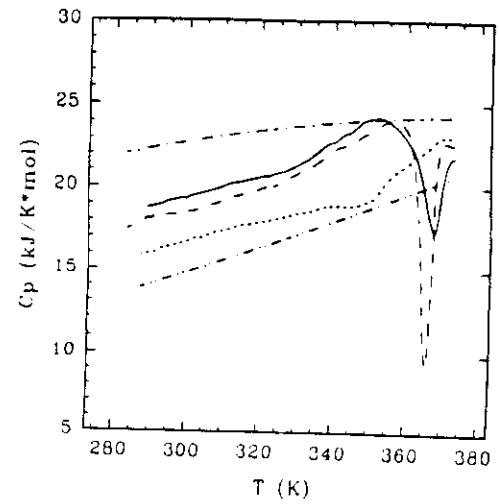

FIGURE 3: Temperature dependence of the partial molar heat capacity of the barstar DM at pH 2.5, 20 mM glycine, 1.9 mg/mL: first heating at 2 K/min (—) and at 1 K/min (— —); second heating at 1 K/min (···). For purposes of comparison we show the calculated heat capacity of the unfolded state (— · —) and the empirical approximation of the heat capacity of the native state (— ·· —).

capacity is much closer to the C_p of the native state than to that of the unfolded one (Figure 3).

The heated protein at pH 2.5 has an increase in light scattering characteristic of an association process. There is an increase in the light scattering of the mutant DM in the order: pH 7.0, pH 2.5 before heating, and pH 2.5 after heating to 100 °C (e.g., the absorbance at 330 nm of these three samples is ≃0, 0.05, and 0.15, respectively, for a concentration of the DM of about 3.5 mg/mL). Size-exclusion chromatography (results not shown) in a Sephadex G-50 column of DM solutions under these conditions showed that the DM at pH 2.5 with or without heating has a very small retention index, very close to the column exclusion volume, whereas the DM at pH 7.0, as well as that at pH 10.0, appears in the DM monomer position. Therefore, the DM clearly behaves as a monomer at pH ≥ 6, while, whatever conformation the protein has at pH 2.5, it shows a certain tendency to association concomitant with an increase in temperature. We also carried out the isothermal calorimetric measurement of the DM denaturation by changing the pH from 7.0 to 2.5 at 25 °C. The expected ΔH value (eq 11) is about 50 kJ/mol, whereas we obtained −95 ± 5 kJ/mol, which means that additional process(es) must occur with a ΔH of approximately 145 kJ/mol. Among other factors (e.g., titration of certain protein groups) this process may well be the association of the protein at pH 2.5, since, for example, the dissociation and unfolding heat of the dimeric CheY molten globule at pH 2.5 has been found to be −155 ± 20 kJ/mol (Filimonov et al., 1993).

DSC of the Barnase−Barstar Complex. Barnase forms a very tight complex with the barstar mutant (DM) at pH 7.0 (almost as tight as with the wild-type barstar) with a dissociation constant of about 2×10^{-13} M (Hartley, 1993; Schreiber & Fersht, 1993a). Such a high affinity should increase considerably, by mass action, the thermal stability of at least one of the components of the complex. This has indeed been observed in DSC experiments (Figure 4), which makes the determination of the binding constant easier.

The barnase−DM complex does not form at pH values below 3.5, and if it does, it is not very soluble in the pH

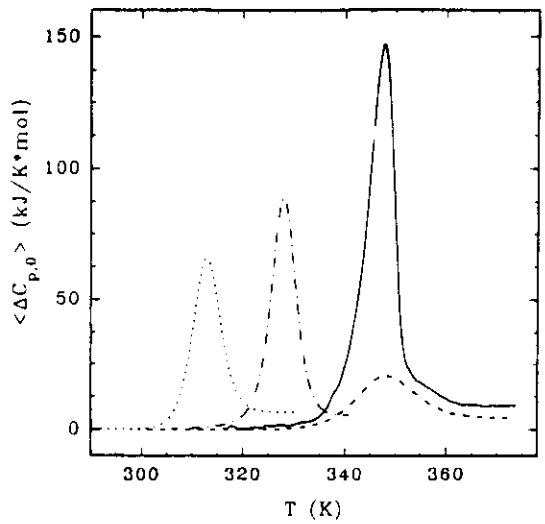

FIGURE 4: Temperature dependence of the $\langle \Delta C_{p,0} \rangle = C_p(T) - C_p^N(T)$ function at pH 7.0, 50 mM PIPES for the DM−barnase complex (—) and of its isolated individual components: DM (– –) and barnase (– · –). The melting of the complex at pH 3.0 is also shown (· · ·); it corresponds to that of barnase since barstar is already unfolded and unbound at this pH.

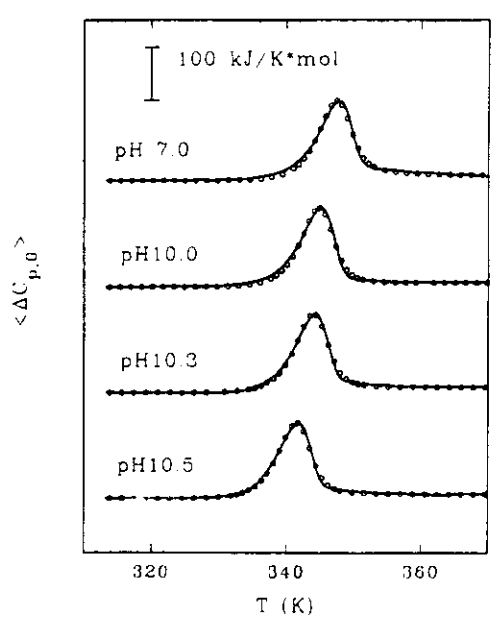

FIGURE 5: Temperature dependence of $\langle \Delta C_{p,0} \rangle$ for the DM−barnase complex at various pH values and their best fittings according to the model of eq 12 in the text. Symbols show the experimental data and solid lines their best fittings.

range 3.5−6.0 (Schreiber & Fersht, 1993a). The inability of barstar to form the complex with barnase at pH ranges around 3 was shown also by the DSC trace, which has only one *symmetric* peak with parameters (T_m and ΔH_m) corresponding to an independent melting of barnase (Figure 4). Hence, at this pH the native conformation of barstar is so energetically unfavorable that, at about 0.1 mM concentration of both proteins in solution, even the high affinity for native barnase cannot compensate for the positive Gibbs energy of barstar folding. Although the solubility of the native complex is high at neutral pH and low temperatures, the unfolding of each component under these conditions is only partially reversible, most probably due to the proximity of their isoelectric points. For example, at pH 6.0 the melting curves of the complex are not reversible on reheating and depend strongly on the heating rate. At pH 7.0 and above the situation alters with a negligible scan-rate effect on the DSC traces and a recovery of the melting profile on sample reheating of at least 60%. It must be emphasized here that the asymmetry observed in the barnase−barstar DSC curves (see Figures 4 and 5) has nothing to do with any irreversible character of the unfolding but is an integral property of any dissociation (or association) process coupled to the unfolding of the protein complex (Brandts & Lin, 1990).

Figure 4 shows that, at pH 7.0, barnase is the component of the complex that becomes more stable (by about 20 K at a working concentration of protein), while under these conditions the complex is only about 2 K more stable than the free DM. Such a low stabilization of barstar means that after dissociation of the complex, accompanied by barnase unfolding, about 40% of barstar molecules can still adopt the native conformation. This native protein fraction should melt in accordance with the unfolding parameters of barstar, i.e., in a rather wide temperature range. Indeed, the unfolding of this barstar fraction was observed as a small shoulder on the right-hand side of the main large peak (Figure 4).

Assuming that under some solvent conditions the temperature-induced unfolding of a 1:1 two-protein complex occurs at equilibrium, one can apply the following reasonable scheme to the DSC data analysis:

$$A^NB^N \overset{K^D}{\rightleftharpoons} A^N + B^N \overset{K_a^U}{\rightleftharpoons} A^U + B^N \qquad A^N + B^N \overset{K_b^U}{\rightleftharpoons} A^N + B^U \tag{12}$$

where superscripts N and U refer to the native and unfolded states of the two proteins, A and B, while the equilibrium constants K^D, K_a^U, and K_b^U refer to the dissociation of the complex followed by the independent unfolding of A and B.

The following equations can then be written for this model:

$$f_{ab} + f_{an} + f_{au} = 1 \tag{13}$$

$$f_{ab} + f_{bn} + f_{bu} = 1 \tag{14}$$

$$f_{ab} = [A^NB^N]/P_0 \tag{15}$$

$$f_{an} = [A^N]/P_0 \tag{16}$$

$$f_{au} = [A^U]/P_0 \tag{17}$$

$$f_{bn} = [B^N]/P_0 \tag{18}$$

$$f_{bu} = [B^U]/P_0 \tag{19}$$

$$K^D = [A^N][B^N]/[A^NB^N] = f_{an}f_{bn}P_0/f_{ab} \tag{20}$$

$$K_a^U = f_{au}/f_{an} \tag{21}$$

$$K_b^U = f_{bu}/f_{bn} \tag{22}$$

where the f values are defined in eqs 15−19 and P_0 stands for the molar concentration of the complex in solution. Simple transformations of these formulas lead to a quadratic equation with the following solutions:

$$f_{au} = 2K_a^U/(1 + K_a^U)Z \quad (23)$$

$$f_{bu} = 2K_b^U/(1 + K_b^U)Z \quad (24)$$

$$f_{ab} = 4P_0/QZ^2 \quad (25)$$

where

$$Q = K^D(1 + K_a^U)(1 + K_b^U) \quad (26)$$

$$Z = 1 + (1 + 4P_0/Q)^{1/2} \quad (27)$$

If we define T_d as the temperature at which $Q(T_d) = P_0/2$, then $Z(T_d) = 4$ and $f_{ab} = 0.5$, and T_d can be defined in this manner as the "temperature of complex dissociation" at a given protein concentration. The overall excess enthalpy, $\langle\Delta H_{ab}(T)\rangle$, over the initial state (A^NB^N) is expressed as

$$\langle\Delta H_{ab}(T)\rangle = (1 - f_{ab})\Delta H^D + f_{au}\Delta H_a^U(T) + f_{bu}\Delta H_b^U(T) \quad (28)$$

and the derivative of this function corresponds to the excess heat capacity function, $\langle\Delta C_{p,ab}(T)\rangle$, over the initial state:

$$\langle\Delta C_{p,ab}(T)\rangle = C_p(T) - C_{p,ab}(T) = d\langle\Delta H_{ab}(T)\rangle/dT \quad (29)$$

This function can be found here without difficulty from the experimental DSC data since, given the relatively high stability of the complex, the $C_{p,ab}(T)$ function can easily be approximated by a straight line.

For the purpose of data analysis by curve fitting, the equilibrium constants and other thermodynamic potentials can be expressed by equations similar to eqs 8−10. To reduce further the number of adjustable parameters for curve fitting, we can use here the known temperature dependencies for $\Delta H_a^U(T)$ and $\Delta H_b^U(T)$. That for barnase was obtained in our previous work (Martínez et al., 1994), and to obtain that for barstar we can use eq 11. This leaves us with only three adjustable parameters, ΔH^D, ΔS^D, and ΔC_p^D, defined as

$$\Delta H^D(T) = \Delta H^D(T_{m,b}) + \Delta C_p^D(T - T_{m,b}) \quad (30)$$

$$\Delta S^D(T) = \Delta S^D(T_{m,b}) + \Delta C_p^D \ln(T/T_{m,b}) \quad (31)$$

$$K^D = \exp(-\Delta G^D(T)/RT) = \exp[(\Delta S^D(T) - \Delta H^D(T)/T)/R] \quad (32)$$

where, once more, all the functions are calculated using the complex as the reference state.

In our analysis, the melting temperature of barstar was taken as a convenient reference to reduce extrapolation errors, since barstar alone melts at almost the same temperature as that at which the whole complex breaks down. The results of the fitting of the experimental data for the barstar(DM)−barnase complex, using the general model described above, are shown in Figure 5 and Table 1.

Isothermal Calorimetry of the Barnase−Barstar Binding. We have determined the heat effects of binding between barnase and the barstar DM at various pH values and in different buffers. The latter was necessary since the heats of buffer ionization at neutral and alkaline pH are relatively high, and also the use of various buffers allows one to

Table 1: DSC Values of the Unfolding Enthalpy, ΔH_m^U, and Melting Temperature, T_m, for Isolated Barnase (BN) and Barstar Double Mutant (DM) Samples and Thermodynamic Parameters of the Barnase Interaction with Barstar−DM at 298 K As Found by DSC and ITC

	DSC						ITC[a]			
conditions	T_m(BN) (K)	ΔH_m^U(BN) (kJ/mol)	T_m(DM) (K)	ΔH_m^U(DM) (kJ/mol)	ΔH^D(298) (kJ/mol)	ΔS^D(298) [J/(K·mol)]	K^D(298) (10^{-14} M)	ΔC_p^D(298)[b] [kJ/(K·mol)]	ΔH^D(298) (kJ/mol)	Δn(298)	Δn(298)[c]
pH 6.0 (no DSC)									49 ± 2	−0.16 ± 0.06	−0.23 ± 0.06
pH 7.0 (50 mM PIPES for DSC)	327.0 ± 0.5	556 ± 20	347.0 ± 0.5	265 ± 15	45 ± 20	−51 ± 5	15 ± 4	0.8 ± 0.1 (62 ± 3)	58 ± 3	−0.37 ± 0.06	−0.31 ± 0.06
pH 10.0 (50 mM CAPS for DSC)	321.6 ± 0.5	510 ± 20	341.6 ± 0.5	245 ± 15	45 ± 20	−93 ± 7	1.2 ± 0.3	0.9 ± 0.1 (71 ± 5)	107 ± 5	0.76 ± 0.06	
pH 10.3 (50 mM CAPS for DSC)	321.4 ± 0.5	507 ± 20	340.0 ± 0.5	240 ± 15	35 ± 20		4.0 ± 1.0	(0.9)			
pH 10.5 (50 mM CAPS for DSC)	320.4 ± 0.5	500 ± 20	338.7 ± 0.5	235 ± 15	54 ± 20		5.5 ± 1.5	(0.9)			

[a] ITC values are corrected for heat buffer effects (Figure 8). The effects of CAPS and PIPES buffers are also shown in parentheses for comparison with the ΔH^D(298) DSC data. [b] ΔC_p^D values at pH 10.3 and 10.5 were assumed to be the same as that at pH 10.0 and used for extrapolation of the DSC binding parameters to 298 K. [c] The number of protons exchanged on binding, Δn, determined directly by pH-stat.

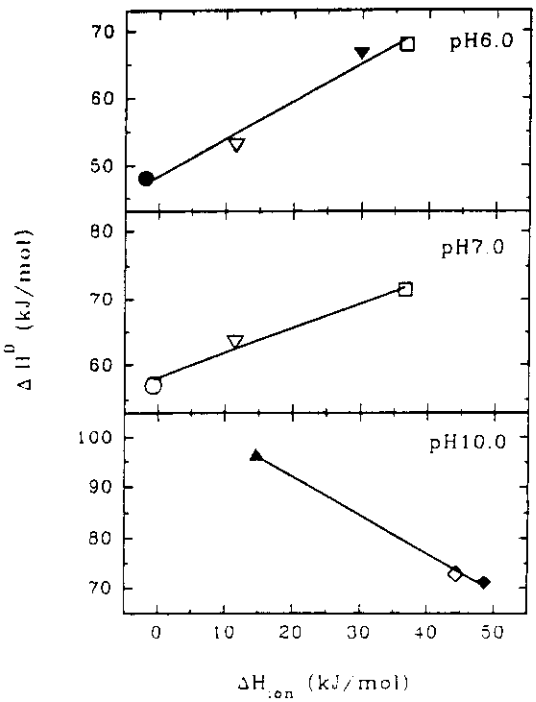

FIGURE 6: Dissociation heats, ΔH^D, of the DM−barnase complex at 25 °C and three pH values plotted *versus* the ionization heat, ΔH_{ion}, of the corresponding buffer: β-glycerophosphate (○); sodium cacodylate (●); PIPES (▽); histidine (▼); imidazole (□); sodium bicarbonate (▲); glycine (◇); CAPS (◆). Solid lines show the linear regressions through the data points.

estimate the proton exchange at binding. We made calorimetric titrations at 15, 20, 25, and 35 °C to obtain the heat capacity increment of binding (experimental points not shown). The heats of the barnase−DM interaction in different buffers at 25 °C are plotted against the heats of ionization of those buffers at three pH values in Figure 6. The straight lines in this figure correspond to the linear regressions through the data points. The slopes of these regression lines should be equal to the number of protons exchanged between the two proteins and the buffer upon binding, whereas their intercepts correspond to the binding enthalpies corrected for the buffer ionization heats. These figures are shown in Table 1 together with other isothermal titration data, as well as the results of the direct determination of the number of exchanged protons using the potentiometric pH-stat technique.

DISCUSSION

In general, heat-induced unfolding of the barstar mutants at the concentrations used in our DSC studies at pH ≥ 6.0 is quite reversible. The DSC peaks are practically independent of scan rate, and the recovery of the melting curves on a second heating of the sample is similar to that of many other globular proteins. Thus, the data analysis in Figure 2 and eq 11 would seem to be correct. Nevertheless, as stated in the results section, reversibility decreases with an increase in both the temperature reached and the time spent at high temperature, as also shown by the CD studies of Khurana and Udgaonkar (1994). Further, there is a systematic tendency for the $C_{p,app}$ to decrease after denaturation (Figure 1A). This behavior usually indicates that the unfolding either deviates from a monomolecular scheme or is highly affected

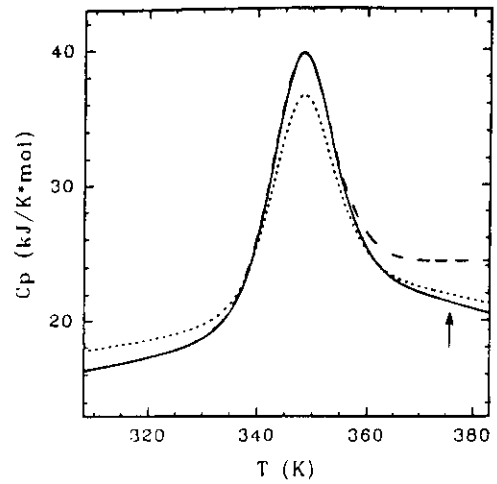

FIGURE 7: Simulations of the DSC curves for the barstar DM using the equilibrium two-state model (− −) and the Lumry−Eyring model with unfolding transition parameters similar to those of the DM at pH 7.0: $C_p^N(T) = 15 + 0.08(T - 293)$; $C_p^U(T) = 24 + 0.01(T - T_m)$; $T_m = 347$ K; $\Delta H_m^U = 265$ kJ/mol. The parameters for the irreversible step (eq 33) were $\Delta H^F = -60$ kJ/mol; $\Delta C_p^F = 0$; $T^* = 435$ K; $E = 90$ kJ/mol; $\nu = 1$ K/min. First heating (—) and reheating (• • •) were both within the Lumry−Eyring model; the first heating went up to 373 K (shown by the arrow), where the population of the F state reached 20%.

by an irreversible process. The first possibility is not consistent with the results of electrophoresis of samples of barstar. These revealed neither degradation nor aggregation of the polypeptide when it is exposed to high temperatures. Conversely, the lack of any apparent distortion of the $\delta C_p^{exc}(T)$ suggests that the irreversible steps are very slow compared to the folding/unfolding kinetics at temperatures just above the T_m of the protein. If these irreversible steps had significant *exothermic* heat effects, however, even their slow development might distort the $C_p^{int}(T)$ by producing an apparent decrease in the posttransitional heat capacity, as can be demonstrated by the following melting curve simulation (Figure 7) according to the Lumry−Eyring model:

$$N \overset{K^U}{\rightleftharpoons} U \xrightarrow{k^F} F \qquad (33)$$

which has already been successfully used for the analysis of the irreversible DSC melting curves of several proteins (Sánchez-Ruiz et al., 1988; Conejero-Lara et al., 1991). The complete development of this model, assuming there to be no heat effect during the final step, was made by Sánchez-Ruiz (1992) and Lepock et al. (1992). Using their formulas with a reasonable combination of thermodynamic and kinetic parameters, but assuming now that the final step is accompanied by a *negative enthalpy change*, one can simulate melting curves such as that shown in Figure 7. Thus, such a model may explain not only the downward slope of the posttransitional $C_{p,app}$ (Figure 1) but also the properties of the reheating curve, which completely resembles the experimental one. Figure 7 shows why such parameters as ΔH_m^U and T_m are almost unchanged by the existence of the irreversible step, while, conversely, the apparent heat capacity of the unfolded state is completely distorted.

We cannot rule out the possibility that at high temperatures the downward slope of the heat capacity may reflect at least

partially an intrinsic temperature dependence. Therefore, in addition to the linear $C^{U}_{p,app}(T)$ function, we have calculated the heat capacity for the completely unfolded state of barstar according to the method proposed by Makhatadze and Privalov (1990). Within the temperature range used, the $C^{U}_{p,calc}(T)$ function of the DM calculated by this method has a typical parabolic shape (Figure 8), which obeys the following empirical equation, obtained by a least-squares fitting of the calculated points with a second-order polynomial:

$$C^{U}_{p,calc}(T) = 22.0 + 0.043(T - 293.2) - (2.45 \times 10^{-4})(T - 293.2)^2 \quad (34)$$

Subtracting eq 34 from eq 1 gives the following $\Delta C^{U}_{p}(T)$ function:

$$\Delta C^{U}_{p,calc}(T) = 7.5 - 0.037(T - 293.2) - (2.45 \times 10^{-4})(T - 293.2)^2 \quad (35)$$

A comparison of this function with the experimental melting curves (Figure 1A) shows that it is in fact very close to the experimental C_p value in the posttransitional temperature range, although remaining somewhat higher. Nevertheless, the calculated $C^{U}_{p}(T)$ does not show any tendency to decrease in the temperature range 350−380 K, which we observed experimentally at neutral pH. Therefore, to simplify the analysis of the melting curves, we have resorted to a linear $C^{U}_{p,app}(T)$ function instead of a parabolic one.

Another approach to evaluate the unfolding heat capacity increase is to analyze the temperature dependence of the unfolding enthalpy. The quality of the least-squares regression through the experimental data hardly depended upon whether a linear or a quadratic function was used (Figure 2). The simplest approach corresponds to the linear approximation of the $\Delta H^{U}_{m}(T_m)$ (eq 11) with a constant $\Delta C^{U}_{p,m}$ of 4.3 kJ/(K·mol). This value not only compares well with the 4.1 kJ/(K·mol) found for $\Delta C^{U}_{p,m}$ from the average of the curve-fitting results but is also reasonably close to the value of 5.3 kJ/(K·mol) (Figure 8) predicted by eq 35 for an "average" melting temperature of 340 K. It must be emphasized though that the results given here for the DM, as with many other data published for small globular proteins, are of dubious use for any reliable extrapolation of the heat effect to 140 °C or even to 110 °C, for the reasons discussed above. For example, the linear approximation of the specific unfolding enthalpy based on eq 11 passes very close to, although slightly below, the "universal" crossing point of 52 J/g at 110 °C, while the best parabolic approximation of the experimental data, which, according to Privalov et al. (1989), should be more realistic, falls further from that value even at 140 °C (Figure 2).

The question still remains as to what extent the application of the two-state model is valid for barstar unfolding. The applicability of this model can be checked by a comparison of the quality of the fitting with that of any other reasonable model. For instance, the introduction of an additional, intermediate step sometimes improves the quality of curve fitting simply because the fitting procedure acquires more freedom with additional variable parameters. In this case it is necessary not only to compare the quality of the fitting but also to consider the populations of the intermediate state.

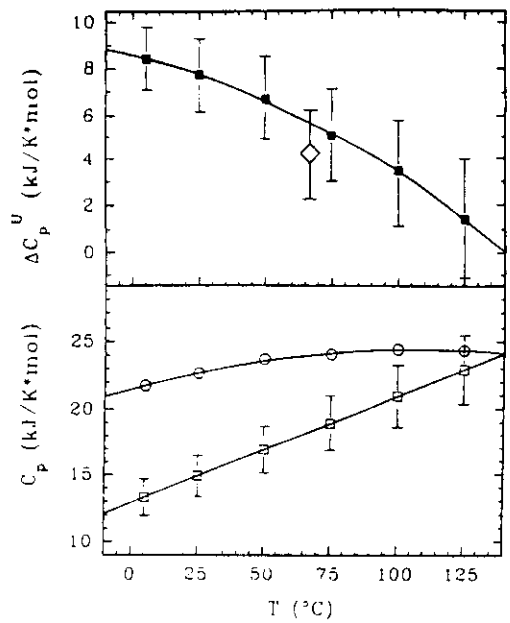

FIGURE 8: Result of the $C^{U}_{p,calc}(T)$ and $\Delta C^{U}_{p,calc}(T)$ calculations of the barstar DM according to Makhatadze and Privalov (1990) (see text). Lower part: calculated $C^{U}_{p,calc}(T)$ values (open circles) and the parabolic least-squares regression through these values; the straight line refers to an empiric $C^{N}_{p}(T)$ linear function found by averaging experimental data (eq 1), where the open squares with bars show the corresponding errors. Upper part: the heat capacity increase upon DM unfolding arising from the difference between the two lines in the lower part, including error bars. The open diamond with error bar corresponds to the average experimental value of $\Delta C^{U}_{p,app}$ at an "average" melting temperature of 340 K (see text).

Thus, when the intermediate state turns out to be only marginally populated, i.e., less than 10% at maximum, it can be concluded that the two-state approach affords a sufficiently good approximation to the experimental data *within the limits of experimental error*. This was actually the case in all our barstar DSC experiments at neutral and alkaline pH.

The DSC traces of barstar at pH 2.5 did not indicate any cooperative unfolding despite the apparent heat capacity of the protein at low temperature being closer to that of the native state than that of the completely unfolded one. Nevertheless, light scattering and chromatography results with this "acid-denatured" form showed that it seems to correspond to protein oligomers rather than to monomers. It appears that protein association can stabilize elements of residual secondary and, to some extent, tertiary structure, in accordance with the molten globule characteristics reported for this "denatured" state (Kurana & Udgaonkar, 1994; Lubienski et al., 1994). Kurana and Udgaonkar (1994) have shown that, although the acidic form of barstar (the A form or molten globule at pH <4) has less secondary and tertiary structure than the native state (pH >5), the former requires higher concentrations of denaturant to unfold than the latter. These authors also describe the unfolding of the A state by urea or GuHCl as a complex, non-two-state transition with at least one intermediate state. All these results are compatible with an association state of barstar at pH 2.5 in our concentration range. It is worth mentioning here that the molten globule state also detected at pH 2.5 for CheY has a strong tendency to form at least dimers in solution (Filimonov et al., 1993). In addition, Sanz et al. (1994) have recently

shown that the A state of barnase undergoes self-association in solution at pH 2.7.

The barnase DSC results shown in Table 1 are new experiments similar to those reported at acid pH (Martinez et al., 1994), with which they correlate very well. The barstar−DM sample mainly used here has been shown to be fully functional both *in vivo* and *in vitro* (Hartley, 1993). The value of ΔG for unfolding, 21.0 ± 1.6 kJ/mol (5.0 ± 0.4 kcal/mol), agrees with that of Schreiber and Fersht (1993b), 4.84 ± 0.18 kcal/mol (both at 25 °C and pH 8.0), obtained from urea denaturation of the DM. The specific enthalpy values of unfolding found for the various mutants used here (Figure 2) are slightly lower at the corresponding T_m than those reported for small, highly compact, globular proteins, whereas the specific ΔC_p of unfolding falls within the lowest limit for these proteins (Privalov, 1979). Barstar has a well-defined hydrophobic core with low solvent accessibility, although the ring of Phe-74 flips freely inside the core, which would indicate that the barstar core is not rigid and well packed but more fluid in character (Lubienski et al., 1994). This character can be reflected in the above-mentioned comparatively low ΔH and ΔC_p values.

DSC and ITC have proved to be very efficient as complementary techniques to characterize the energetics of the barnase−DM interaction. The binding constant at 25 °C, determined from the combined ITC and DSC analysis (Table 1), agrees very well with those calculated from kinetic studies (Hartley, 1989, 1993; Schreiber & Fersht, 1993a), despite the fact that our value had to be extrapolated over a temperature range of 50 °C. The errors in the binding enthalpy obtained by DSC are obviously higher than those directly obtained by ITC because the former were calculated from other, much higher heat effects. Nevertheless, the DSC enthalpy values at 25 °C compare with those obtained from ITC within experimental uncertainty (Table 1). The entropy values shown in Table 1 were obtained from the K_d and ITC enthalpy data, whereas the ΔS values obtained from the DSC data analysis had a higher error (about 30%), just as had the ΔH values.

The barnase−barstar binding is overall both enthalpy- and entropy-driven, although the enthalpy term is about 4 times higher than the entropic one at pH 7.0 at 25 °C. This high negative enthalpy binding value correlates very well with our present knowledge of the structural information of the complex (Hartley, 1993; Jones et al., 1993; Guillet et al., 1993; Buckle et al., 1994). Thus, the barstar−barnase interface is formed by highly polar and charged surfaces, forming a network of polar interactions with 14 hydrogen bonds and several electrostatic bridges, interactions characterized by a few kilocalories per mole [cf. Gillet et al. (1993) and Buckle et al. (1994)]. In addition, a number of well-ordered water molecules are at the interface, some of them forming hydrogen bond bridges between barnase and barstar, allowing for some flexibility at the protein−protein interface. The binding enthalpy should, therefore, come mainly from the creation of this whole net of electrostatic interactions. Given the polar character of the protein binding surfaces and the remaining ordered water, one should expect a comparatively small entropic contribution, as is in fact the case. The negative entropy sign, however, suggests that some water is still released on binding and/or the overall structure becomes less rigid. Apart from the flexible character of the interface region, barstar seems to expand on binding, with localized, minor changes in barnase (Guillet et al., 1993; Buckle et al., 1994). In addition, negative entropy contributions should be expected from strong, localized salt bridges. Nevertheless, a hydrophobic effect should also be taken into account, considering the concomitant negative ΔC_p value of binding, which is generally accepted to have a mainly hydrophobic origin besides the change in internal degrees of freedom. The splitting of the binding ΔC_p, according to the method proposed by Sturtevant (1977), leads in fact to negative values for both the hydrophobic and the vibrational contributions of ΔC_p [−168 and −23 cal/(K·mol), respectively]. Consequently, both a certain release of water molecules and a more flexible protein complex structure are to be expected as a result of barnase−barstar interaction.

NOTE ADDED IN PROOF

During the preparation of this paper another publication on the DSC of the barnase−barstar complex has appeared (Makarov et al., 1994), and a development of the Lumry−Eyring model similar to ours has also been described in detail by Milardi et al. (1994).

ACKNOWLEDGMENT

We thank Dr. A. Parody for allowing us to use the Gill-type ITC and Drs. M. E. Harrous and L. García for helping us in our use of the technique.

REFERENCES

Azuaga, A. I., Galisteo, M. L., Mayorga, O. L., Cortijo, M., & Mateo, P. L. (1992) *FEBS Lett. 309*, 258−260.
Brandts, J. F., & Lin, L.-N. (1990) *Biochemistry 29*, 6927−6940.
Buckle, A. M., Schreiber, G., & Fersht, A. R. (1994) *Biochemistry 33*, 8878−8889.
Bycroft, M., Ludvigsen, S., Fersht, A. R., & Poulsen, F. M. (1991) *Biochemistry 30*, 8697−8701.
Conejero-Lara, F., Sanchez-Ruiz, J. M., Mateo, P. L., Burgos, F. J., Vendrell, J., & Avilés, F. X. (1991) *Eur. J. Biochem. 200*, 663−670.
Filimonov, V. V., Prieto, J., Martínez, J. C., Bruix, M., Mateo, P. L., & Serrano, L. (1993) *Biochemistry 32*, 12906−12921.
Gill, S. C., & von Hippel, P. H. (1989) *Anal. Biochem. 182*, 319−326.
Guillet, V., Lapthorn, A., Hartley, R. W., & Mauguen, Y. (1993) *Curr. Opin. Struct. Biol. 1*, 165−167.
Hartley, R. W. (1968) *Biochemistry 7*, 2401−2408.
Hartley, R. W. (1989) *Trends Biochem. Sci. 14*, 450−454.
Hartley, R. W. (1993) *Biochemistry 32*, 5978−5984.
Janin, J., & Chothia, C. (1990) *J. Biol. Chem. 265*, 16027−16030.
Jones, D. N. M., Bycroft, M., Lubienski, M. J., & Fersht, A. R. (1993) *FEBS Lett. 331*, 165−172.
Kellis, J. T., Jr., Nyberg, K., & Fersht, A. R. (1989) *Biochemistry 28*, 4914−4922.
Khurana, R., & Udgaonkar, J. B. (1994) *Biochemistry 33*, 106−115.
Klibanov, A. M., & Ahern, T. J. (1987) *Protein Engineering* (Oxender, D. L., & Fox, C. F., Eds.) pp 213−218, Alan R. Liss, New York.
Lepock, J. R., Ritchie, K. P., Rodahl, A. M., Heinz, K. A., & Kruuv, J. (1992) *Biochemistry 31*, 12706−12712.
Lubienski, M. J., Bycroft, M., Jones, D. N. M., & Fersht, A. R. (1993) *FEBS Lett. 332*, 81−87.
Lubienski, M. J., Bycroft, M., Freund, S. M. V., & Fersht, A. R. (1994) *Biochemistry 33*, 8866−8877.
Lumry, R., & Eyring, H. (1954) *J. Phys. Chem. 58*, 110−120.
Makarov, A. A., Protasevich, I. I., Lobachev, V. M., Kirpichnikov, M. P., Yakovlev, G. I., Gilli, R. M., Briand, C. M., & Hartley, R. W. (1994) *FEBS Lett. 354*, 251−254.
Makhatadze, G. I., & Privalov, P. L. (1990) *J. Mol. Biol. 213*, 375−384.

Martínez, J. C., El Harrous, M., Filimonov, V. V., Mateo, P. L., & Fersht, A. R. (1994) *Biochemistry 33*, 3919−3926.
Mauguen, Y., Hartley, R. W., Dodson, E. J., Dodson, G. G., Bricogne, G., Chothia, C., & Jack, A. (1982) *Nature 297*, 162−164.
Milardi, D., La Rosa, C., & Grasso, D. (1994) *Biophys. Chem. 52*, 183−189.
Privalov, P. L. (1979) *Adv. Protein Chem. 33*, 167−241.
Privalov, P. L. (1989) *Annu. Rev. Biophys. Biophys. Chem. 18*, 47−69.
Privalov, P. L., & Potekhin, S. V. (1986) *Methods Enzymol. 114*, 4−51.
Privalov, P. L., & Makhatadze, G. I. (1990) *J. Mol. Biol. 213*, 385−391.
Privalov, P. L., Tiktopoulo, E. I., Venyaminov, S. I., Griko, Y. V., Makhatadze, G. I., & Khechinashvili, N. N. (1989) *J. Mol. Biol. 205*, 737−750.
Sanchez-Ruiz, J. M. (1992) *Biophys. J. 61*, 921−935.
Sanchez-Ruiz, J. M., Lopez-Lacomba, J. L., Cortijo, M., & Mateo, P. L. (1988) *Biochemistry 27*, 1648−1652.
Sanz, J. M., Johnson, C. M., & Fersht, A. R. (1994) *Biochemistry 33*, 11189−11199.
Schreiber, G., & Fersht, A. R. (1993a) *Biochemistry 32*, 5145−5150.
Schreiber, G., & Fersht, A. R. (1993b) *Biochemistry 32*, 11195−11203.
Serrano, L., Horovitz, A., Avron, B., Bycrosft, M., & Fersht, A. R. (1990) *Biochemistry 29*, 9343−9352.
Sturtevant, J. M. (1977) *Proc. Natl. Acad. Sci. U.S.A. 74*, 2236−2240.
Takahashi, K., & Sturtevant, J. M. (1981) *Biochemistry 20*, 6185−6190.

BI942516Z

Differential Scanning Calorimetry of the Irreversible Thermal Denaturation of Thermolysin†

José M. Sánchez-Ruiz, José L. López-Lacomba, Manuel Cortijo,‡ and Pedro L. Mateo*
Departamento de Química Física, Facultad de Ciencias, Universidad de Granada, 18071 Granada, Spain
Received June 5, 1987; Revised Manuscript Received October 9, 1987

ABSTRACT: A differential scanning calorimetry study of the thermal denaturation of *Bacillus thermoproteolyticus rokko* thermolysin was carried out. The calorimetric traces were found to be irreversible and highly scan-rate dependent. The shape of the thermograms, as well as their scan-rate dependence, can be explained by assuming that the thermal denaturation takes place according to the kinetic scheme $N \xrightarrow{k} D$, where k is a first-order kinetic constant that changes with temperature, as given by the Arrhenius equation, N the native state, and D the unfolded state or, more probably, a final state, irreversibly arrived at from the unfolded one. On the basis of this model, the value of the rate constant as a function of temperature and the activation energy have been calculated. It is shown that the proposed model may be considered as being one particular case of that proposed by Lumry and Eyring [Lumry, R., & Eyring, H. (1954) *J. Phys. Chem. 58*, 110] $N \rightleftharpoons D \rightarrow I$, where N is the native state, D the unfolded one, and I a final state, irreversibly arrived at from D. Lastly, some comments are made on the use of the scan-rate effect on the calorimetric traces as an equilibrium criterion in differential scanning calorimetry.

The study of the in vitro unfolding process in proteins has been a subject of increasing interest during recent years. Thus, the transition from the native to the denatured state for many proteins has been followed by different techniques, using mainly the kinetic or the thermodynamic approach (Tanford, 1968, 1970; Lapanje, 1978; Ghelis & Yon, 1982). This transition has generally been achieved by denaturant agents, such as urea or Gdn-HCl,[1] by changes in the pH and/or ionic strength, or by temperature. In this latter case the development of high-sensitivity differental scanning microcalorimetry (DSC) (Privalov, 1980) has been very important, since this technique permits the direct calculation of all the unfolding thermodynamic functions and, furthermore, can also be used to check the validity of the two-state model for the process by calculating and comparing both the calorimetric and the van't Hoff enthalpies of denaturation (Sturtevant, 1974; Privalov, 1979; Pfeil, 1981; Mateo, 1984). In addition, a knowledge of the heat capacity value of the protein as a function of temperature permits the calculation of its molecular partition function and, through the appropriate algorithm (Freire & Biltonen, 1978; Privalov et al., 1981), the deconvolution of the unfolding thermal profile into two-state-type processes. This analysis has already been applied to several proteins of various sizes and complexity, leading to the definition and characterization of submolecular cooperative blocks as structural domains of the macromolecule (Privalov et al., 1981; Privalov, 1982; Potekhin & Privalov, 1982; Privalov & Medved, 1982; Novokhatny et al., 1984; Rigell et al., 1985; Tsalkova & Privalov, 1985).

An essential prerequisite for these thermal studies, however, is that there should be thermodynamic equilibrium in the sample throughout the temperature-induced unfolding process. The equilibrium criterion usually applied is the reproducibility of the trace in a second heating of the sample, the so-called calorimetric reversibility. In many cases, however, the second thermogram shows no thermal effect and, therefore, according to the above-mentioned criterion, thermodynamic functions for the process, such as changes in entropy and Gibbs function, cannot be extracted from the first trace.

It has recently been shown, nevertheless, that the DSC thermograms for the thermal denaturation of several proteins can be interpreted in terms of the van't Hoff equation, in spite of the calorimetric irreversibility (Manly et al., 1985; Edge et al., 1985; Hu & Sturtevant, 1987). This can be explained if we assume that an irreversible alteration of the unfolded state takes place, with little heat effect, at temperatures higher than those at which the calorimetric transition occurs. These results indicated that the lack of calorimetric reversibility does not necessarily preclude the derivation of thermodynamic information from the calorimetric trace. It is still conceivable, of course, to find DSC traces that do not follow equilibrium thermodynamics, that is, traces that are kinetically controlled and, therefore, scan-rate dependent.

In this paper we describe a simple model for this type of DSC thermogram, and we show that the traces for the thermal denaturation of thermolysin can be quantitatively interpreted according to this working scheme.

Experimental Procedures

Thermolysin (EC 3.4.24.4), as a crystallized and lyophilized powder (lot 95F-0551), FAGLA, and HEPES were obtained from Sigma, and NaCl was obtained from Merck. All chemicals used were of the highest available purity. Distilled, deionized water was used throughout.

Prior to use, the thermolysin was additionally purified by crystallization according to the method of Holmquist and Vallee (1974) and its concentration calculated from the absorbance at 280 nm by using an $E^{1\%}$ value of 17.65 (Ohta et al., 1966). The enzymatic assay of thermolysin was carried out by measuring the peptidase activity of the enzyme, using the chromophore FAGLA as substrate and following the de-

† This research was supported by CAICYT Grant 1233/84.
‡ Present address: Departamento de Química Física Farmacéutica, Facultad de Farmacia, Universidad Complutense, 28071 Madrid, Spain.

[1] Abbreviations: DSC, differential scanning calorimetry; FAGLA, *N*-[3-(2-furyl)acryloyl]glycyl-L-leucinamide; Gdn·HCl, guanidine hydrochloride; HEPES, *N*-(2-hydroxyethyl)piperazine-*N*'-2-ethanesulfonic acid; SDS, sodium dodecyl sulfate.

0006-2960/88/0427-1648$01.50/0

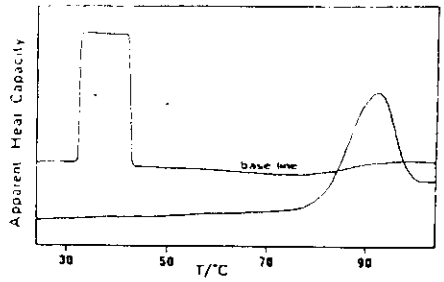

FIGURE 1: Original calorimetric recording of heat absorption of thermolysin solution at 1 K/min and pH 7.5, protein concentration 0.6 mg/mL. The endotherm on the base line corresponds to a 50-μW calibration mark.

crease in absorbance at 322 nm (Khan & Darnall, 1978).

All absorbance measurements were carried out in a Cary 210 spectrophotometer with the cells maintained at 25 °C. DSC experiments were performed in a DASM-1M calorimeter with cell volumes of 1 mL under an extrapressure of 1 atm to prevent any degassing during the heatings. Four different scan rates were used within the range of about 0.2–2 K/min. The calorimetric reversibility of the thermally induced transition was checked by reheating the protein solution in the calorimetric cell after the cooling from the first run. The calculation of the denaturation enthalpy was as has been described elsewhere (Mateo, 1984).

Protein solutions were prepared by dissolving dry samples in buffer solutions. Before the calorimetric experiments, the sample solutions were dialyzed for 24 h at 4 °C against three changes of a large volume of the dialysis buffer. The buffer used was 10 mM HEPES, 0.1 M NaCl, and 10 mM $CaCl_2$ at pH 7.5. For all the measurements the protein concentrations were in the range of 0.5–1.0 mg/mL. In the calculations of molar quantities the molecular weight used for the protein was 34 600, estimated from the known sequence of thermolysin (Matthews et al., 1974).

Results

Figure 1 shows an original DSC recording for the thermal denaturation of thermolysin at pH 7.5 and at a scan rate of 1 K/min. The traces were corrected for the calorimetric base line (see Figure 1) and for the difference in heat capacity between the initial and final states by using a linear chemical base line traced between the initial and final temperatures of the transition. The use of a sigmoidal base line, as described by Takahashi and Sturtevant (1981), leads to practically the same corrected traces. The corrected calorimetric traces, i.e., the excess heat capacity function versus temperature profiles, are given in Figure 2A at four different scan rates.

The reversibility of the process was checked as described under Experimental Procedures, and no transition was obtained in the second run of all the samples. As is evident in Figure 2A, the temperature corresponding to the maximum heat capacity, T_m, is highly dependent on the scan rate, which suggests that the denaturation process is kinetically determined.

In order to explain these results we have assumed that the process taking place in the calorimetric cell is a two-state irreversible process that can be represented as

$$N \xrightarrow{k} D$$

where N is the native state, D the unfolded state or, more probably, a final state, arrived at irreversibly from the unfolded one (see Discussion), and k a first-order kinetic constant, which changes with temperature according to the Arrhenius equation. The calorimetric experiment is assumed to start at a temperature low enough to make the reaction rate negligible and

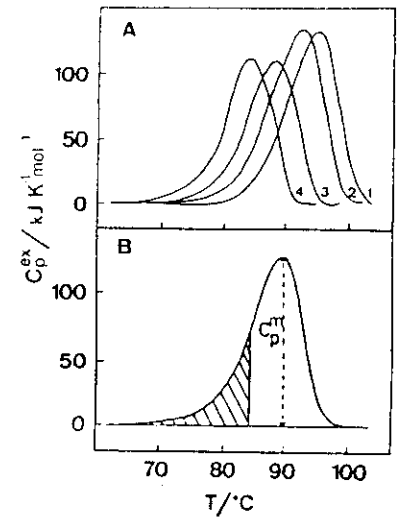

FIGURE 2: (A) Excess heat capacity of thermolysin at pH 7.5 versus temperature obtained at four different scan rates: (1) 1.9; (2) 1.0; (3) 0.5; and (4) 0.2 K/min. (B) Theoretical excess heat capacity curve versus temperature obtained according to eq A18; values used were T_m = 90 °C, specific denaturation enthalpy 39 J/g, and E = 282 kJ/mol.

hence the concentration of the native state equal to the total protein concentration.

A mathematical elaboration of this model (see Appendix) allows us to calculate the activation energy of the kinetic process in several different ways.

(A) The rate constant of the reaction at a given temperature, T, can be obtained by using

$$k = vC_p/(Q_t - Q) \qquad (1)$$

where v (K/min) stands for the scan rate, C_p for the excess heat capacity, Q_t for the total heat of the process, and Q for the heat evolved at a given temperature, T (proportional to the hatched area in Figure 2B). The energy of activation, E, can then be obtained from the values of k at several temperatures by using the Arrhenius equation $k = A \exp(-E/RT)$. The corresponding Arrhenius plot, ln k versus $1/T$, including data from the four scan rates used, is given in Figure 3A. There is excellent agreement between the rate constants calculated from the traces obtained at four different scan rates. A value of 275 ± 5 kJ/mol for the energy of activation can be calculated from the slope of the Arrhenius plot in Figure 3A.

(B) The proposed kinetic model predicts that the temperature value corresponding to the maximum of the heat capacity curve, T_m, should change with the scan rate according to

$$\frac{v}{T_m^2} = \frac{AR}{E} e^{-E/RT_m} \qquad (2)$$

Therefore, a plot of ln (v/T_m^2) versus $1/T_m$ should result in a straight line with a slope equal to $-E/R$. This plot is shown in Figure 3B for the four scan rates involved; the four data points fit a straight line very well, and the calculated activation energy is 269 ± 5 kJ/mol.

(C) The dependence of the heat evolved with temperature can be expressed as

$$\ln\left(\ln\frac{Q_t}{Q_t - Q}\right) = \frac{E}{R}\left(\frac{1}{T_m} - \frac{1}{T}\right) \qquad (3)$$

Thus, a plot of ln [ln $[Q_t/(Q_t - Q)]$] versus $1/T$ should give rise to straight lines, the slope of each one being $-E/R$. These plots are given in Figure 3C, and the average activation energy

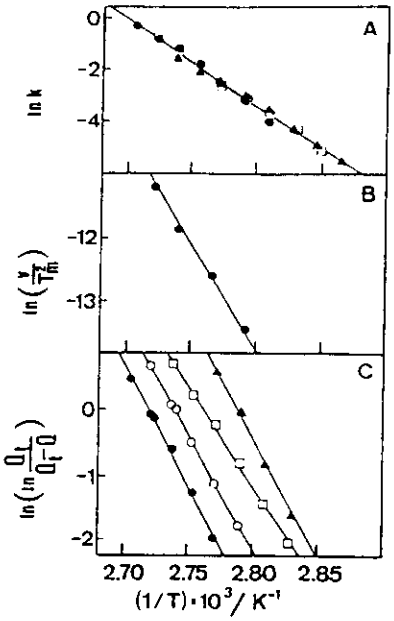

FIGURE 3: (A) Arrhenius plot including k data from the four scan rates used (Figure 2A): (●) 1.9; (○) 1.0; (□) 0.5; and (▲) 0.2 K/min. At the four scan rates only k values corresponding to the thermal effects higher than 5% or lower than 95% of the total unfolding heat were used to avoid the relative higher uncertainty at the beginning and the end of the transition. (B) Plot of ln (υ/T_m^2) versus $1/T_m$. Here the $1/T$ coordinate actually represents $1/T_m$. Each data point corresponds to one of the four scan rates used. (C) Values of ln [ln $[Q_t/(Q_t - Q)]$] plotted versus $1/T$. Symbols are the same as those used in (A).

thus obtained is 296 ± 14 kJ/mol.

In addition, the values of T_m can be calculated from the X-axis intercepts in these plots. The values obtained were 367.6, 365.0, 362.0, and 358.6 K for the scan rates 1.9, 1.0, 0.4, and 0.2 K/min, respectively. These T_m values compare well with the corresponding ones obtained directly from the calorimetric traces: 367.2, 364.8, 361.5, and 358.1 K.

It is interesting to note that, according to eq 3, when $T = T_m$, the value of ln [ln$(Q_t - Q)$]] must be equal to zero, and therefore $Q_t/(Q_t - Q_m) = e$, where Q_m is the heat evolved at T_m. The average value of $Q_t/(Q_t - Q_m)$ for the four scan rates is 2.59 ± 0.1, with a percentage deviation from the e value of lower than 5%.

(D) The activation energy can also be calculated from the heat capacity at the maximum of the trace, C_p^m, according to

$$E = eRC_p^m T_m^2/Q_t \qquad (4)$$

When this expression is applied to the four traces of Figure 3C, an average activation energy of 287 ± 9 kJ/mol is obtained.

We must point out that the four methods employed to obtain the activation energy involve different approximations (see Appendix) and use different experimental information. Thus, method D uses parameters from the maximum of the excess heat capacity curve, while method C is based on the effect of the scan rate on the temperature of the maximum and method B tests the shape of the traces. These three methods assume that the Arrhenius equation holds true. Method A, on the other hand, checks that the rate constants calculated from the traces obtained at different scan rates agree and would continue to be valid even if the Arrhenius equation did not hold good or if the activation energy were strongly temperature dependent (nonlinear Arrhenius plot). It is clear that the excellent agreement between the results obtained by using all of these four methods supports the validity of the proposed kinetic model for the thermal denaturation of thermolysin.

The overall average value for the activation energy (at pH 7.5, including all the results obtained, by using the four methods) is 282 ± 8 kJ/mol, which compares well with the values reported by Fujita et al. (1979), 330 kJ/mol at pH 8.2, and Voordouw et al. (1976), 275 kJ/mol at pH 6, using noncalorimetric techniques. The slight differences observed can be attributed to a certain small pH dependence of the energy of activation. In fact, we have carried out DSC experiments on the thermolysin thermal unfolding under the same conditions as those of Fujita et al. (1979) and found an E value of 329 ± 5 kJ/mol, which agrees exactly with their value (results not reported). There is also agreement between the rate constants given by these authors and those calculated from the calorimetric traces by using our method A.

Finally, the denaturation calorimetric enthalpy of thermolysin increases slightly with the scan rate, that is, with the T_m value. The average specific enthalpy obtained was 38.6 ± 1.5 J/g (1336 ± 50 kJ/mol), a value that compares well with those published for compact globular proteins of similar denaturation temperatures (Privalov, 1979).

DISCUSSION

We have shown that the DSC thermograms for the thermal denaturation of thermolysin can be interpreted in terms of a kinetic process

$$N \xrightarrow{k} D$$

where k is a first-order kinetic constant that changes with temperature as described by the Arrhenius equation.

This model predicts that the calorimetric traces should be highly dependent on the scan rate, as is the case for thermolysin. It should be borne in mind, however, that the time response of the calorimeter may also produce a scan-rate dependence of the traces, especially when one is dealing with sharp transitions such as, for instance, the main lipid transition. Lechuga (1985) has shown how the effect of the finite time response of the instrument can be corrected for. When his procedure is applied to thermolysin calorimetric traces, it is found that the corrected and noncorrected traces are virtually identical, which is to be expected given the broadness of thermolysin transitions. It is clear, therefore, that the observed scan-rate dependence can be attributed to chemical kinetic factors. The analysis carried out under Results demonstrates that the proposed kinetic model is able consistently to explain such a dependence.

This model would appear to suggest that the unfolded state is thermodynamically more stable than the native one throughout the temperature range of the calorimetric experiment. We must emphasize, however, that while the proposed model is the simplest one, other more complex models may come back to a first-order kinetic process. For instance, a more realistic representation of the irreversible thermal denaturation of a protein might be (Lumry & Eyring, 1954)

$$N \underset{k_2}{\overset{k_1}{\rightleftharpoons}} D \xrightarrow{k_3} I$$

where I is a final state irreversibly arrived at from the unfolded state, D. If we assume that all three processes are first-order ones and that $k_3 \gg k_2$ at any moment, most of the D molecules will be converted to I instead of returning to N through the process D → N. As a result the equilibrium between N and D will not be established, the concentration of D always being very low, and thus the denaturation may be considered as being an irreversible process, N → I, kinetically controlled by the

relatively slow conversion from N to D. That is

$$N \xrightarrow{k_3} I$$

which would lead to the same kinetic equations as those resulting from our original model, N → D. It is of interest to note that if the D → I process is much faster than the D → N one, the kinetic order of the former is immaterial.

The irreversible step in the denaturation pathway of many proteins has been put down to a variety of mechanisms, including protein aggregation, deamination of Asn/Gln residues, isomerization of proline residues, chain separation in oligomeric proteins, loss of cofactor, etc. [see Privalov (1982), Ahern and Klibanov (1985), and Zale and Klibanov (1986)]. As far as the irreversible thermal denaturation of thermolysin is concerned, autolysis might be playing a part, and this would appear to be borne out by SDS gel electrophoresis of the scanned samples. It is worth pointing out, however, that the thermal denaturation of thermolysin does not seem to be a unique case, and, in fact, results obtained in the authors' laboratory indicate that the DSC traces for other proteins, such as procarboxypeptidase A, in which no evidence for autolysis has been found, may also be interpreted according to the proposed kinetic model (manuscript in preparation).

In order to apply equilibrium thermodynamics to the analysis of DSC transitions, the prime necessity is for chemical equilibrium to exist throughout the temperature range of the transition. It is usually assumed that this condition is fulfilled in those cases in which calorimetric reversibility is found. Furthermore, it has recently been reported (Edge et al., 1985; Manly et al., 1985; Hu & Sturtevant, 1987) that some calorimetric transitions corresponding to thermal denaturation of proteins can be adequately analyzed in terms of equilibrium thermodynamics, in spite of calorimetric irreversibility. In these cases the equilibrium criterion applied was the agreement between the van't Hoff enthalpy values calculated from the shape of the trace and those calculated from the effect of the ligands and from the protein concentration on the transition temperature. Within the context of the model N ⇌ D → I, these results can be easily understood if we assume that $k_3 \ll k_2$ within the temperature range at which the transition occurs; the irreversible step may, nevertheless, be faster at higher temperatures, thus originating the calorimetric irreversibility.

A conclusion that can be drawn from this work, as well as from general principles, is that if the process giving rise to the calorimetric transition is kinetically controlled, the calorimetric traces should be dependent on the scan rate. Accordingly, we would like to suggest that the effect of scan rate on the thermograms (after correcting, if necessary, for the effect of the finite time response of the instrument) may be used as an alternative equilibrium criterion in differential scanning calorimetry. Thus, the detection of a clear scan-rate dependence of the traces should preclude their interpretation in terms of equilibrium thermodynamics. This idea has been advanced before by several authors, but rarely heeded. For instance, Jackson and Sturtevant (1978) proposed that equilibrium thermodynamics could be applied to the 80 °C transition of *Halobacterium halobium* purple membranes on the basis of its scan-rate independence.

ACKNOWLEDGMENTS

We gratefully acknowledge the technical assistance of M. L. Galisteo.

APPENDIX

We will consider here a two-state endothermic transition, from the native, N, to the denatured, D, state of a protein, which takes place upon heating at a scan rate of v K/min and which is determined by a first-order kinetic process

$$N \xrightarrow{k} D$$

where k is a first-order kinetic constant that changes with temperature according to the Arrhenius equation.

A simple irreversible DSC melting profile of the form found for several proteins is shown in Figure 2B. For the sake of simplicity we will consider that there is no net heat capacity change on denaturation, that is, $\Delta_d C_p = C_p(D) - C_p(N) = 0$.

(A) For a given temperature, T, the heat evolved, Q, will be proportional to the hatched area in Figure 2B. This value, as well as the total heat of the process, Q_t, can be expressed by

$$Q = [D]\Delta HV \qquad Q_t = c\Delta HV \tag{A1}$$

where [D] stands for the molar concentration of the denatured state at the temperature T, c for the total molar concentration of protein in the sample cell, V for the cell colume, and ΔH for the total heat (enthalpy) of the process per mole of protein. The Q_t value is thus proportional to the total area under the transition curve.

For a first-order kinetic process

$$d[N]/dt = -k[N]$$

and since the scan rate is $v = dT/dt$

$$k = -\frac{v}{[N]}\frac{d[N]}{dT} \tag{A2}$$

where [N] is the concentration of the native state at the temperature T. This value can also be expressed as

$$[N] = c - [D] = (Q_t - Q)/\Delta HV \tag{A3}$$

and thence

$$\frac{d[N]}{dT} = \frac{-1}{\Delta HV}\frac{dQ}{dT} = \frac{-C_p}{\Delta HV} \tag{A4}$$

and by substitution in (A2)

$$k = vC_p/(Q_t - Q) \tag{A5}$$

which is eq 1 used in method A under Results.

(B) From eq A2 and the Arrhenius relationship, we have

$$\frac{d \ln [N]}{dT} = -\frac{k}{v} = -\frac{A}{v}\exp(-E/RT) \tag{A6}$$

The value of $d^2 \ln [N]/dT^2$ will, then, be

$$\frac{d^2 \ln [N]}{dT^2} = -\frac{A}{v}\frac{E}{RT^2}\exp(-E/RT) = \frac{E}{RT^2}\frac{d \ln [N]}{dT} \tag{A7}$$

but also

$$\frac{d^2 \ln [N]}{dT^2} = \frac{1}{[N]}\frac{d^2[N]}{dT^2} - \frac{1}{[N]^2}\left(\frac{d[N]}{dT}\right)^2 \tag{A8}$$

Now from eq A4 it follows that

$$C_p = -V\Delta H\frac{d[N]}{dT} \tag{A9}$$

where, for $T = T_m$, we have that $dC_p/dT = 0$ and therefore $|d^2[N]/dT^2|_{T=T_m} = 0$.

Comparing (A7) and (A8), for $T = T_m$, we arrive at

$$\frac{E}{RT_m^2}\frac{1}{[N]}\left(\frac{d[N]}{dT}\right)_{T_m} = -\frac{1}{[N]^2}\left(\frac{d[N]}{dT}\right)^2_{T_m} \tag{A10}$$

or

$$\frac{E}{RT_m^2} = -\left(\frac{d \ln [N]}{dT}\right)_{T_m} \quad (A11)$$

Taking eq A6 into account and rearranging, we have

$$\frac{v}{T_m^2} = \frac{AR}{E} \exp(-E/RT_m) \quad (A12)$$

which is eq 2 in the text used in method B to calculate the energy of activation.

(C) The derivation, from (A6), of an explicit equation giving the concentration of the native state as a function of temperature requires the evaluation of the so-called Arrhenius integral; this must be done numerically (Norris, 1981) or by carrying out some approximation.

We can relate T_m to any temperature by $T = T_m + \Delta T$ and apply the Taylor expansion of $1/T$ in the neighborhood of $1/T_m$ using only the first expansion term, given that within the range of the calorimetric transition $\Delta T \ll T_m$

$$1/T = 1/T_m + (d(1/T)/dT)_{T_m}(T - T_m) = 1/T_m - \Delta T/T_m^2 \quad (A13)$$

Substituting (A13) in (A6) and using (A12), we arrive at

$$d \ln [N]/dT = -A/v \exp(-E/RT_m) \exp[(E/RT_m^2)\Delta T] = -W \exp(W\Delta T) \quad (A14)$$

where $W = A/v \exp(-E/RT_m) = E/RT_m^2$ (see eq A12).

Upon integration from $\Delta T_0 = T_0 - T_m$, where T_0 is a temperature low enough to make the reaction rate negligible, we obtain

$$\ln [N]/[N]_0 = \exp(W\Delta T_0) - \exp(W\Delta T) \quad (A15)$$

If T_0 is low enough, and for the temperature range of the calorimetric transition, $\exp(W\Delta T) \gg \exp(W\Delta T_0)$ (note that $\Delta T_0 < 0$). Therefore

$$\ln \frac{[N]_0}{[N]} = \exp(W\Delta T) = \exp\left[\frac{E}{R}\left(\frac{T - T_m}{T_m^2}\right)\right] \quad (A16)$$

Now, from eq A1 we have

$$\frac{[N]_0}{[N]} = \frac{Q_t}{Q_t - Q} \quad (A17)$$

and taking into account that, within the relatively narrow range of the transition $(T - T_m)/T_m^2 = 1/T_m - 1/T$ (eq A13), we finally obtain

$$\ln\left(\ln \frac{Q_t}{Q_t - Q}\right) = \frac{E}{R}\left(\frac{1}{T_m} - \frac{1}{T}\right) \quad (A18)$$

which is eq 3 in the text used in method C. Clearly, we could have used an equation similar to (A18) with $(T - T_m)/T_m^2$ instead of $1/T_m - 1/T$ in the right-side term. Both equations, in fact, lead to the same results; we have used (A18) because it allows us to use the same X axis for the three plots in Figure 3.

Note that for $T = T_m$ eq A18 leads to

$$\ln \frac{Q_t}{Q_t - Q_m} = 1 \qquad \frac{Q_t}{Q_t - Q_m} = e \quad (A19)$$

(D) Finally, at $T = T_m$ and by use of eq A6 and A12, eq A5 becomes

$$\frac{v C_p^m}{Q_t - Q_m} = \frac{Ev}{RT_m^2} \quad (A20)$$

from whence, and by application of eq A19, we obtain

$$E = \frac{RT_m^2 C_p^{-1}}{Q_t - Q_m} = \frac{eRT_m^2 C_p^m}{Q_t} \quad (A21)$$

which is eq 4 in the text used in method D.

Registry No. Thermolysin, 9073-78-3.

REFERENCES

Ahern, T. J., & Klibanov, A. M. (1985) *Science (Washington, D.C.) 228*, 1280.

Edge, V., Allenwell, N. M., & Sturtevant, J. M. (1985) *Biochemistry 24*, 5899.

Freire, E., & Biltonen, R. L. (1978) *Biopolymers 17*, 463.

Fujita, S. C., Go, N., & Imakori, K. (1979) *Biochemistry 18*, 24.

Ghelis, C., & Yon, J. (1980) *Protein Folding*, Academic, New York.

Holmquist, B., & Vallee, B. L. (1974) *J. Biol. Chem. 249*, 4601.

Hu, C. Q., & Sturtevant, J. M. (1987) *Biochemistry 26*, 178.

Jackson, M. B., & Sturtevant, J. M. (1978) *Biochemistry 17*, 911.

Jackson, W. M., & Brandts, J. F. (1970) *Biochemistry 9*, 2294.

Khan, S. M., & Darnall, D. W. (1978) *Anal. Biochem. 86*, 332.

Lapanje, S. (1978) *Physicochemical Aspects of Protein Denaturation*, Wiley, New York.

Lechuga, A. (1985) Master's Thesis, University of Granada.

Lumry, R., & Eyring, H. (1954) *J. Phys. Chem. 58*, 110.

Manly, S. P., Matthews, K. S., & Sturtevant, J. M. (1985) *Biochemistry 24*, 3842.

Mateo, P. L. (1984) in *Thermochemistry and Its Applications to Chemical and Biochemical Systems* (Ribeiro da Silva, M. A. V., Ed.) pp 541–568, Reidel, Dordrecht, Holland.

Matthews, B. W., Weaver, L. H., & Kestler, W. R. (1974) *J. Biol. Chem. 249*, 8030.

Norris, A. C. (1981) *Computational Chemistry. An Introduction to Numerical Methods*, pp 194–199, Wiley, New York.

Novokhatny, V. V., Kudinor, S. A., & Privalov, P. L. (1984) *Mol. Biol. 179*, 215.

Ohta, Y., Ogura, Y., & Wada, A. (1966) *J. Biol. Chem. 241*, 5919.

Pfeil, W. (1981) *Mol. Cell. Biochem. 40*, 3.

Potekhin, S. A., & Privalov, P. L. (1982) *J. Mol. Biol. 159*, 519.

Privalov, P. L. (1979) *Adv. Protein Chem. 33*, 167.

Privalov, P. L. (1980) *Pure Appl. Chem. 52*, 479.

Privalov, P. L. (1982) *Adv. Protein Chem. 35*, 1.

Privalov, P. L., & Medved, L. V. (1982) *J. Mol. Biol. 159*, 665.

Privalov, P. L., Mateo, P. L., Khechinashvili, N. N., Stepanov, V., & Revina, L. (1981) *J. Mol. Biol. 152*, 445.

Rigell, C. W., Saussure, C. de, & Freire, E. (1985) *Biochemistry 24*, 5638.

Sturtevant, J. M. (1974) *Annu. Rev. Biophys. Bioeng. 3*, 35.

Takahashi, K., & Sturtevant, J. M. (1981) *Biochemistry 20*, 6185.

Tanford, C. (1968) *Adv. Protein Chem. 23*, 121.

Tanford, C. (1970) *Adv. Protein Chem. 24*, 1.

Tsalkova, T. M., & Privalov, P. L. (1985) *J. Mol. Biol. 181*, 533.

Voordouw, G., Milo, C., & Roche, R. S. (1976) *Biochemistry 15*, 3716.

Zale, S. A., & Klibanov, A. M. (1986) *Biochemistry 25*, 5432.